AD-A119 673 AIR FORCE INST OF TECH WRIGHT-PATTERSON AFB OH F/G 13/1
OPTIMAL CONTROL OF RESIDENTIAL HEATING AND COOLING SYSTEMS.(U)
1982 R C WINN
UNCLASSIFIED AFIT/CI/NR-82-54D NL

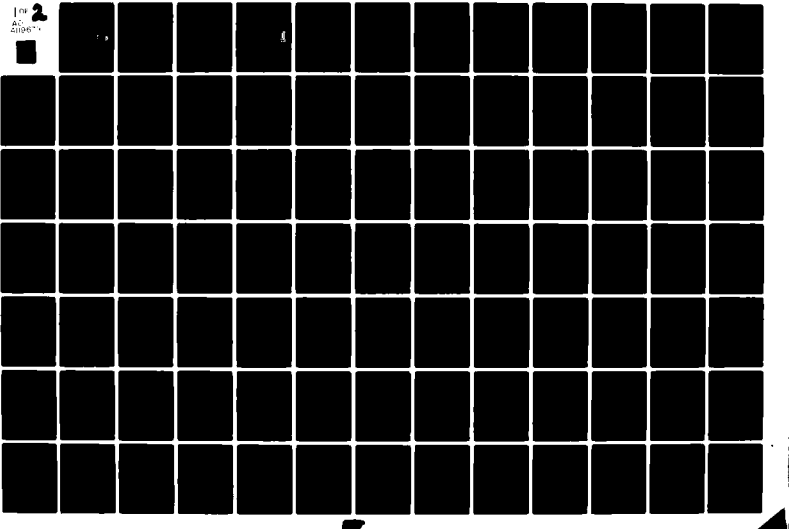

UNCLASS

SECURITY CLASSIFICATION OF THIS PAGE *(When Data Entered)*

REPORT DOCUMENTATION PAGE		READ INSTRUCTIONS BEFORE COMPLETING FORM
1. REPORT NUMBER AFIT/CI/NR-82-54D	2. GOVT ACCESSION NO. A119673	3. RECIPIENT'S CATALOG NUMBER
4. TITLE *(and Subtitle)* Optimal Control of Residential Heating and Cooling Systems		5. TYPE OF REPORT & PERIOD COVERED THESIS/DISSERTATION 6. PERFORMING ORG. REPORT NUMBER
7. AUTHOR(s) Robert C. Winn		8. CONTRACT OR GRANT NUMBER(s)
9. PERFORMING ORGANIZATION NAME AND ADDRESS AFIT STUDENT AT: Colorado State University		10. PROGRAM ELEMENT, PROJECT, TASK AREA & WORK UNIT NUMBERS
11. CONTROLLING OFFICE NAME AND ADDRESS AFIT/NR WPAFB OH 45433		12. REPORT DATE Summer, 1982 13. NUMBER OF PAGES 114
14. MONITORING AGENCY NAME & ADDRESS*(if different from Controlling Office)*		15. SECURITY CLASS. *(of this report)* UNCLASS 15a. DECLASSIFICATION/DOWNGRADING SCHEDULE

16. DISTRIBUTION STATEMENT *(of this Report)*

APPROVED FOR PUBLIC RELEASE; DISTRIBUTION UNLIMITED

DTIC ELECTE SEP 28 1982 H

17. DISTRIBUTION STATEMENT *(of the abstract entered in Block 20, if different from Report)*

18. SUPPLEMENTARY NOTES

APPROVED FOR PUBLIC RELEASE: IAW AFR 190-17

16 SEPT 1982

LYNN E. WOLAVER
Dean for Research and
Professional Development
AFIT, Wright-Patterson AFB OH

19. KEY WORDS *(Continue on reverse side if necessary and identify by block number)*

20. ABSTRACT *(Continue on reverse side if necessary and identify by block number)*

ATTACHED

180

AD A119673

FILE COPY

DD FORM 1 JAN 73 1473 EDITION OF 1 NOV 65 IS OBSOLETE

UNCLASS

SECURITY CLASSIFICATION OF THIS PAGE *(When Data Entered)*

ABSTRACT OF DISSERTATION

OPTIMAL CONTROL OF RESIDENTIAL HEATING AND COOLING SYSTEMS

In recent years, several heating and cooling systems have come into use for the purpose of reducing energy costs. Unfortunately, due to limitations of the conventional control strategies, the use of these systems does not always result in significantly reduced costs of operation. The purpose of this study is to develop control strategies for these systems which will ensure that their use results in the desired savings in energy costs.

The methods of dynamic optimization are used to develop the improved control strategies for three types of systems. The system types which are analyzed are a passive solar home with an electrically heated thermal storage floor, solar and/or off-peak storage heating and cooling systems, and an active solar energy collection system. Optimal control strategies are presented for each of the analyzed systems. Simulation results are presented for each system. In addition, experimental results from an implementation of the optimal collection of solar energy are presented.

Robert C. Winn
Department of Mechanical Engineering
Colorado State University
Fort Collins, Colorado 80523
Summer, 1982

AFIT/CI/NR/82-54D

AFIT RESEARCH ASSESSMENT

The purpose of this questionnaire is to ascertain the value and/or contribution of research accomplished by students or faculty of the Air Force Institute of Technology (ATC). It would be greatly appreciated if you would complete the following questionnaire and return it to:

AFIT/NR
Wright-Patterson AFB OH 45433

RESEARCH TITLE: Optimal Control of Residential Heating and Cooling Systems

AUTHOR: Robert C. Winn

RESEARCH ASSESSMENT QUESTIONS:

1. Did this research contribute to a current Air Force project?

( ) a. YES ( ) b. NO

2. Do you believe this research topic is significant enough that it would have been researched (or contracted) by your organization or another agency if AFIT had not?

( ) a. YES ( ) b. NO

3. The benefits of AFIT research can often be expressed by the equivalent value that your agency achieved/received by virtue of AFIT performing the research. Can you estimate what this research would have cost if it had been accomplished under contract or if it had been done in-house in terms of manpower and/or dollars?

( ) a. MAN-YEARS _____ ( ) b. $_____

4. Often it is not possible to attach equivalent dollar values to research, although the results of the research may, in fact, be important. Whether or not you were able to establish an equivalent value for this research (3. above), what is your estimate of its significance?

( ) a. HIGHLY SIGNIFICANT ( ) b. SIGNIFICANT ( ) c. SLIGHTLY SIGNIFICANT ( ) d. OF NO SIGNIFICANCE

5. AFIT welcomes any further comments you may have on the above questions, or any additional details concerning the current application, future potential, or other value of this research. Please use the bottom part of this questionnaire for your statement(s).

NAME GRADE POSITION

ORGANIZATION LOCATION

STATEMENT(s):

FOLD DOWN ON OUTSIDE - SEAL WITH TAPE

AFIT/NR
WRIGHT-PATTERSON AFB OH 45433

OFFICIAL BUSINESS
PENALTY FOR PRIVATE USE. $300

NO POSTAGE
NECESSARY
IF MAILED
IN THE
UNITED STATES

BUSINESS REPLY MAIL
FIRST CLASS PERMIT NO. 73236 WASHINGTON D.C.

POSTAGE WILL BE PAID BY ADDRESSEE

AFIT/ DAA
Wright-Patterson AFB OH 45433

FOLD IN

DISSERTATION

OPTIMAL CONTROL OF RESIDENTIAL HEATING AND COOLING SYSTEMS

Submitted by

Robert C. Winn

Department of Mechanical Engineering

In partial fulfillment of the requirements

for the Degree of Doctor of Philosophy

Colorado State University

Fort Collins, Colorado

Summer, 1982

COLORADO STATE UNIVERSITY

SUMMER 1982

WE HEREBY RECOMMEND THAT THE DISSERTATION PREPARED UNDER OUR SUPERVISION BY ROBERT C. WINN ENTITLED OPTIMAL CONTROL OF RESIDENTIAL HEATING AND COOLING SYSTEMS BE ACCEPTED AS FULFILLING IN PART REQUIREMENTS FOR THE DEGREE OF DOCTOR OF PHILOSOPHY.

Committee on Graduate Work

Adviser

Department Head

ABSTRACT OF DISSERTATION

OPTIMAL CONTROL OF RESIDENTIAL HEATING AND COOLING SYSTEMS

In recent years, several heating and cooling systems have come into use for the purpose of reducing energy costs. Unfortunately, due to limitations of the conventional control strategies, the use of these systems does not always result in significantly reduced costs of operation. The purpose of this study is to develop control strategies for these systems which will ensure that their use results in the desired savings in energy costs.

The methods of dynamic optimization are used to develop the improved control strategies for three types of systems. The system types which are analyzed are a passive solar home with an electrically heated thermal storage floor, solar and/or off-peak storage heating and cooling systems, and an active solar energy collection system. Optimal control strategies are presented for each of the analyzed systems. Simulation results are presented for each system. In addition, experimental results from an implementation of the optimal collection of solar energy are presented.

Robert C. Winn
Department of Mechanical Engineering
Colorado State University
Fort Collins, Colorado 80523
Summer, 1982

ACKNOWLEDGEMENTS

I would like to express my appreciation to the people who have contributed their time and experience to this study. The encouragement, assistance, and understanding of my major professor, Dr. C. Byron Winn, made this research a rewarding, as well as enjoyable, experience. The cooperation of Dr. Susumu Karaki, a member of my graduate committee, during the work at Solar House II made that phase of the research possible. I also wish to thank the remainder of my committee, Dr. Paul Wilbur and Dr. Charles Mitchell. The encouragement and approval of such learned men means a lot to me.

I also wish to express my appreciation to several organizations for financial support during the course of the research. The Department of Energy funded some of the work on the implementation of the optimal controller in Solar House II. The Electric Power Research Institute supported the work on the storage discharge problems. The United States Air Force supported me. I am extremely thankful for the assistance.

TABLE OF CONTENTS

LIST OF TABLES

LIST OF FIGURES

CHAPTER I

INTRODUCTORY REMARKS

Many residential heating and cooling systems have been developed recently which are intended to reduce the cost of heating or cooling a house. Solar heating systems and off-peak storage devices are designed to reduce energy costs; however, they are not always successful. The conventional control strategies used to operate these systems have limitations which can reduce the effectiveness of the systems. The purpose of this study is to develop control strategies for these systems which ensure that their operation results in a reduced cost of operation.

Solar heating systems attempt to reduce energy cost by reducing the total amount of purchased energy required for heating relative to conventional heating systems. Over a long period of time, a solar heating system will require less purchased energy than a conventional heating system. However, if the heating load on a particular day is high, the peak instantaneous demand is about the same for solar and conventional houses. As a result, the utility must maintain the generating capacity to satisfy the instantaneous demand of all of the houses in its service area, not just the conventional houses. In addition, the operation of the pumps and fans in an active solar heating system may result in a large electrical requirement during the time of day when the utility's overall demand is high. Improved control strategies can help prevent these undesirable performance characteristics.

Off-peak storage devices are designed to require electricity during the utility's low demand time of day so that the utility's demand is more uniform throughout the day. Off-peak storage systems can take several forms. The

simplest form of off-peak storage system is one in which water in a storage tank is heated or cooled at night and discharged during the day. A modification of this system is one in which an off-peak heater is added to a solar storage tank. Another variation is to use off-peak electricity to heat a large solid mass in a passive solar home. In any of these systems, if the storage is depleted before the end of the utility's high demand time of day, a large, instantaneous, electrical load is experienced at the residence. Again, the utility must have the capability to satisfy this load. Improved conrol strategies can ensure that the use of off-peak storage will have the desired effect of significantly reducing on-peak electrical demand.

Methods of dynamic optimization are used in this study to develop optimal control strategies for the systems mentioned above. Specifically, analyses are conducted on a system in which off-peak electrical energy is input to a passive solar home, an active solar and/or off-peak storage system, and an active solar energy collection system. Each of these analyses represents a different level of control complexity which is the result of specific characteristics of the energy storage systems.

The study of the passive heating system is presented in Chapter II. In this problem, the energy storage medium is in thermal contact with the conditioned space. As a result, the discharge from storage is determined by the dynamics of the storage and the governing heat transfer relationships. Control is achieved by the rate and timing of energy delivery to storage. The optimal control in this problem depends heavily on the dynamics of the storage and requires accurate load prediction.

Systems with energy storage isolated from the conditioned space are studied in Chapter III. In these systems, the control is achieved by turning a

pump on or off. As such, the characteristics of the storage are not as important as in the problem in Chapter II. The optimal control in this case requires some load prediction, but a rough estimate of the load gives an excellent approximation to the optimal control.

In Chapter IV, the collection of solar energy in an active solar heating system is analyzed. In this problem, the storage dynamics may be safely ignored, and the dynamic optimization is equivalent to a series of point optimizations. No load prediction is required. A controller designed to approximate the optimal control has been built and results of actual system performance using this controller are presented in Chapter IV.

The optimal control problems presented in Chapters II, III, and IV are all solved using a dynamic optimization technique. The solutions to the problems differ significantly due to the differing importance of the characteristics of the storage. In each case, however, the optimal control strategy ensures that the system operation has the effect that was intended in the initial design of the system.

CHAPTER II

PASSIVE SOLAR RESIDENCE WITH ELECTRICALLY HEATED THERMAL STORAGE

In this chapter, optimal control strategies are developed for a passive solar residence which has thermal energy storage which can be electrically heated. This problem is one in which the storage characteristics are extremely important in the control determination. The control of the system is the electrical heating of the thermal energy storage.

INTRODUCTION

The use of off-peak electricity to heat thermal energy storage has been investigated as a technique for reducing electrical demand during the utility high demand hours. Typically, the storage is isolated from the living space, and the discharge of energy from storage is easily controlled. In some designs, however, the storage is thermally coupled to the living space. Such a design is incorporated in a house built in the LaVereda subdivision of Santa Fe, New Mexico as a joint venture of the Public Service Company of New Mexico, the Los Alamos National Laboratory, and a contractor in Santa Fe [1]. The building is heated using an indirect gain passive solar heating system (Trombe wall) and an electrically heated thermal storage floor.

The operation of an energy storage system such as the one described above requires a control strategy which is designed specifically for the system. A simple thermostat is inadequate because of the long time delay between energy input into storage and the response of the building temperature. In addition,

because the energy storage is coupled to the living space, the discharge from storage is determined by the governing heat transfer equations and cannot be switched on or off. An effective control strategy must take into account the time delay between energy input and release as well as the governing heat transfer relationships. The results of simulations using several different control strategies as applied to a residence similar to the one in Santa Fe are presented and, in particular, several optimal control strategies are proposed.

SYSTEM MODEL

For the purpose of this study, the Santa Fe residence is modeled by the system shown in Figure 1. The enclosure, the storage wall, and the storage floor are modeled using a single node for each; i.e., lumped capacitance. This is not an adequate model for use in a detailed simulation because the wall, floor, and enclosure are not isothermal; however, this model, which gives qualitatively correct results, is used to develop and compare the control strategies.

For the model in Figure 1, the heat transfer (in Watts) are given by

$$\dot{Q}_s = H_t \tau\alpha A_w \tag{1}$$

$$\dot{Q}_w = h_{we} A_w (T_w - T_e) \tag{2}$$

$$\dot{Q}_{w,loss} = U_{wa} A_w (T_w - T_a) \tag{3}$$

$$\dot{Q}_f = U_{fe} A_f (T_f - T_e) \tag{4}$$

$$\dot{Q}_{f,loss} = U_{fg} A_f (T_f - T_g) \tag{5}$$

$$\dot{Q}_{e,loss} = U A_e (T_e - T_a) \tag{6}$$

$\dot{Q}_{aux}$ is the electrical power to the floor

where

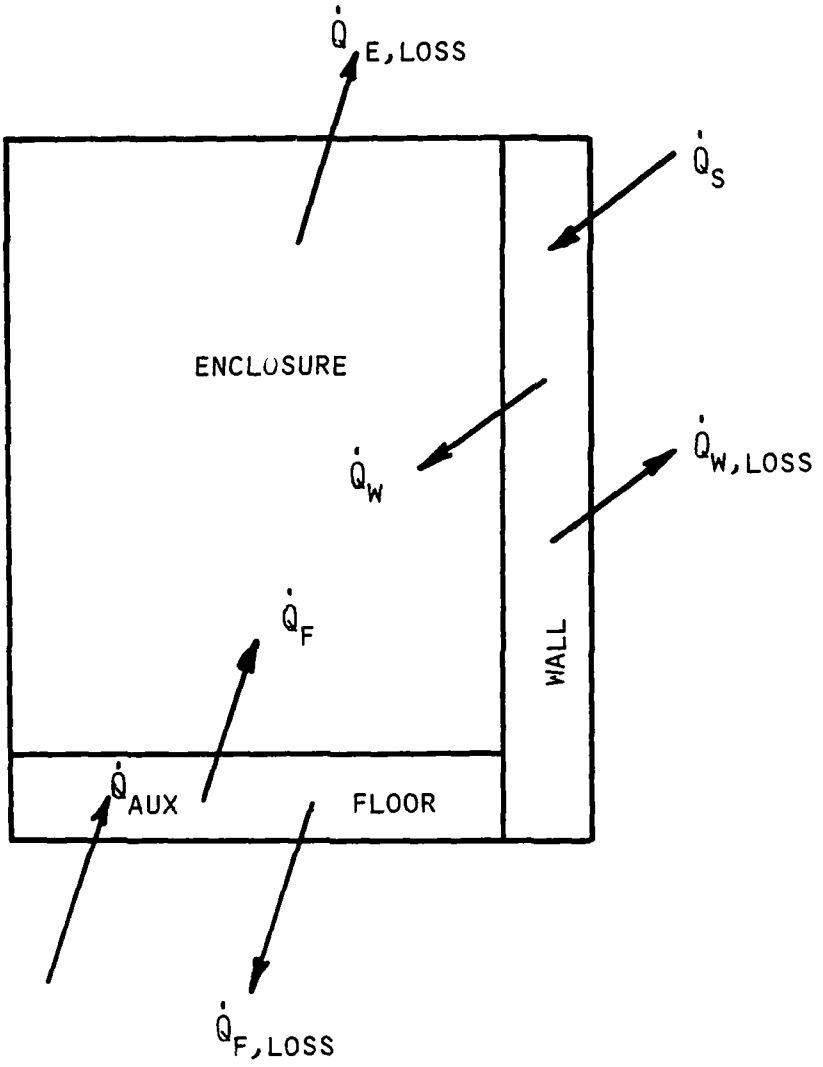

Figure 1. Schematic of Passive Solar Residence.

H_t is the solar radiation incident on the glazing surface

$\tau\alpha$ is the glazing transmittance-absorptance product

A_w is the glazing area

h_{we} is the connective heat transfer coefficient, Trombe wall to enclosure

U_{wa} is the overall heat transfer coefficient, Trombe wall to ambient

U_{fe} is the overall heat transfer coefficient, floor to enclosure

A_f is the floor area

U_{fg} is the overall heat transfer coefficient, floor to ground

UA_e is the overall enclosure heat transfer coefficient-area product

T_w is the enclosure temperature

T_a is the ambient temperature

T_f is the floor temperature

T_g is the ground temperature.

All properties and heat transfer coefficients are assumed constant. Performing an energy balance on each node and using the above relationships yields

$$g_1 = dT_e/dt = -(a_1+a_2+a_3)T_e+a_1T_w+a_2T_f+a_3T_a \quad (7)$$

$$g_2 = dT_w/dt = a_5T_e-(a_5+a_6)T_w+a_4H_T+a_6T_a \quad (8)$$

$$g_3 = dT_f/dt = a_7T_e-(a_7+a_8)T_f+Q_{aux}/C_f+a_8T_g \quad (9)$$

where

$$a_1 = h_{we}A_w/C_e$$

$$a_2 = U_{fe}A_f/C_e$$

$$a_3 = UA_e/C_e$$

$$a_4 = \tau\alpha A_w/C_w$$

$$a_5 = h_{we}A_w/C_w$$

$a_6 = U_{wa}A_w/C_w$

$a_7 = U_{fe}A_f/C_f$

$a_8 = U_{fg}A_f/C_f$

C_e is the thermal capacitance of the Trombe wall (kJ/^oC)

C_f is the thermal capacitance of the floor (kJ/^oC)

Equations (7), (8), and (9) describe the performance of the system in Figure 1. A more detailed model could easily be developed using multiple nodes throughout the structure, but these equations will suffice for the following development.

OPTIMAL CONTROL DETERMINATION

Equations (7), (8), and (9) describe the dynamic performance of the system depicted in Figure 1. That performance is driven by external inputs (ambient temperature, ground temperature, and solar radiation) and is controlled by the auxiliary heat input. The optimal use of auxiliary heat input, that is, the optimal control, can be determined using a dynamic optimization technique. The technique used in this problem is Pontryagin's Maximum Principle [2].

To apply the Maximum Principle to the problem at hand, a statement of what is to be optimized must be made. There are many possible statements, and two will be used in this study. The first statement is

$$J_1 = \int_{t_o}^{t_f} [f\dot{Q}_{aux}^2 + C(T_e - T_{set})^2]dt \qquad (10)$$

which is the quadratic objective function. The second statement is

$$J_2 = \int_{t_o}^{t_f} f\dot{Q}_{aux}dt \qquad (11)$$

which is called the minimum cost objective function. In these statements, f represents the cost per unit of energy, C is a comfort weighting coefficient,

and T_{set} is the desired temperature, all of which may be functions of time of day. In equation (10) the first term represents a measure of energy cost and the second is measure of discomfort. Because $\dot{Q}_{aux}$ is squared in the first term, it is not strictly and energy cost term, but is, in fact, the product of energy cost, $f\dot{Q}_{aux}dt$, and power demand, $\dot{Q}_{aux}$. To minimize energy cost, the term must be linear in $\dot{Q}_{aux}$, as in the equation (11).

The controls which minimize the above objective functions are determined from the solution of a set of differential equations which form a two point boundary value problem. For equation (10), the optimal control is determined numerically; for equation (11) it is determined by a combination of analytical and numerical methods. For a complete discussion of the optimal control determination for both objective functions see Appendix A.

Equations (9) and (10) contain the energy cost, f, which may be a function of time. The utility rate structure may be used as the energy cost, but utility rates may not accurately reflect true energy costs. To avoid this problem, actual utility fuel cost of supply information is used. Utility unit fuel costs depend on the total systemwide demand imposed on the utility at any time. The projected unit fuel cost of supply for the peak utility demand day in Albuquerque in 1990 is presented in Figure 2. The unit fuel cost is high at the times of day corresponding to the morning and afternoon utility peaks.

In each of the problems described above, the period of the optimization is arbitrary. Ideally, the objective function should be optimized over the entire heating season. This, however, is not practical because of computer limitations as well as the dependence of the optimal control on weather. If, however, the optimization were to be performed over an entire heating season, one would expect the enclosure temperature to fluctuate around the desired

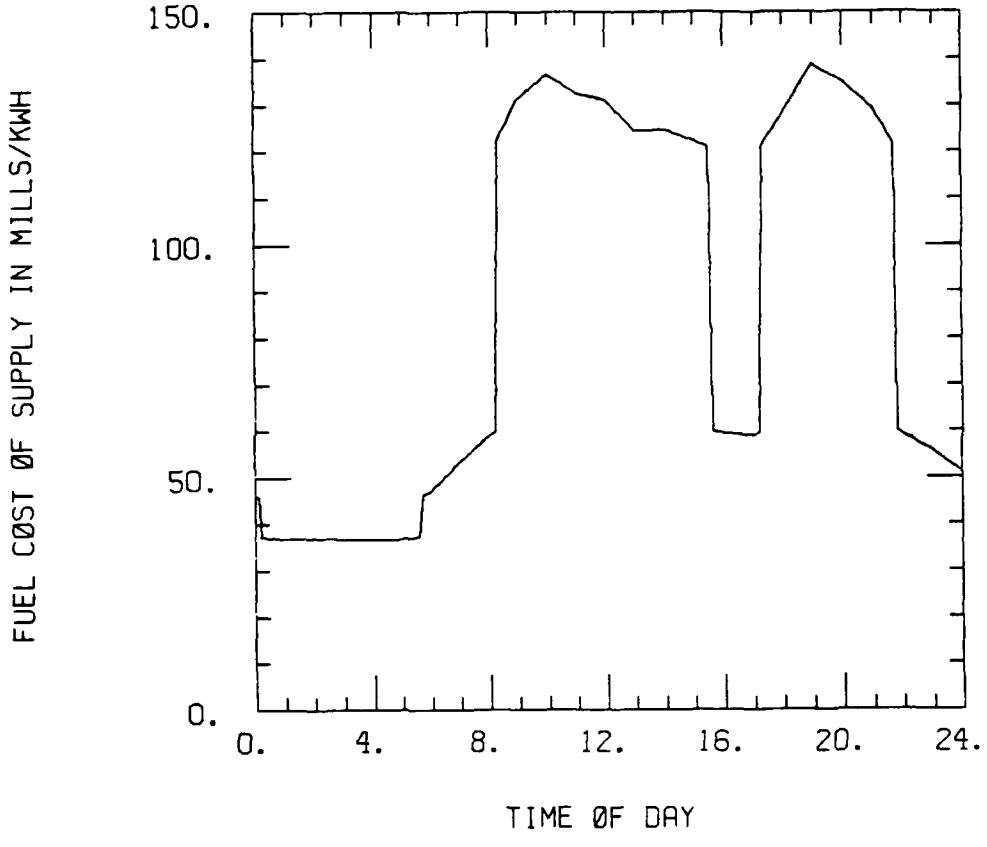

Figure 2. Fuel Cost of Supply on Utility Peak Day.

temperature throughout the season. As an approximation to this seasonal optimization, the objective function is minimized on a daily basis, and the enclosure temperature is forced to equal the desired temperature at midnight.

Typical optimal control strategies which were developed using the fuel costs and enclosure temperature conditions described above are presented in Figures 3 and 4 for a sunny and cloudy day, respectively. The corresponding enclosure temperature variations are given in Figures 5 and 6. On the sunny day, the enclosure temperature is kept closer to the desired temperature as the comfort weighting factor, C, is increased. When the comfort weighting factor is high, large instantaneous values of $\dot{Q}_{aux}^{*}$ can occur; when the factor is low, $\dot{Q}_{aux}^{*}$ has less variation throughout the day. The apparent discontinuities in the controls are caused by the rapid changes in f (see Figure 2). On the cloudy day, the control strategies differ considerably from those on the sunny day. The reason for the difference is that much more electrical energy is required to make up for the lack of solar energy. The minimum cost control requires two on periods during the cloudy day compared to one for the sunny day. The second on period occurs during the time that the fuel cost is low in the middle of the day. The high fuel cost in the morning and evening ensures that the minimum cost control will not call for heat at those times. If the fuel cost were constant all day, the minimum cost control would call for heat in the late afternoon only.

The large difference between the controls for the sunny day and for the cloudy day implies that accurate net heating load prediction is important in proper control determination. If an error is made in the control determination, the principle effect is lack of control of enclosure temperature. Over a long time, the net load for the building, and, therefore, the electrical energy

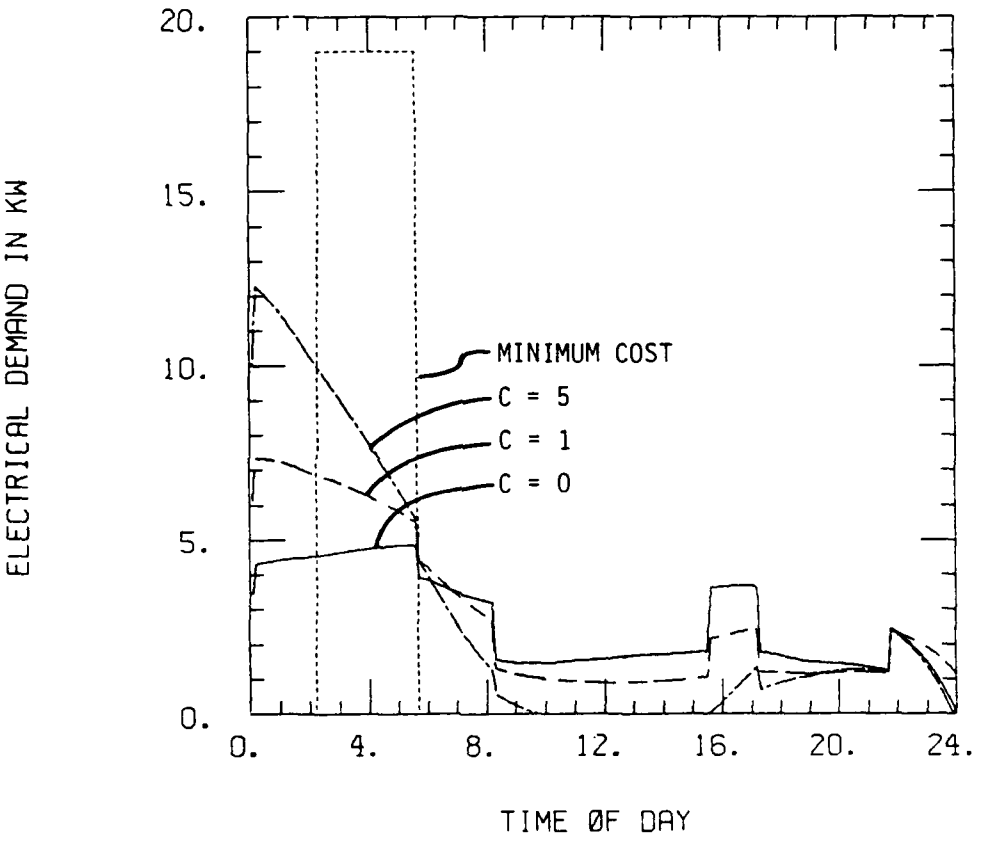

Figure 3. Optimal Control Strategies, Sunny Day.

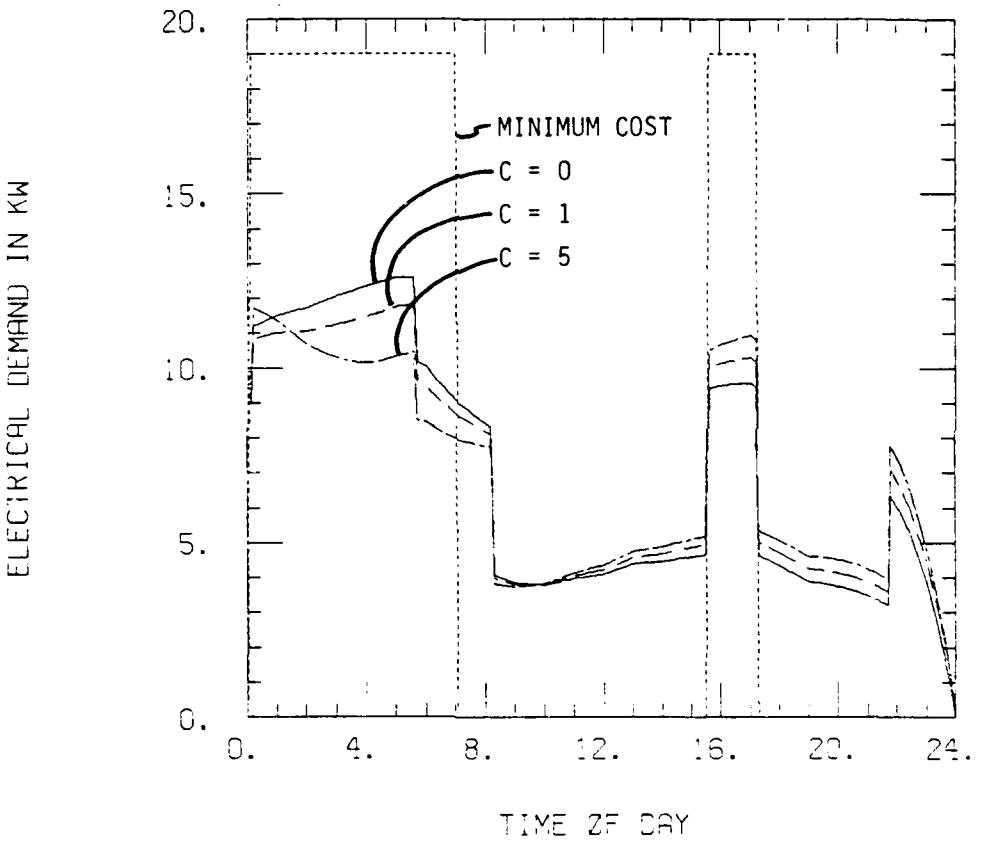

Figure 4. Optimal Control Strategies, Cloudy Day.

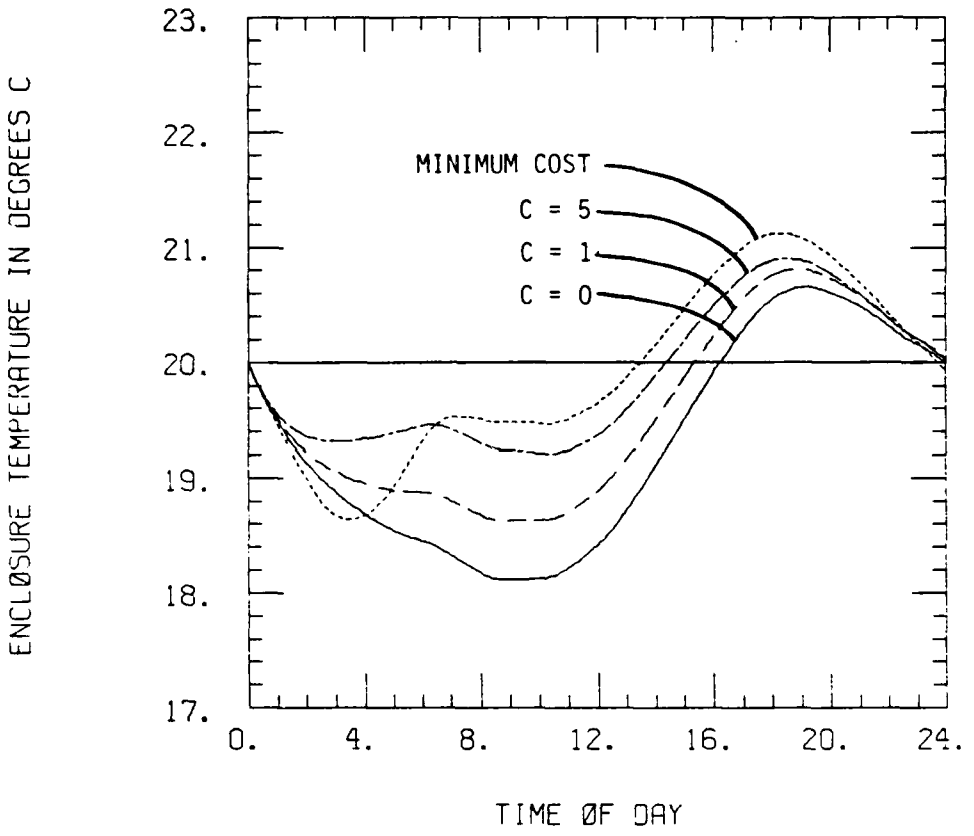

Figure 5. Enclosure Temperature Response to Optimal Control, Sunny Day.

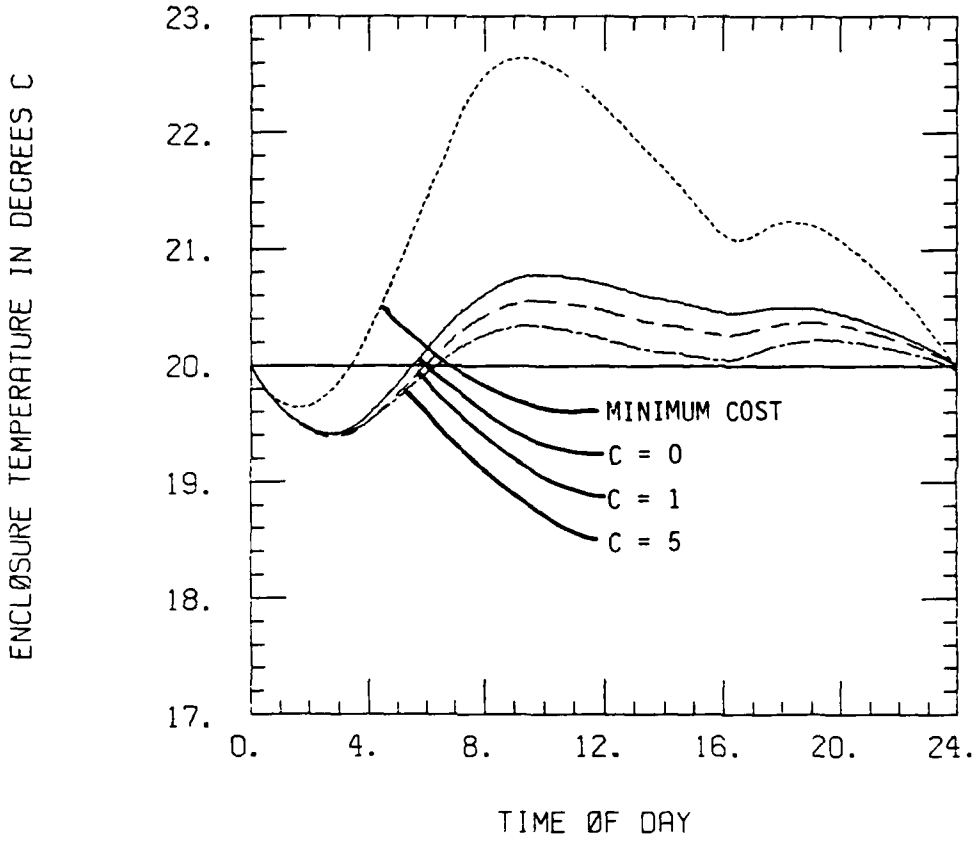

Figure 6. Enclosure Temperature Response to Optimal Control, Cloudy Day.

requirement, is relatively independent of control accuracy. The enclosure temperature excursions, however, are sensitive to the control.

COMPARISON OF STRATEGIES

Several different control strategies were employed in simulations of the system in Figure 1. Weather data from the Albuquerque Typical Meteorological Year (TMY) for the month of February were used in the simulations. The control strategies which are considered are those that result from minimizing the quadradic objective function with several different comfort weighting factors, the minimum cost control, a control which requires $\dot{Q}_{aux}$ to be constant all day so as to minimize the daily peak $\dot{Q}_{aux}$, and a thermostat control in which energy is delivered directly to the enclosure instead of the floor.

In each control strategy except thermostat control, the estimate of temperature and solar radiation for the next day is very important. If future knowledge of these weather features is available, rather precise temperature control can be maintained in the enclosure. This, however, is not possible, but there are several ways to estimate weather 24 hours in advance. The least sophisticated estimate is to assume that tomorrow's weather will be exactly like today's. A further improvement is to use an automatic observer/predictor [4]. Another method is to use a direct input from a forecaster. The forecasted high temperature, low temperature, and cloudiness are sufficient to give a reasonable estimate of the net heating load to be encountered during the next day. Simulations were performed to compare the extremes of the weather predictions, perfect prediction versus day old weather. Values for system parameters shown in Table 1 were used in the simulations.

The results of month long simulations using exact knowledge of future weather and one day old weather are presented in Tables 2 and 3, respectively.

Table 1. Passive Heating System Parameter Values.

$\tau\alpha = 0.8$

$h_{we} = 5.67$ W/m^2 ^oC (1. Btu/hr ft^2 ^oF)

$U_{wa} = 2.84$ W/m^2 ^oC (0.5 Btu/hr ft^2 ^oF)

$U_{fe} = 8.52$ W/m^2 ^oC (1.5 Btu/hr ft^2 ^oF)

$U_{fg} = 0.57$ W/m^2 ^oC (0.1 Btu/hr ft^2 ^oF)

$UA_e = 264$ W/^oC (500 Btu/hr ^oF)

$A_w = 18.6$ m^2 (200 ft^2)

$A_f = 139$ m^2 (1500 ft^2)

$C_e = 1900$ kJ/^oC (10,000 Btu/^oF)

$C_w = 950$ kJ/^oC (5000 Btu/^oF)

$C_f = 3800$ kJ/^oC (20,000 Btu/^oF)

Table 2. One Month Simulation Results Using Perfect Weather Prediction.

Control	Enclosure Temperature Range, ^{o}C	Avg. Temp. Diff. from $T_{set}=20^{o}C$	Energy Used, kWh	Fuel Cost, $	$\int fu^2 dt$ kw-$
Thermostat	19.3-21.1	0.33	2259	177	13.99
Optimal, C=0	17.8-21.1	0.62	2359	163	3.04
Optimal, C=1	18.2-21.0	0.53	2377	156	3.14
Optimal, C=5	18.9-21.3	0.39	2398	147	3.30
Minimum Cost	17.6-22.5	0.94	2554	101	7.97
Constant	17.6-21.0	0.68	2310	201	3.66

Table 3. One Month Simulation Results Using One Day Old Weather.

Control	Enclosure Temperature Range, ^{o}C	Avg. Temp. Diff. from $T_{set}=20^{o}C$	Energy Used, kWh	Fuel Cost, $	$\int fu^2 dt$ kw-$
Thermostat	19.3-21.1	0.33	2259	177	13.99
Optimal, C=0	15.6-22.4	0.97	2316	160	3.35
Optimal, C=1	15.7-22.3	0.88	2320	152	3.42
Optimal, C=5	16.0-22.0	0.73	2363	145	3.55
Minimum Cost	15.6-23.5	1.38	2512	103	8.12
Constant	15.6-22.3	1.08	2256	196	4.02

The enclosure temperature range and the average temperature difference are presented to quantify discomfort. The integral included as the last column is the integrated product of fuel cost and instantaneous demand.

If perfect weather prediction is used, rather precise control of the enclosure temperature can be achieved. Thermostat control results in the best enclosure temperature control and the least energy consumption but does not take advantage of the energy storage capabilities of the residence, as evidenced by the fuel cost of $177. Temperature control almost as precise is achieved by using optimal control with a high discomfort weighting (C=5). This performance is achieved with a reduction of 17 percent in fuel cost compared to thermostat control. The minimum cost control results in the lowest fuel cost but at the expense of the largest electrical energy use and the least precise temperature control of all of the studied strategies. The energy requiremnet is large because the average enclosure temperature is generally higher with the minimum cost control than with any other strategy (see Figures 5 and 6). Because the enclosure temperature is high, the building losses are high, and, therefore, the electrical energy requirement is high. This control strategy makes maximum use of the energy storage capability of the residence. Energy is input to the floor only when electricity is inexpensive. The constant control results in the lowest peak demand of all of the control strategies tested but results in a fuel cost almost twice as large as that for the minimum cost control.

The results in Table 2 are useful for comparison, but it is unrealistic to expect perfect weather prediction in an actual controller. The results presented in Table 3 represent the system performance when the least sophisticated form of weather prediction is used. The control can vary

significantly depending on the predicted weather which can be seen by comparing Figures 3 and 4. Even though the control may be significantly in error, the fuel cost and energy usage are not greatly affected by the accuracy of weather prediction. The decrease in the accuracy of the temperature control is the primary result of imperfect weather prediction. The average temperature difference increases only slightly but the temperature range increases significatly. In other words, the performance of the system is usually quite good, but on a few days in the month, the temperature control is rather poor. The worst problems occur when expected radiation does not occur. Even on the worst days, however, the enclosure temperature remains within tolerable limits partly due to the large amount of mass in the building. Because the results in Table 3 represent the minimum in weather prediction, results for a real system will be between those in Tables 2 and 3.

IMPLEMENTATION

In order to implement one of the optimal control strategies for the quadratic objective function, a good deal of computational ability must be available because a set of six differential equations must be solved numerically several times. Approximations to these strategies, however, are possible. The constant control weighted inversely with the rate structure is close to the optimal control and easily determined once an estimate of the energy requirement for the next day is made. The minimum cost cntrol is also easily implemented in a like manner. Regardless which control is used, some form of weather prediction is required.

CHAPTER III

SYSTEMS WITH ISOLATED STORAGE

In the previous chapter, the storage in the system is in thermal contact with the conditioned space. In this chapter, the systems are all characterized by a storage which is isolated from the living space and control is maintained by turning a circulating pump on or off. Because storage is isolated, its characteristics are not very important in control determination.

INTRODUCTION

Several heating, ventilating, and air conditioning (HVAC) systems have come into use recently which are intended to reduce the cost of space heating or cooling using electrical energy. Solar heating systems decrease the overall energy requirement, and off-peak energy storage systems move the energy requirement to a low demand time of day. Unfortunately, the use of these systems does not always result in the desired impact on the utility. For example, when the available energy in an off-peak energy storage system is depleted, a high electric power requirement is imposed on the utility because the auxiliary heating system must satisfy the entire load. If this depletion occurs while the overall utility demand is high, an undesireable situation has developed. The utility must maintain the capacity necessary to satisfy this peak load, regardless of how infrequently it should occur. The purpose of this study is to develop control strategies for these heating systems which will ensure that their use will have a favorable impact on both the consumer and the utility.

Methods of dynamic optimization are applied in order to determine improved control strategies. The improved control strategies are then evaluated using a computer program developed for the Electric Power Research Institute (EPRI) by Arthur D. Little, Inc. The program, "EPRI Methodology for Preferred Solar Systems" (EMPSS), performs detailed simulations of the thermal performance of buildings with various heating systems. In addition, the program uses the results of the simulation to estimate the cost of electric energy from a particular utility's actual cost of supply [5]. EMPSS was modified locally to accept the different improved control strategies.

SYSTEM DESCRIPTIONS

There are four residential heating systems considered in this chapter. The four systems are a baseline heating and cooling system, an off-peak storage system, a solar heating system, and a combination solar heating and off-peak storage system. Each system is used to satisfy the space heating and cooling and domestic water requirement of the residence with back up, as required, provided by electric resistance heat or vapor compression cooling. Schematic diagrams for the systems are shown in Figure 7. The residence for each system is a well insulated single story dwelling with an attic. Because of the long lead time required for decisions made by utilities, the impact of each of the heating systems is determined for the year 1990. The analyses are conducted using data representative of the Albuquerque utility service area.

The baseline system provides heat to the residence via a duct mounted electric resistance heater. The energy is distributed by forced air. Cooling is provided by a central vapor compression air conditioner. The system is controlled by a room thermostat. The baseline system is used to provide a basis for comparison for the other systems.

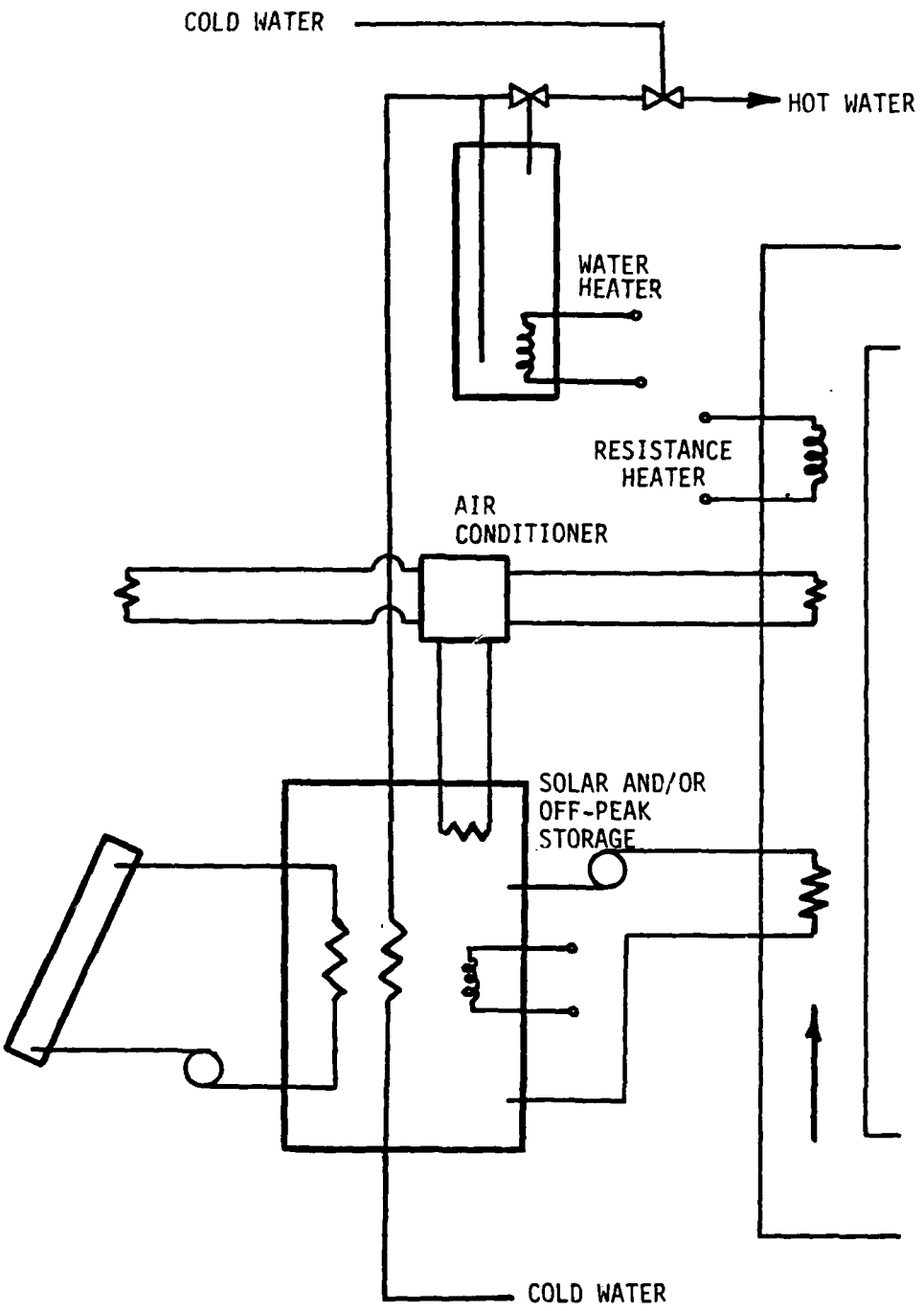

Figure 7. Schematic of Solar and/or Off-Peak Storage Systems.

The off-peak storage heating and cooling system is composed of a 3785 liter (1000 gallon) storage tank and a 250 Watt circulating pump. The conventional operating strategy is to heat or cool the water to some previously determined temperature when the utility's off-peak period begins and then, during the utility's on-peak period, to satisfy the heating or cooling and domestic hot water load by circulation of storage water through a duct mounted heat exchanger until the storage has reached some limiting temperature.

The solar heating system is liquid based. There are 14 square meters (150 sq. ft.) of collector area. The collectors are single glazed and have a selective surface. The storage tank contains 1135 liters (300 gal.) of water. The conventional strategy is to satisfy the heating load by circulating the hot water through a duct mounted heat exchanger whenever the storage temperature is above some set minimum. Cooling is provided by vapor compression air conditioning with no cool storage.

The combined off-peak and solar heating system is identical to the solar heating system except that a heater is added to the tank. The storage tank is heated to some previously determined temperature at the beginning of the utility's off-peak period.

ELECTRICAL COST OF SUPPLY

The purpose of this study is to develop control strategies for the above-mentioned systems which will ensure a favorable impact on the consumer and the utility. The impact on the utility is determined using the utility's cost of supply. The utility's cost of supply is used instead of utility rates because rates do not always accurately reflect true costs. A control strategy which is based on an imperfect rate structure may result in an unnecessarily high real

cost. In addition, any savings to the utility will ultimately find their way to the consumer.

In this study, the utility's cost of supply is composed of energy and capacity related costs. Energy related costs are comprised mainly of the costs of fuel, taking into account the efficiencies of the generating units needed to satisfy the systemwide load. Energy costs generally increase with systemwide load but are essentially independent of the power draw at the residence. Capacity related costs are composed of the various costs associated with owning and maintaining generating equipment. In this study, the capacity related costs are charged whenever the residence has an electric power draw coincident with the utility's on-peak period. This coincident demand charge is either zero (off-peak) or some number of dollars per kilowatt (on-peak). The total cost of supply as determined by EMPSS is the sum of the energy costs and the coincident demand charges.

The cost of supply resulting from the operation of a particular heating or cooling system in a particular building will depend not only on the building load but also on the particular make up of the utility serving the residence. For example, a utility which uses a large amount of natural gas will incur much higher energy costs than one with a large amount of hydroelectric generating capability. For this reason EMPSS has the capability to accept data which describe the expected systemwide load with variability due to weather, fuel costs, and coincident demand charges which are applicable to a particular utility. For this study, data representative of the Public Service Company of New Mexico (Albuquerque) for 1990 were used [3]. The methodology for the computation of the cost of supply is illustrated in Figure 8.

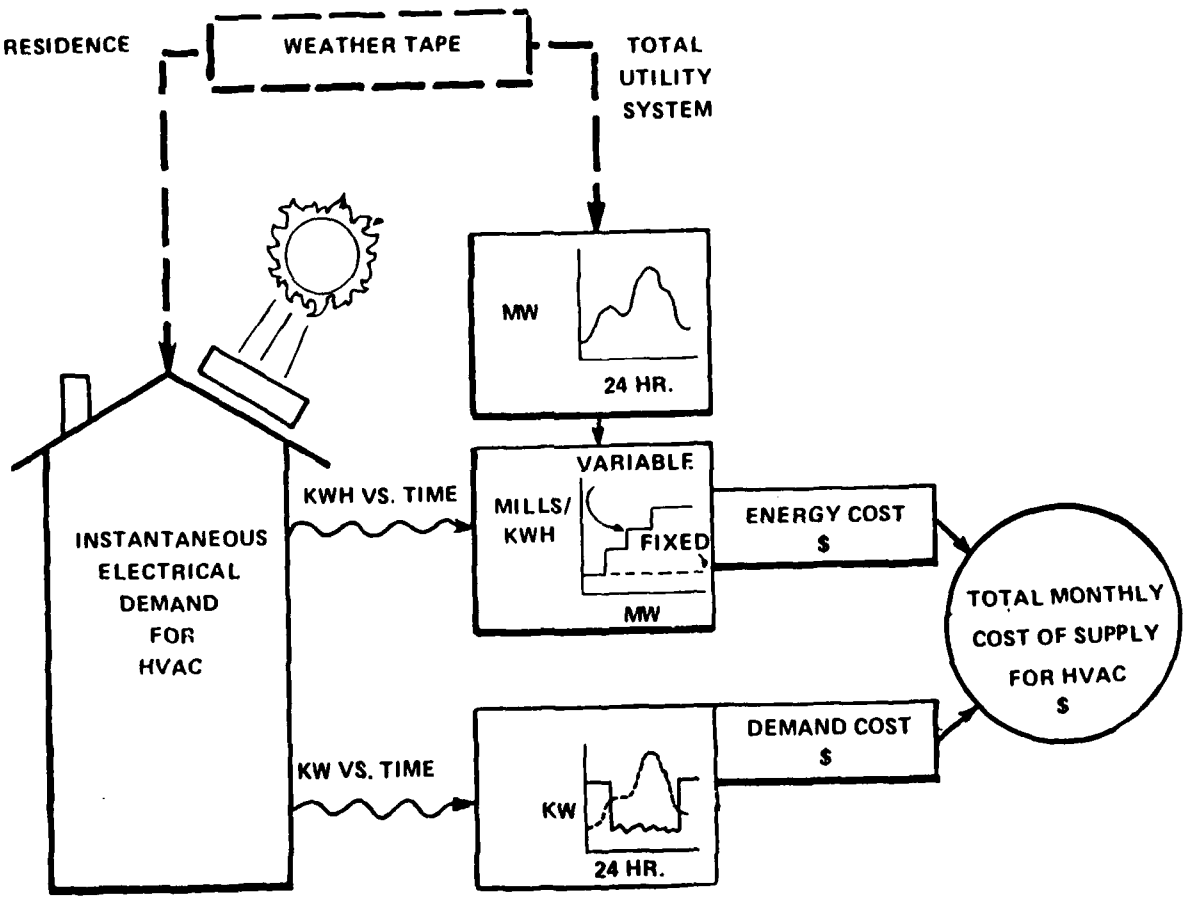

Figure 8. Cost of Supply Methodology. (Abstracted from Ref. [5])

CONTROL STRATEGIES

The conventional strategy for energy discharge from off-peak or solar storage is to use the energy as required to satisfy the load until the temperature in storage reaches some limiting temperature. The problem with this strategy is that, if the available energy in storage is depleted before the end of the utility high demand period, a very large coincident demand may result. This is illustrated in Figure 9, which shows the HVAC electrical demand for a residence in Albuquerque, New Mexico, for the day on which the utility experiences its maximum systemwide load for the heating season. The available internal energy from storage has been depleted by 2000 hours and there is a resulting electrical demand of approximately 9kW at the residence at that time. The fuel cost of supply for energy provided by the utility on that day is shown in Figure 2. The residential demand, shown on Figure 9, is quite large at the same time that the cost of supply, shown on Figure 2, is high. Clearly the use of the off-peak storage system with conventional control has not led to much of a decrease in the generation capabilities required of the utility. An improved control strategy can significantly reduce the coincident demand and consequently reduce the maximum power required of the utility.

To determine the best control strategy for the discharge of off-peak or solar storage, the methods of dynamic optimization may be employed. The optimization problem is formulated to determine the on-peak power draw to minimize

$$J = \int_{t_o}^{t_f} [\dot{Q}_{on-peak}(t)]^2 dt \tag{12}$$

subject to the dynamic equations of the enclosure and the storage,

$$C_e dT_e/dt = \dot{Q}_{on-peak} + \dot{Q}_{st} - \dot{Q}_{load}$$

$$C_s dT_s/dt = \dot{Q}_{sol} - \dot{Q}_{st} - \dot{Q}_{loss}$$

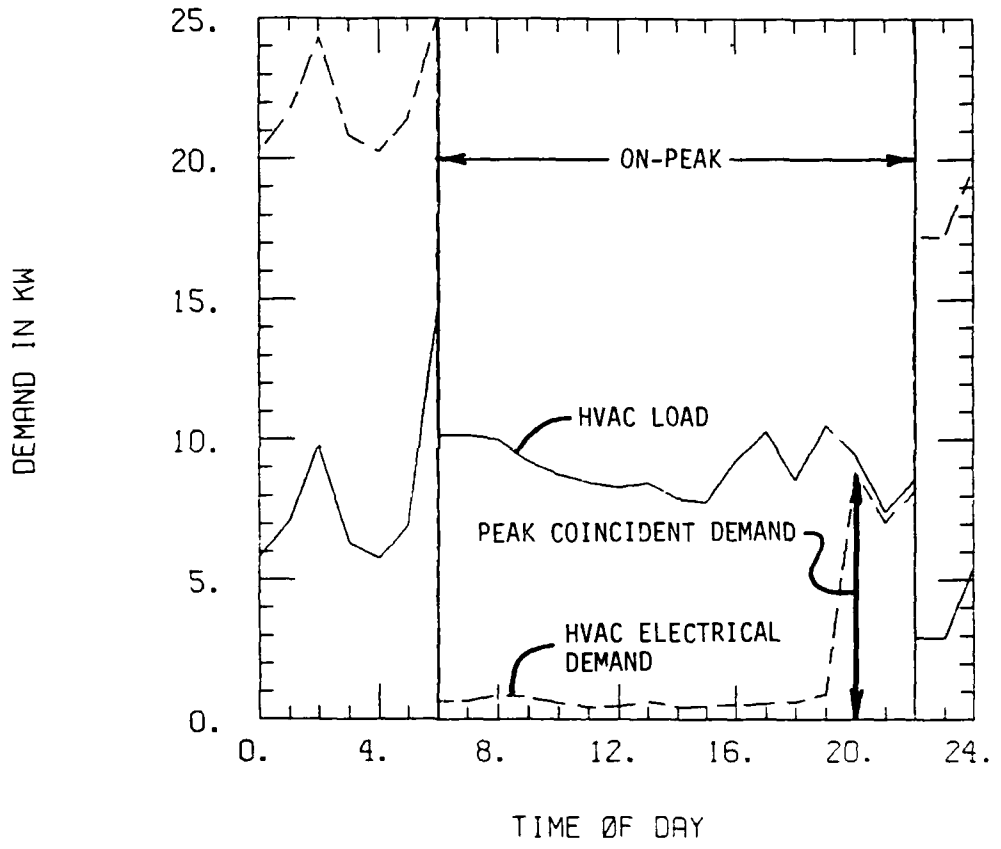

Figure 9. Conventional Strategy for Off-Peak Storage on January 14.

where

t_o is the current time

t_f is the time at the end of the on-peak period

C_e is the thermal capacitance of the storage, kJ/^oC (Btu/^oF)

T_e is the enclosure temperature, ^oC(^oF)

C_s is the thermal capacitance of the storage, kJ/^oC(Btu/^oF)

T_s is the storage temperature, ^oC(^oF)

$\dot{Q}_{on-peak}$ is the on-peak resistance heat rate, kJ/hr (Btu/hr)

$\dot{Q}_{st}$ is the rate of energy removal from storage, kJ/hr (Btu/hr)

$\dot{Q}_{sol}$ is the rate of supply of solar energy to storage kJ/hr (Btu/hr)

$\dot{Q}_{load}$ is the heating load, kJ/hr (Btu/hr)

$\dot{Q}_{loss}$ is the rate of energy loss from storage, kJ/hr (Btu/hr).

Minimizing J will minimize the product of coincident demand ($\dot{Q}_{on-peak}$) and on-peak energy consumption ($\dot{Q}_{on-peak}dt$) while satisfying the dynamic equations which describe the thermal performance of the residence and the storage. The dynamic equations used in this problem formulation assume a well-mixed storage and a uniform (but not constant) enclosure temperature. EMPSS, and most other detailed simulations, use a much more elaborate system of equations, but the purpose of those simulations is to provide accurate load and temperature histories. The purpose of this optimization problem is to develop an analytical expression for the optimal control, and, as such, the dynamic equations above are quite adequate. Once the optimal control strategy is determined, it may then be programed into the more detailed EMPSS simulation to determine its effect on system performance and cost.

Several reasonable assumptions make this a very straight-forward problem to solve. First, in a well designed system, the storage losses are small and

can safely be ignored in formulating a control strategy. Second, the enclosure temperature is held nearly constant during the on-peak period by the thermostat in the enclosure. Certainly, when diversity is considered, the utility sees the enclosure temperature as constant, and, therefore, the time derivative of enclosure temperature is effectively zero. Third, the boundary conditions on the storage temperature can be specified. The storage temperature at t_o is the current temperature. If the current time is the beginning of the on-peak period, the storage temperature is the predetermined charging temperature which is determined by reasonable design practice or by an optimization of the charging process. The charging process is independent of the depletion process and is not covered in this study. The temperature at t_f is the temperature, $T_{s,min}$, below which the pump is deactivated. With these assumptions, the problem is now solved using Pontryagin's Maximum Principle. The resulting optimal discharge rate is

$$\dot{Q}_{st}^{*} = \dot{Q}_{load} - \overline{\dot{Q}}_{load} + \overline{\dot{Q}}_{sol} + C_s(T_s - T_{s,min})/(t_f - t_o) \tag{13}$$

where the overbar indicates the average over the entire on-peak period. When discharge from cool storage is considered, the optimal control is

$$\dot{Q}_{st}^{*} = \dot{Q}_{load} - \overline{\dot{Q}}_{load} + C_s(T_{s,max} - T_s)/(t_f - t_o) \tag{14}$$

where $T_{s,max}$ is the temperature above which the circulating pump is disabled. The complete derivation of these optimal control strategies, including the effect of storage losses, is presented in Appendix B.

Implementation of either strategy requires a knowledge of the current heating or cooling load, the total load during the on-peak period, and, in the case of solar heating, the total amount of solar energy delivered to storage during the on-peak period. This is a difficult task to achieve; however, some approximations to the optimal control strategy are easily determined by

approximating the load and the solar energy collection. For example, if the load is modeled as constant throughout the on-peak period and it is assumed that no solar energy will be collected, the approximation to the optimal discharge from hot storage is

$$\dot{Q}_{st} = C_s(T_s - T_{s,min})/(t_f - t_o). \quad (15)$$

This approximation is called the proportional discharge because the energy in storage is proportioned equally throughout the on-peak period. If an approximation for the load other than constant is used, a weighted proportional discharge strategy results. It is called weighted proportional because a larger storage discharge rate is allowed when the load is expected to be high. For an example of the development of a weighted proportional strategy for discharge from cool storage, see Appendix C.

SIMULATION RESULTS

The performance of the selected systems under the various control strategies was compared using the EMPSS computer program. All of the simulations used weather and utility data applicable to Albuquerque in 1990. The optimal strategy was implemented in the simulation by saving the heating and cooling loads and the solar energy collection rates which were calculated by EMPSS and then this information was used to calculate the optimal control. This is not a practical implementation procedure, but it provides an upper limit on the performance of the different systems against which the performance under conventional and proportional control can be compared.

A. Off-Peak Storage Heating And Cooling System

The peak HVAC coincident demand for the peak heating months (December, January and February) and the associated costs of supply that result from using conventional, proportional and optimal discharge of off-peak storage for

the entire year of 1990 are presented in Table 4. The proportional strategy reported on in this section is the proportional strategy for heating and the weighted proportional strategy for cooling. The peak coincident demand information is presented only for the heating season because the peak heating demand is about three times as large as the peak cooling demand. The cost information presented in Table 4 represents annual cost, that is, heating and cooling costs. For comparison, the results for the baseline heating and cooling system are also shown.

The use of proportional or optimal control reduces the peak coincident demand relative to the conventional control in each month except December. In December, the total on-peak heating load never exceeded the energy storage capacity so the system performances are identical, regardless of control strategy. The use of the optimal strategy, as expected, results in the best system performance; however, the performance is only slightly better than if proportional control were used.

Implementation of the optimal control strategy requires a knowledge of the current instantaneous heating load and the load for the rest of the on-peak period. For a typical day, these terms can be estimated quite well by using a best fit of weather data procedure; however, the monthly peak coincident demand does not occur on a typical day. The monthly peak coincident demand occurs on the day that has the largest heating load during the on-peak period. An analysis of the Albuquerque weather shows that these "worst" days have temperatures which are nearly constant all day long. Therefore, a best fit of weather data will not be adequate to accurately predict the building loads on the "worst" days. On these "worst" days, the building HVAC load is nearly constant all through the on-peak period. Therefore, on the "worst" days, the

Table 4. Off-Peak Storage Discharge Strategy Comparisons.

		Off-Peak Storage System		
	Baseline Heating System	Conventional Strategy	Proportional Strategy	Optimal Strategy
December Peak HVAC Coincident Demand	7.28 kW	.63 kW	.63 kW	.63 kW
January Peak HVAC Coincident Demand	13.32 kW	12.61 kW	5.59 kW	3.60 kW
February Peak HVAC Coincident Demand	12.32 kW	10.33 kW	4.69 kW	3.49 kW
HVAC Coincident Demand Annual Cost of Supply in 1990 Dollars and % of Baseline	$2551 100%	$1340 53%	$783 31%	$658 26%
HVAC Fuel Annual Cost of Supply in 1990 Dollars and % of Baseline	$1396 100%	$979 70%	$913 65%	$909 65%
HVAC Total Annual Cost of Supply in 1990 Dollars and % of Baseline	$3946 100%	$2319 59%	$1697 43%	$1567 40%

optimal control would be expected to perform much like the proportional control; this is confirmed by the results in Table 4.

Figures 9, 10, and 11 depict the HVAC load and electrical demand required to satisfy that load for conventional, proportional, and optimal control, respectively, on January 14. January 14 was the day on which the highest utility load for the entire heating season occurred. The use of the conventional strategy results in a large coincident demand at 2000 hours because storage was depleted before the end of the on-peak period. The use of proportional discharge from storage ensures that energy will be left in storage for use at the end of the on-peak period so no large coincident demand occurs. The same is true of the optimal control. Proportional control is a good approximation to optimal control for this heating system because both have relatively constant on-peak HVAC elecrical demand curves. Because of the difficulty in actually implementing the optimal strategy and the excellent system performance under the proportional strategy, the recommended strategy for the discharge from storage for heating is the proportional discharge strategy.

For the discharge from cool storage, the proportional strategy does not result in system performance that is much like the performance when optimal control is used. The reason that the proportional strategy is not a good approximation to the optimal strategy is that, on the "worst" days of the cooling season, the cooling load varies widely throughout the day, reaching a maximum at about 1800 hours. A much better approximation to the optimal strategy is obtained by assuming a cooling load profile for the entire on-peak period of the "worst" day, which is typically a very hot, sunny day. The cooling load on these days is usually low in the morning hours, increases until about

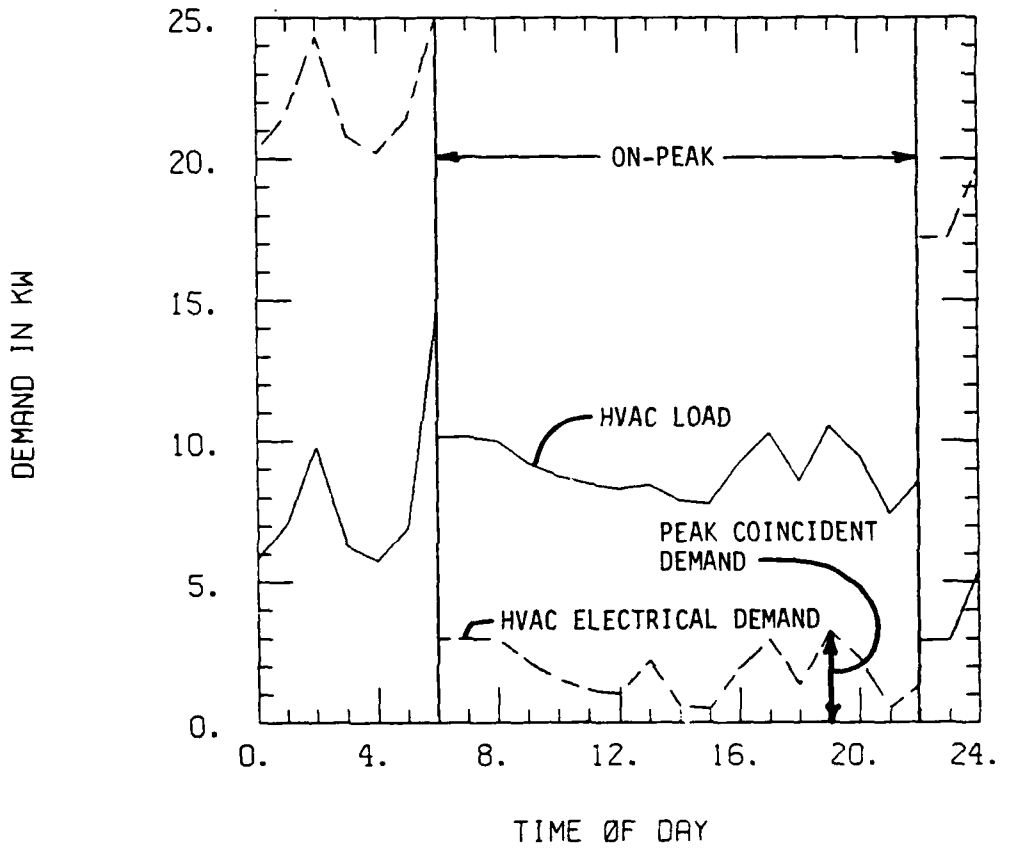

Figure 10. Proportional Strategy for Off-Peak Storage on January 14.

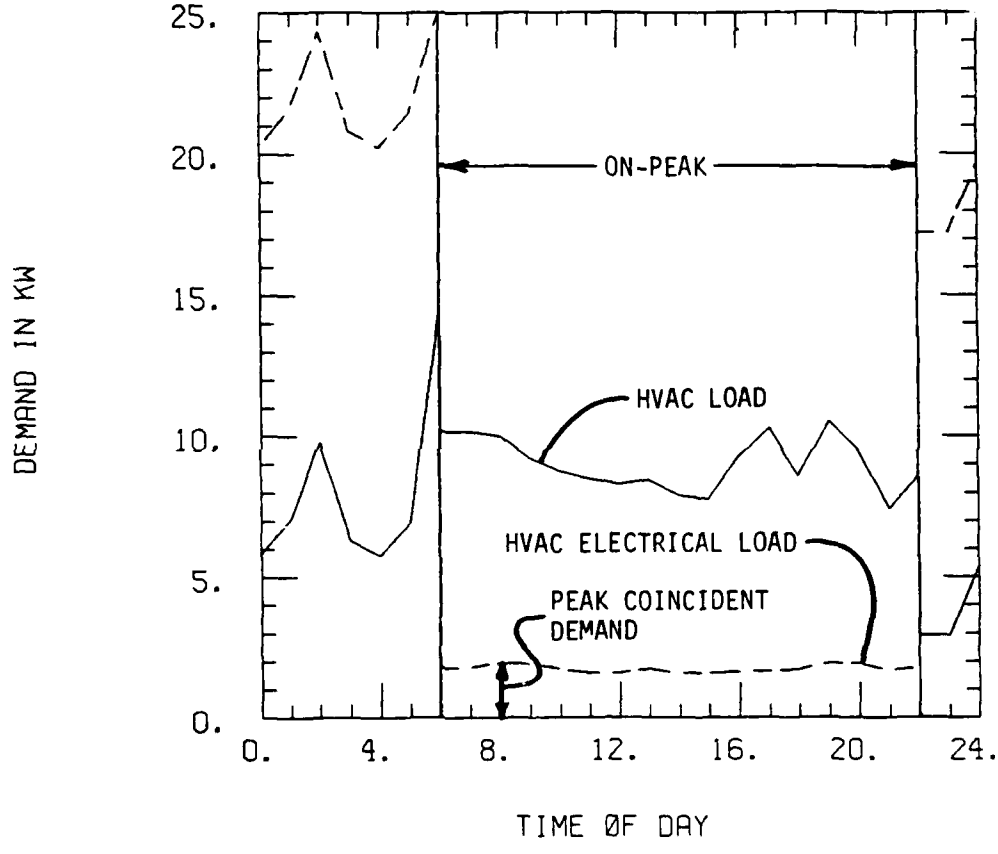

Figure 11. Optimal Strategy for Off-Peak Storage on January 14.

1800 hours, and then decreases thereafter. This load profile is easily modeled using a sine wave which is then used in the equation for the optimal discharge rate to obtain a weighted proportional discharge strategy. The development of a weighted proportional discharge strategy is presented in Appendix C.

Cooling system performance is depicted in Figures 12 through 15 for systems using conventional, proportional, weighted proportional, and optimal discharge from storage, respectively. The day for which Figures 12 through 15 were generated was the Albuquerque utility's peak load day for the summer. In each figure, the HVAC electrical load and the electrical demand required to satisfy that load are presented. The HVAC load is the electrical load which would be required if no storage were present. Using conventional discharge (Figure 12), the storage is depleted before the end of the on-peak period and a large coincident demand occurs. The use of proportional discharge (Figure 13) reduces the peak coincident demand but it is still rather large. The use of the weighted proportional discharge (Figure 14) reduces the peak coincident demand still further. For comparison, the performance of the system when optimal discharge is used is presented in Figure 15.

For the entire year, the greatest improvement in performance over the conventional strategy was achieved by proportional control in January; however, any time the storage is not sufficient to meet the heating or cooling load, some reduction in coincident demand is expected using the improved control strategies. During the spring and fall the heating and cooling load is so small and the storage so large that any strategy will satisfy the entire on-peak load.

The optimal discharge from storage resulted in the best system performance, but implementation of that control requires exact knowledge of

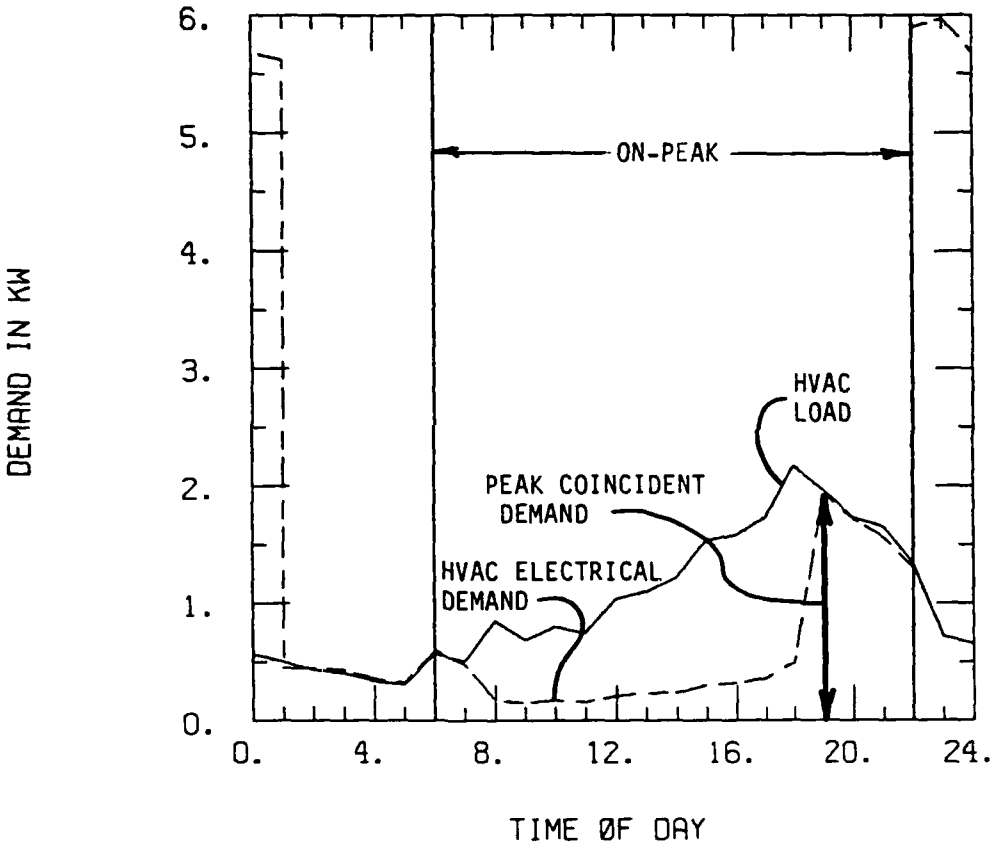

Figure 12. Conventional Strategy for Off-Peak Storage on July 26.

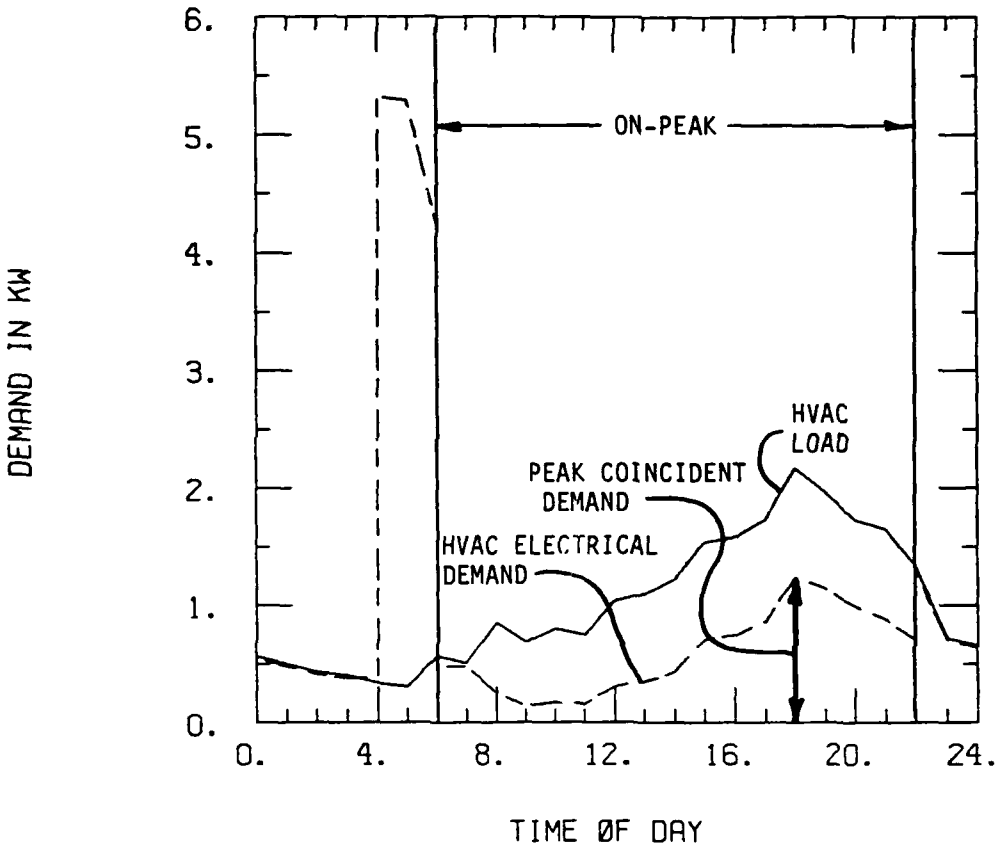

Figure 13. Proportional Strategy for Off-Peak Storage on July 26.

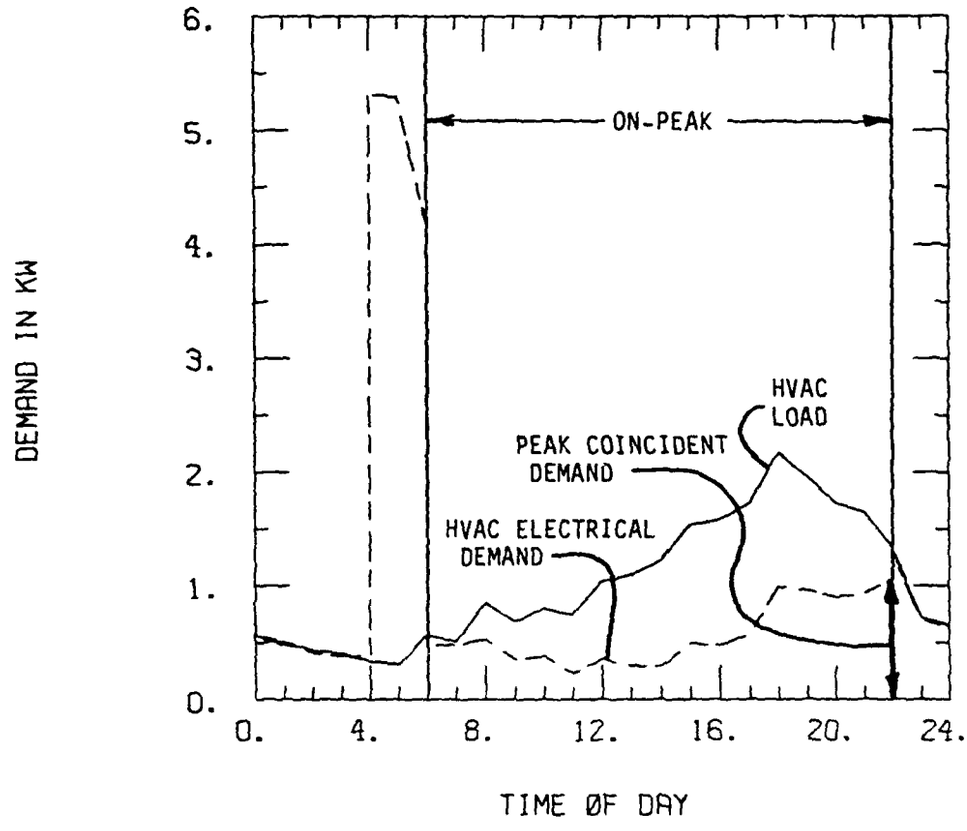

Figure 14. Weighted Proportional Strategy for Off-Peak Storage on July 26.

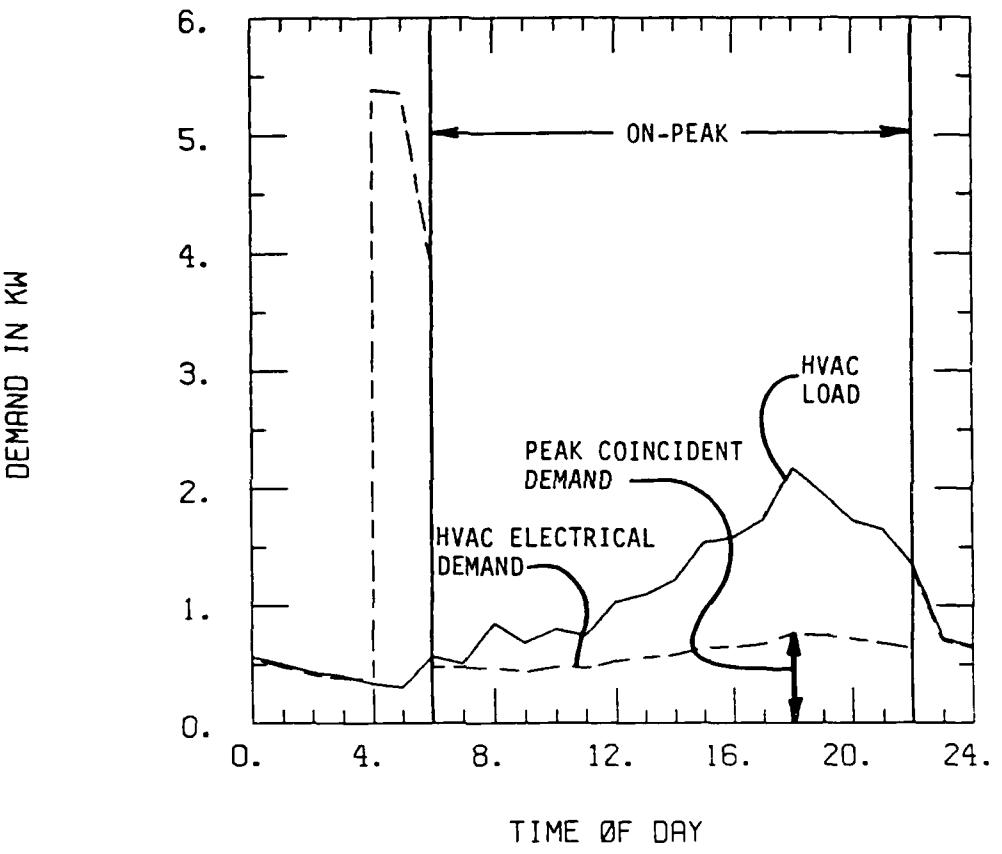

Figure 15. Optimal Strategy for Off-Peak Storage on July 26.

the heating or cooling load for the upcoming day. Implementation of the proportional or weighted proportional strategy, on the other hand, does not require any load prediction capability. If relatively accurate load prediction were available, one would expect the system to perform between the above two cases. To determine how accurate the load prediction must be in order to improve upon the performance of the proportional or weighted proportional strategy, simulations were performed with known errors in the loads used to determine the control. A specified error was assigned to each hourly load using a Bernoulli distribution. The results of the year long simulations are presented in Figure 16. The use of proportional discharge for heating and weighted proportional for cooling corresponds to a load prediction error of about 17 percent. By contrast, using yesterday's loads as today's is equivalent to a load prediction error of 28 percent. Rather sophisticated load prediction is required to improve upon the performance of the proportional or weighted proportional control.

The widespread use of proportional or weighted proportional discharge of off-peak storage will have a significant impact on the utility. An assessment of this impact was made assuming that 66,000 new homes would be built in the Albuquerque service area from 1981 to 1990. The impact is summarized in Table 5 which presents the cumulative impact of the use of many off-peak storage heating and cooling systems. The impact is based on the assumption that the off-peak storage systems replace conventional resistance heating and vapor compression cooling systems. In Table 5, Delta Energy is the net change in the energy consumption resulting from use of the system for one year. This term is positive because off-peak storage systems use more energy than conventional systems. The Delta Cost values presented are in millions of 1990

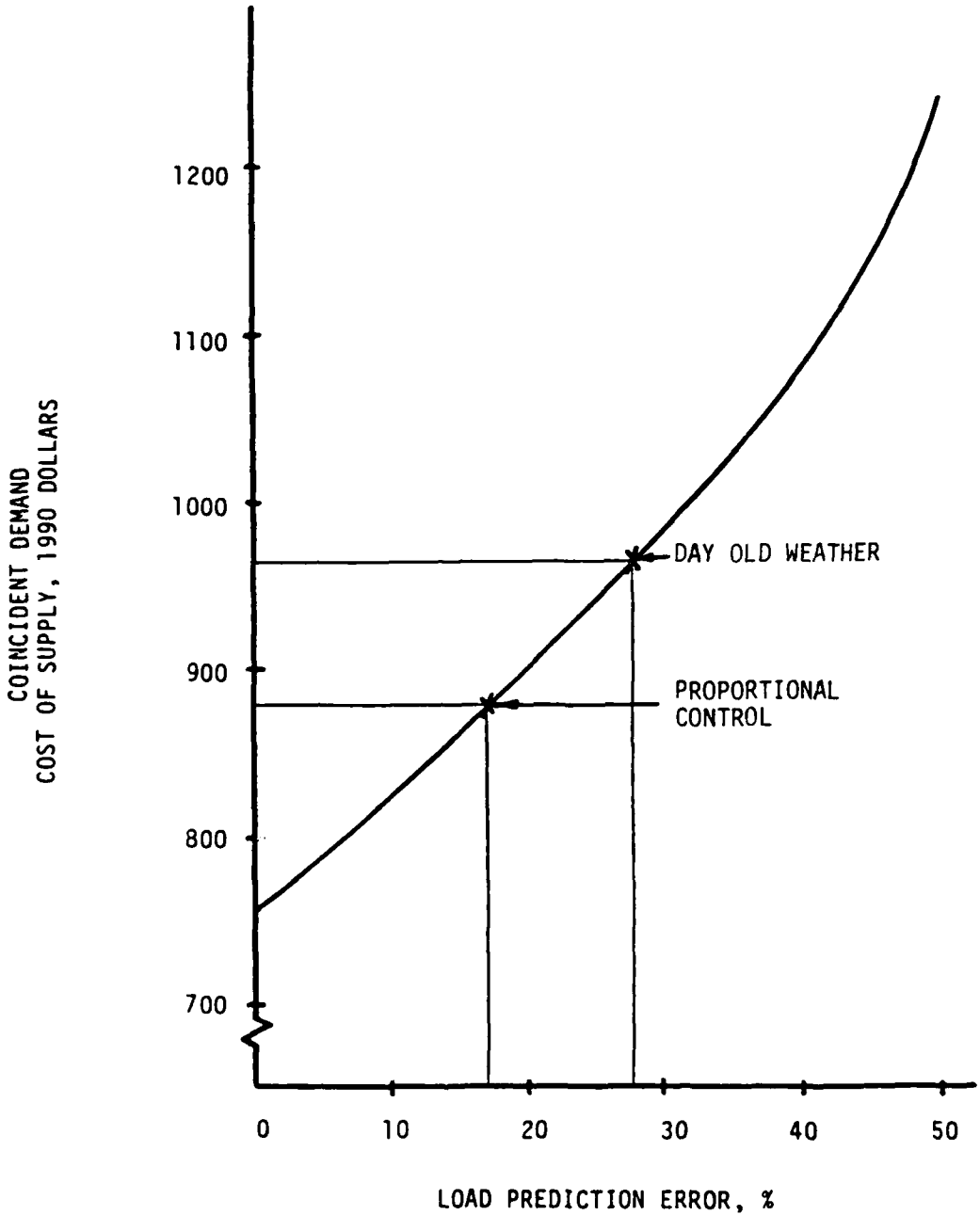

Figure 16. Influence of Load Prediction Error on Coincident Demand Cost of Supply.

Table 5. Utility Impact Assessment.

Market Saturation	Delta Energy, MWh	Delta Demand Cost	Delta Fuel Cost	Delta Cost of Supply	Delta Demand Peak, MW
100%	35,100	-117	-32	-147	-61
50%	17,600	-58	-16	-74	-31
25%	8,800	-29	-8	-37	-15

Note: Costs are in Millions of 1990 Dollars.

dollars. The negative values indicate annual savings. The Delta Demand Peak is the change in the utility demand at the hour of the annual peak utility demand. The annual peak utility demand time is determined before the off-peak systems were included.

The information presented in Table 5 was generated assuming linear relationships between market saturation and the quantities listed. This relationship may not be linear. In fact, in January in Albuquerque, for market saturations beyond 16 percent, the systemwide load has a peak a night. Any increases in market saturation beyond 16 percent will increase the systemwide load even though the daytime load continues to decrease.

The effect that the use of many off-peak storage systems has on the systemwide load curve on the peak load days is shown in Figures 17 through 20. In Figure 17, the solid line is the expected load curve for the peak load day in January; the dashed line is the load curve if 16 percent of the new homes use off-peak storage with the conventional discharge strategy. Notice that the two curves are identical for the last few hours of the on-peak period. The change in the utility load curve if 16 percent of the new homes use proportional discharge of off-peak storage is presented in Figure 18. The demand at the end of the on-peak period is significantly reduced. A market saturation of 16 percent gives the most uniform load curve. The changes in the systemwide load curve for the peak load day in July are presented in Figure 19 and 20 for conventional and weighted proportional discharge of cool storage. The dashed line represents the load curve if 100 percent of the new homes used cool storage. Again, the weighted proportional strategy reduces the demand at the end of the on-peak period. The impact on the utility is smaller for cooling than for heating because the demand for each house is smaller for cooling than for heating.

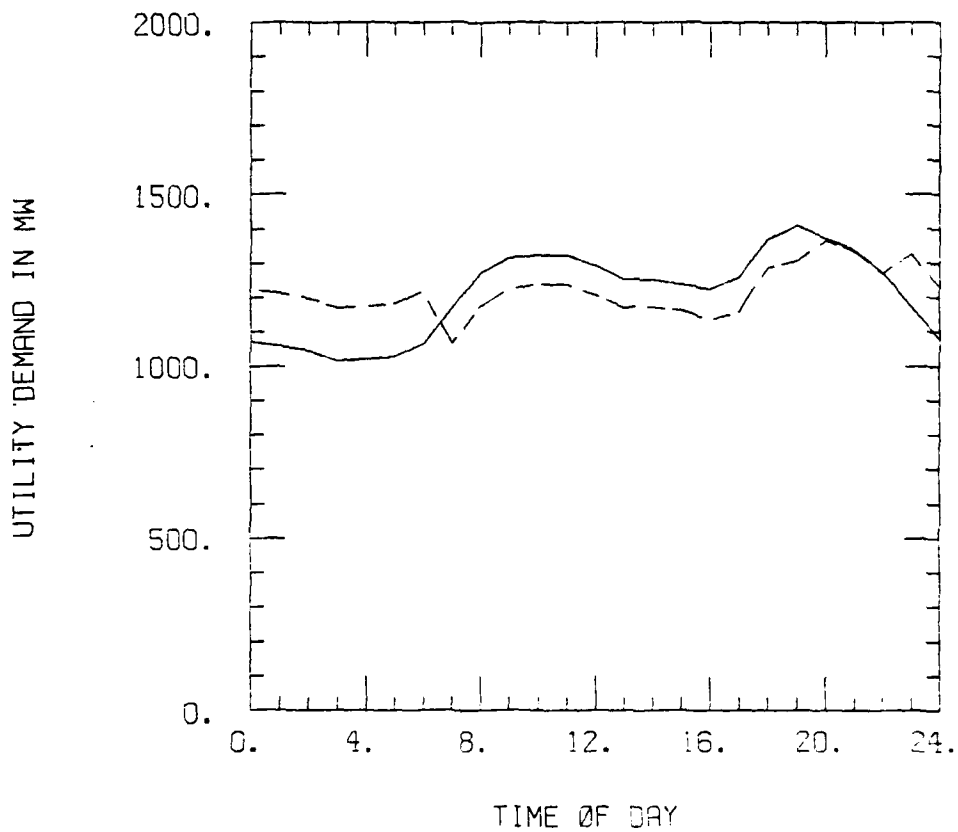

Figure 17. January Peak Day Utility Impact Due To 16% Saturation of Off-Peak Storage Systems With Conventional Discharge.

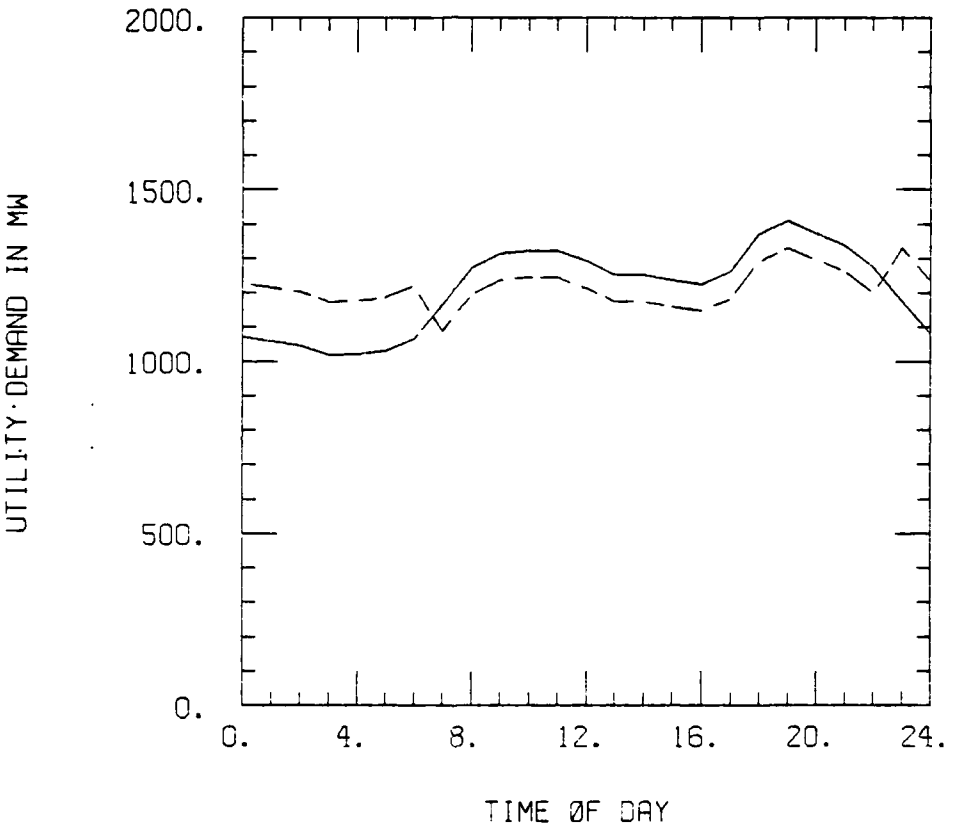

Figure 18. January Peak Day Utility Impact Due To 16% Saturation of Off-Peak Storage Systems With Proportional Discharge.

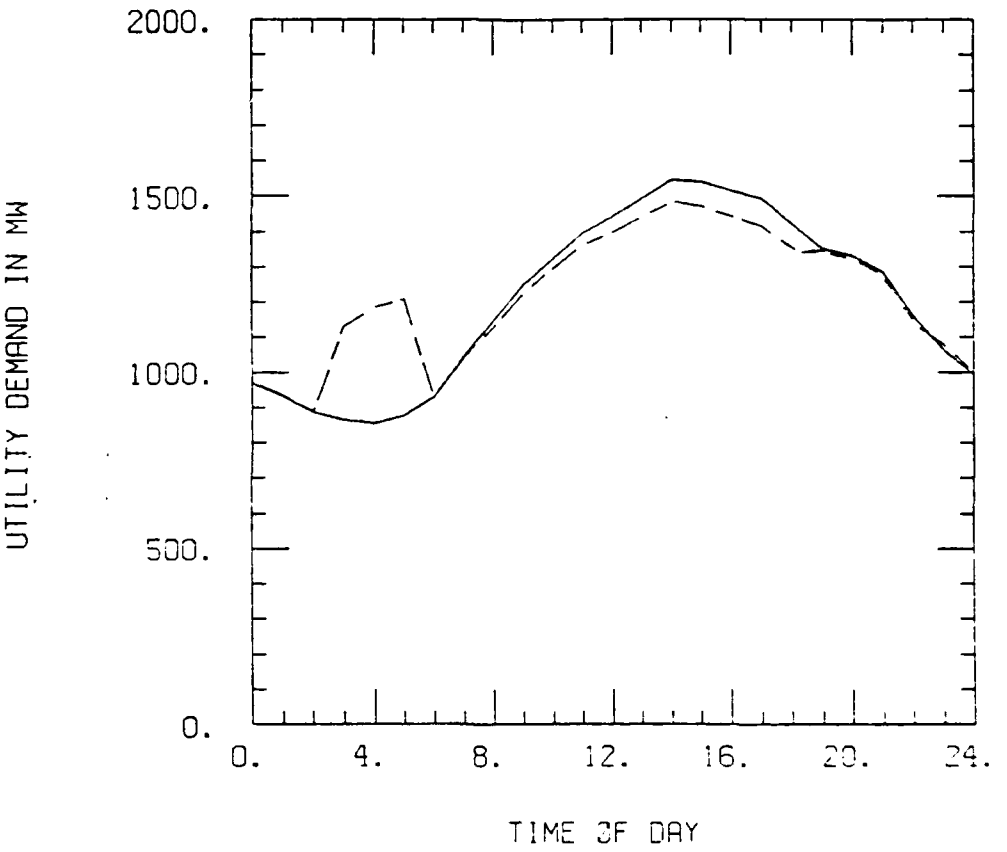

Figure 19. July Peak Day Utility Impact Due To 100% Saturation of Off-Peak Storage Systems With Conventional Discharge.

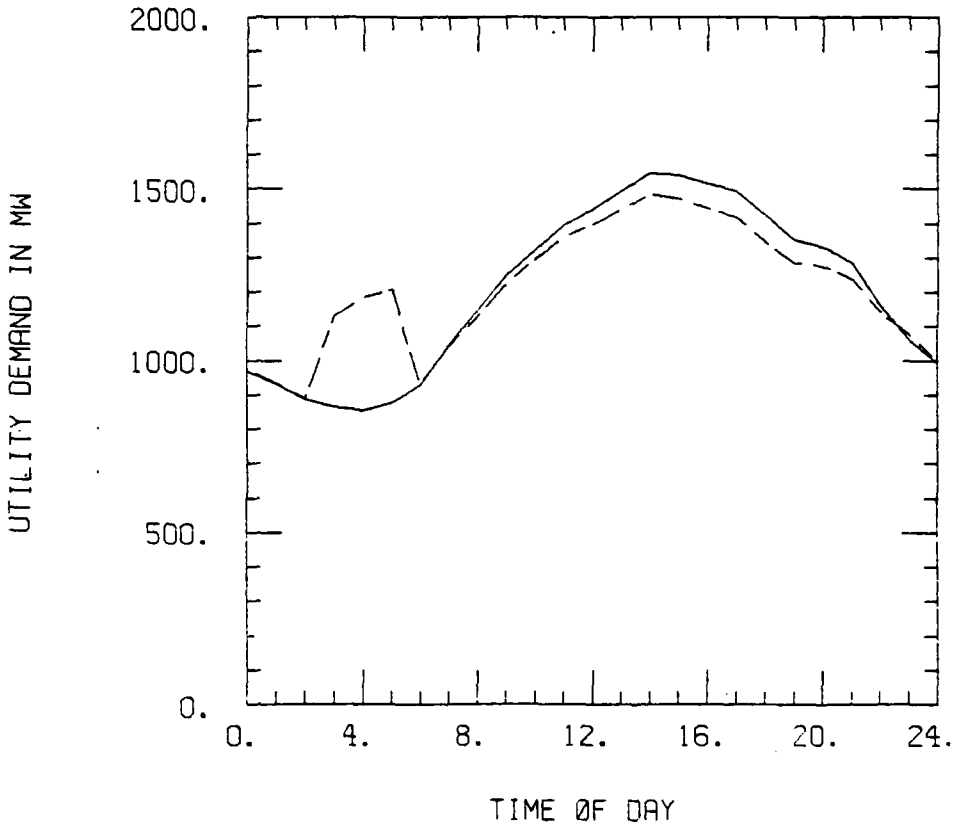

Figure 20. July Peak Day Utility Impact Due To 100% Saturation of Off-Peak Storage Systems With Weighted Proportional Discharge.

B. Solar Heating System

The conventional strategy for the discharge of solar storage is to use energy from storage if it is available, and, as a result, little thought has been given in the past to control strategies designed to reduce coincident demand. The optimal control strategy described by equation (13) is designed to reduce coincident demand. For a solar heating system, the proportional discharge strategy is a good approximation to this optimal control because of the characteristics of the utility's "worst" day as described earlier.

There are two variations to this proportional discharge strategy which are considered in this study. In variation one, if energy is available, it is discharged from storage during the off-peak period. In variation two, no energy is dicharged during the off-peak period. Variation two is designed to keep more energy available for on-peak use. Simulations were performed comparing these two variations of the proportional control. The systems which were simulated for this comparison had their cooling systems disabled so the costs were for heating only. The use of variation one resulted in an annual coincident demand cost of supply of $1809 compared to $1704 for variation two. This decrease in coincident demand cost results from the fact that variation two causes more energy to be available for on-peak use. The fuel cost of supply was $648 with 9808 kWh of solar energy collected when variation one was used. For variation two, the fuel cost of supply was $637 with 9238 kWh of solar energy collected. By having more energy available for on-peak use with variation two compared to variation one, the average storage temperature is higher and, therefore, less solar energy is collected. However, the fuel cost of supply does not necessarily decrease as more solar energy is collected. The cost of fuel depends on the overall utility demand at the time of use as shown

earlier in Figure 2. Because the use of variation two causes the collected solar energy to be saved for use only during the on-peak period, it replaces only expensive energy. For that reason, even though less solar energy is collected and more electrical energy is required, the fuel cost of supply is lower for variation two. Because of the overall better performance when variation two is used, for the remainder of this study, the proportional discharge strategy for solar storage refers to proportional control without off-peak use of energy in storage.

The conventional, proportional, and optimal discharge strategies for the utility's peak winter load day are depicted in Figures 21, 22 and 23. The conventional strategy results in a very low electrical demand during the middle of the day. Comparison of the HVAC electrical demand in Figure 17 with the utility fuel cost in Figure 2 shows that the solar contribution occurs at a low utility demand time of day. In fact, the characteristics of the heating system under conventional control tend to accentuate the difference between the "peaks" and "valleys" on the utility load curve. The proportional and the optimal discharge strategies reduce the afternoon peak electrical demand. The peak coincident demand still occurs in the morning because there is little energy in storage at the beginning of the day. It is not until some energy has been collected that differences in the discharge strategies can be seen. It should be noted that January 14 happened to be a sunny day. If January 14 were a cloudy day, all three strategies would have appeared to be identical.

The results of simulations of a solar heating system with conventional, proportional and optimal control are presented in Table 6. In January, the peak coincident demand is reduced significantly by using proportional or optimal control, but the same is not true in December and February. The reason for the

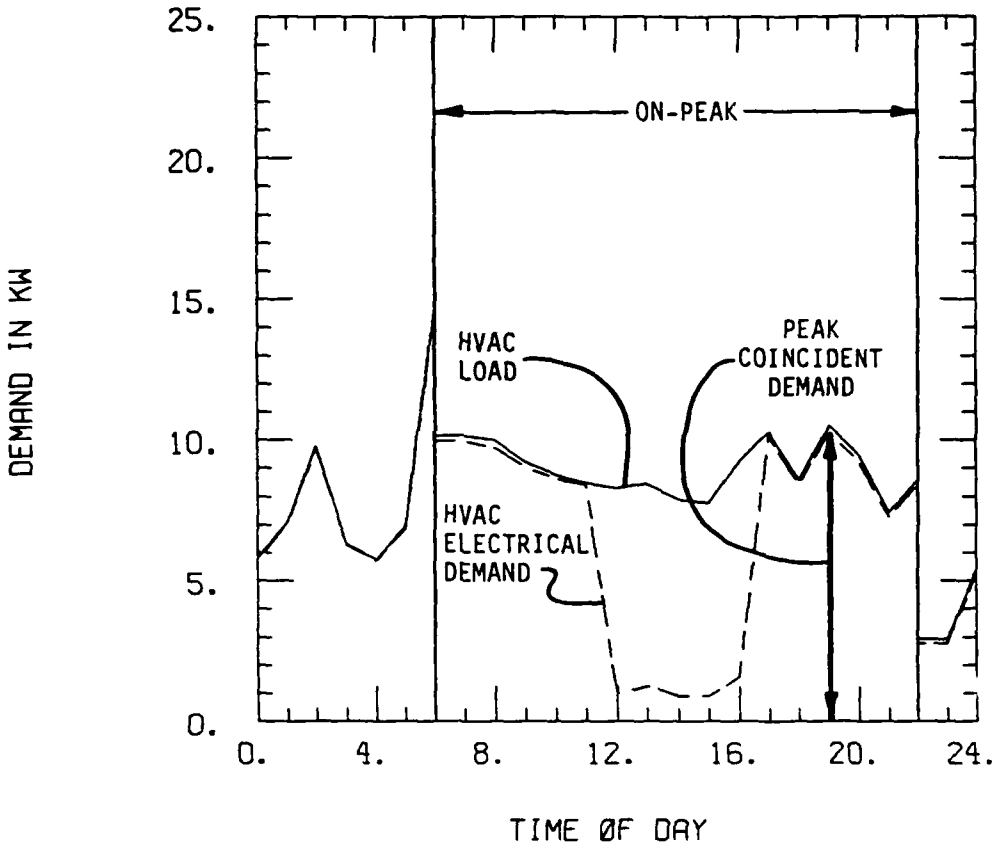

Figure 21. Conventional Strategy for Solar Storage on January 14.

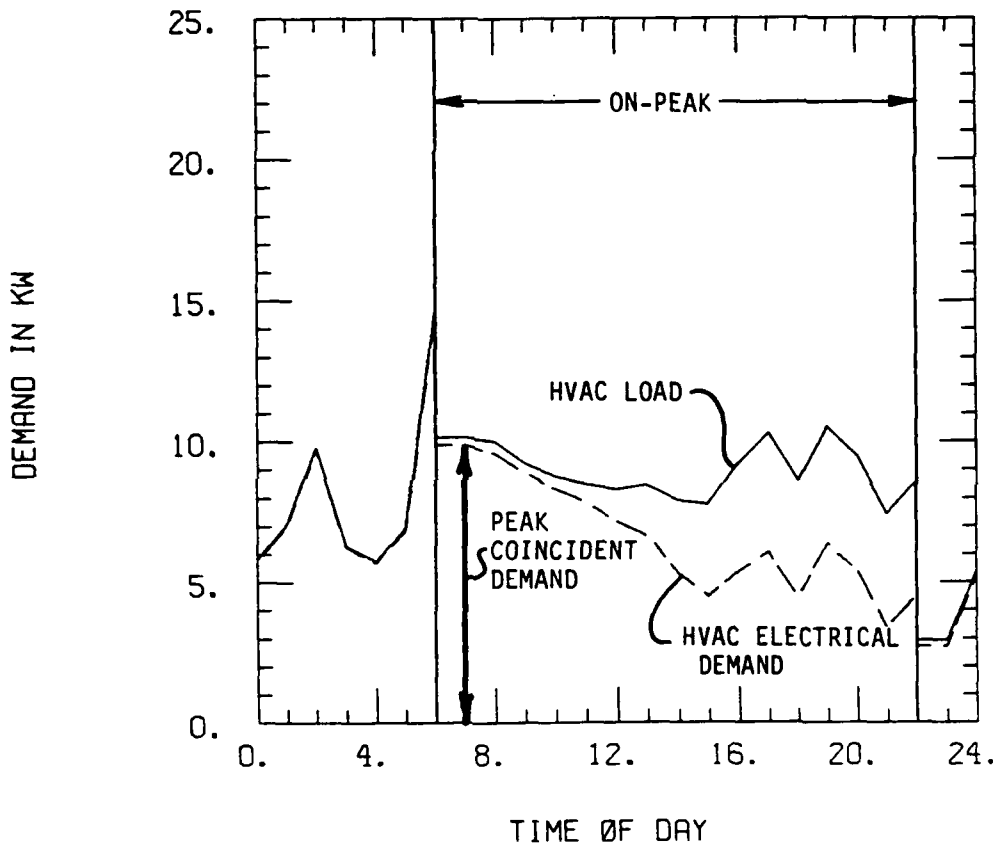

Figure 22. Proportional Strategy for Solar Storage on January 14.

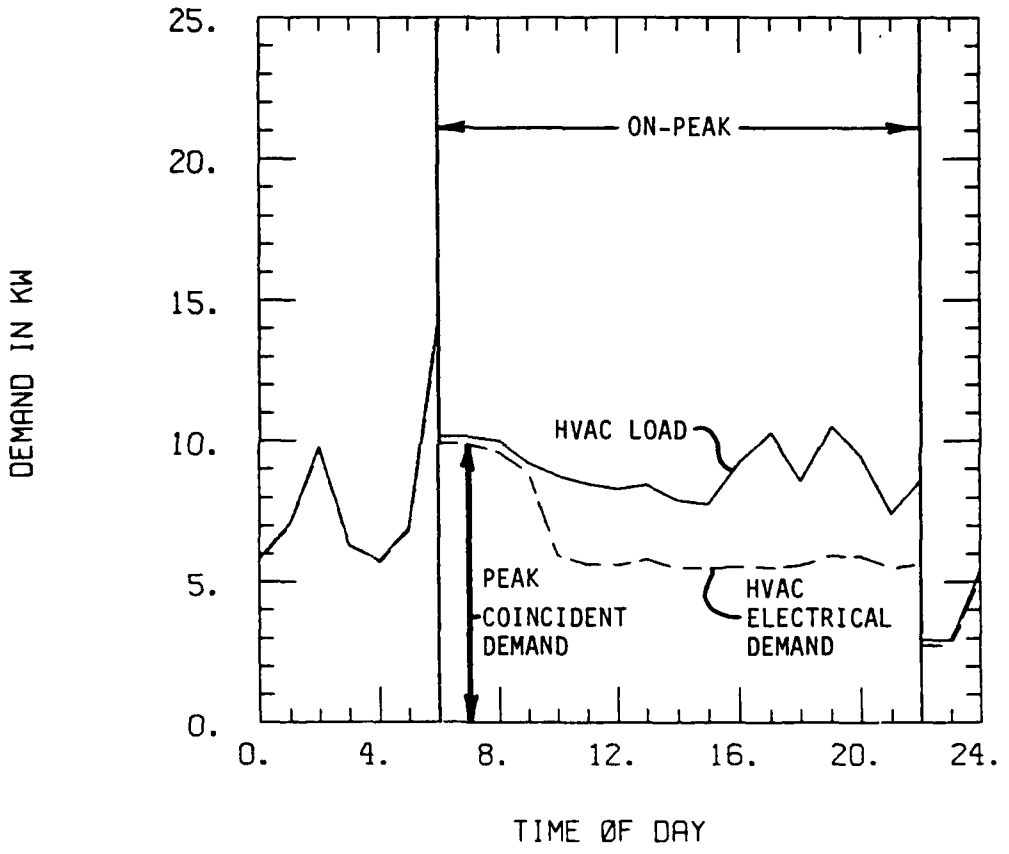

Figure 23. Optimal Strategy for Solar Storage on January 14.

Table 6. Solar Storage Discharge Strategy Comparisons.

	Baseline Heating System	Solar Heating System		
		Conventional Strategy	Proportional Strategy	Optimal Strategy
December Peak HVAC Coincident Demand	7.28 kW	6.83 kW	6.87 kW	6.78 kW
January Peak HVAC Coincident Demand	13.32 kW	13.07 kW	10.29 kW	9.59 kW
February Peak HVAC Coincident Demand	12.32 kW	11.84 kW	11.73 kW	11.74 kW
HVAC Coincident Demand Annual Cost of Supply in 1990 Dollars and % of Baseline	$2551 100%	$2227 87%	$2020 79%	$1905 75%
HVAC Fuel Annual Cost of Supply in 1990 Dollars and % of Baseline	$1396 100%	$705 51%	$730 52%	$691 49%
HVAC Total Annual Cost of Supply in 1990 Dollars and % of Baseline	$3946 100%	$2932 74%	$2749 70%	$2596 66%

lack of improvement in December and February is that the day on which the peak coincident demand occurred was the second of two successive cloudy days. There was very little energy in solar storage so the discharge strategy has little effect on system performance. A completely discharged storage is a rather common occurence during the peak heating season. During the spring and fall, the heating load is low, so storage is completely depleted less often, and the different discharge strategies have a larger effect on overall system performance. The decrease in the annual coincident demand cost of supply for the proportional and optimal strategies is largely due to the improved performance during the spring and fall. The fuel cost of supply is virtually the same for each control strategy even though less solar energy is collected when either proportional or optimal control is used because the proportional and optimal strategies save the collected energy to replace only expensive on-peak electrical energy.

Implementation of the optimal discharge strategy for solar storage is more difficult than in the case of off-peak storage systems. In addition to needing an estimate for the heating load for the entire on-peak period, the optimal discharge of solar storage requires advanced knowledge of the amount of solar energy to be collected. Accurate prediction of the collection of solar energy is very difficult to achieve. Because of the high cost and difficulty in implementing the optimal control, the recommended strategy for solar systems is proportional discharge of solar storage.

The changes in the load curve on the peak heating load day if 34 percent of the new homes used solar heating systems with conventional and proportinal discharge of storage are presented in Figures 24 and 25. The conventional strategy actually makes the utility load curve more uneven. The peak demand

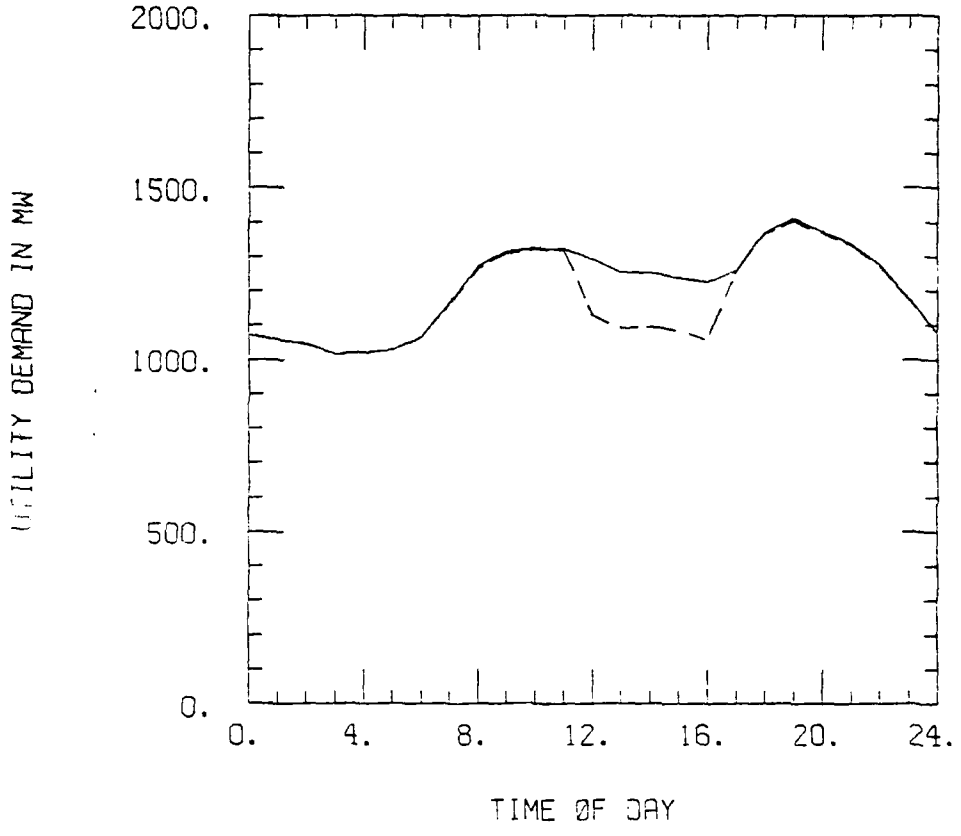

Figure 24. January Peak Day Utility Impact Due to 34% Saturation of Solar Heating Systems With Conventional Discharge.

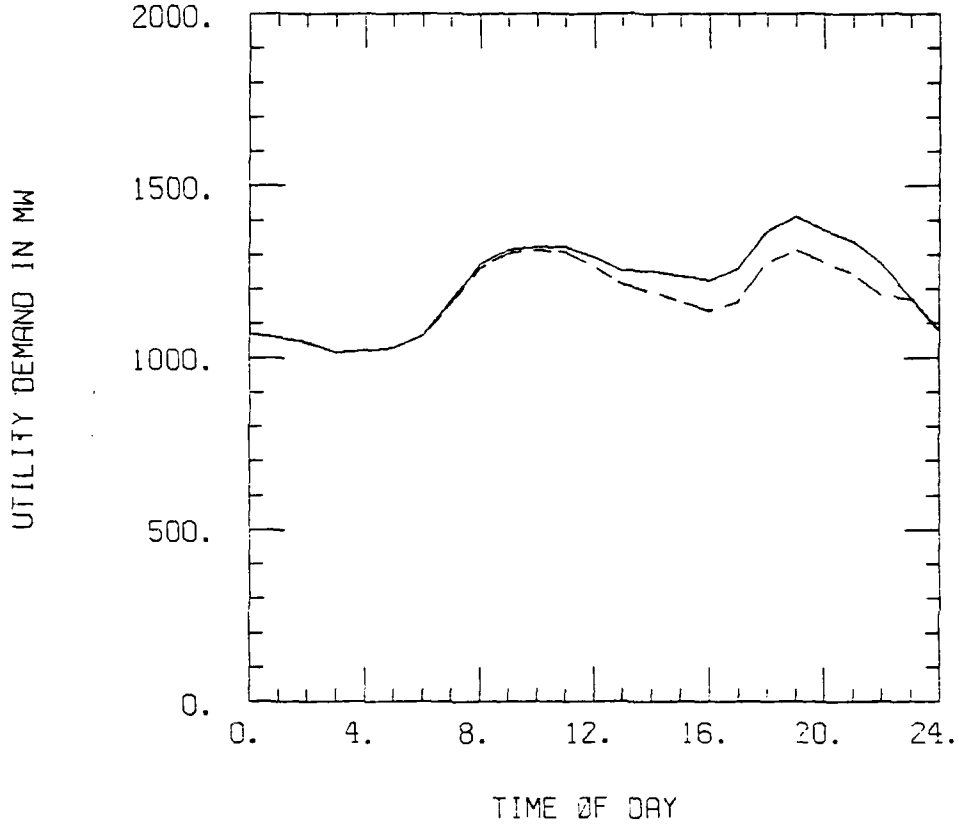

Figure 25. January Peak Day Utility Impact Due to 34% Saturation of Solar Heating Systems With Proportional Discharge.

is unchanged. The use of solar heating systems with proportional discharge of storage results in a more uniform load curve with a reduced peak demand. A saturation of 34 percent results in the most uniform curve.

C. Combined Solar Plus Off-Peak Storage System

The optimal control strategy for a combined solar plus off-peak storage system is again given by equation (13). The proportional approximation to the optimal strategy again effectively makes the conservative approximation that the heating load is constant and no solar energy is collected. The results of simulations of this system under the various control strategies are presented in Table 7. Although the use of the proportional strategy results in a significant reduction in the coincident demand during January and February, the reduction in the coincident demand cost of supply is small. The explanation of this apparent contradiction lies in an examination of the performace of the system during the spring and fall. The days on which the largest heating load occurs in the spring and fall are unlike those described earlier for the middle of the heating season. In the spring and fall, these "worst" days have a very high heating load in the morning with the load decreasing throughout the on-peak period. For this reason, the proportional discharge strategy is a poor approximation to the optimal strategy during the spring and fall. In fact, the conventional strategy is a close approximation to the optimal strategy at these times because it is designed to be able to satisfy the morning load. The difference between the conventional and the proportional strategy can be seen by comparing Figures 26 and 27 which are load profiles for March 14, the utility peak demand day in March. The reason that the combined solar plus off-peak storage has the spring and fall performance described above and the off-peak storage system does not is that the storage for the combined system is only 30

Table 7. Solar Plus Off-Peak Storage Discharge Strategy Comparisons.

	Baseline Heating System	Solar Plus Off-Peak Storage Heating System		
		Conventional Strategy	Proportional Strategy	Optimal Strategy
December Peak HVAC Coincident Demand	7.28 kW	5.48 kW	4.86 kW	2.08 kW
January Peak HVAC Coincident Demand	13.32 kW	12.97 kW	8.18 kW	6.66 kW
February Peak HVAC Coincident Demand	12.32 kW	11.63 kW	9.80 kW	8.84 kW
HVAC Coincident Demand Annual Cost of Supply in 1990 Dollars and % of Baseline	$2551 100%	$1895 74%	$1714 67%	$1267 50%
HVAC Fuel Annual Cost of Supply in 1990 Dollars and % of Baseline	$1396 100%	$645 46%	$686 49%	$627 45%
HVAC Total Annual Cost of Supply in 1990 Dollars and % of Baseline	$3946 100%	$2540 64%	$2427 62%	$1894 48%

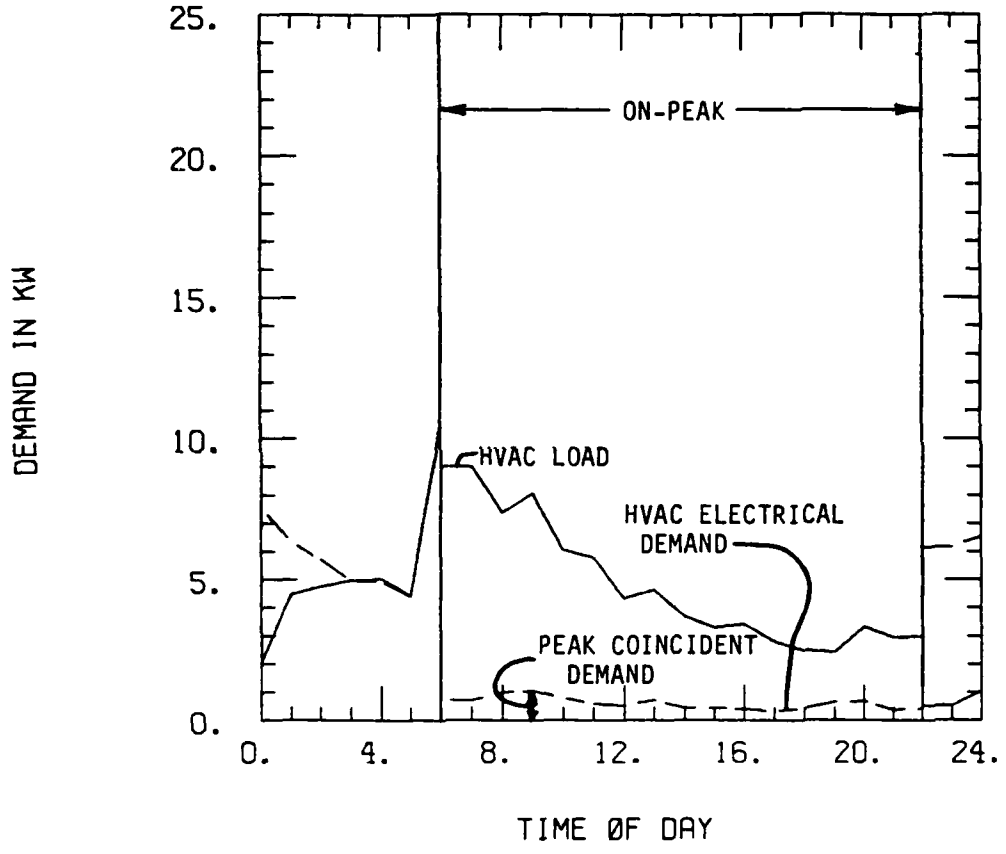

Figure 26. Conventional Strategy for Solar Plus Off-Peak Storage on March 14.

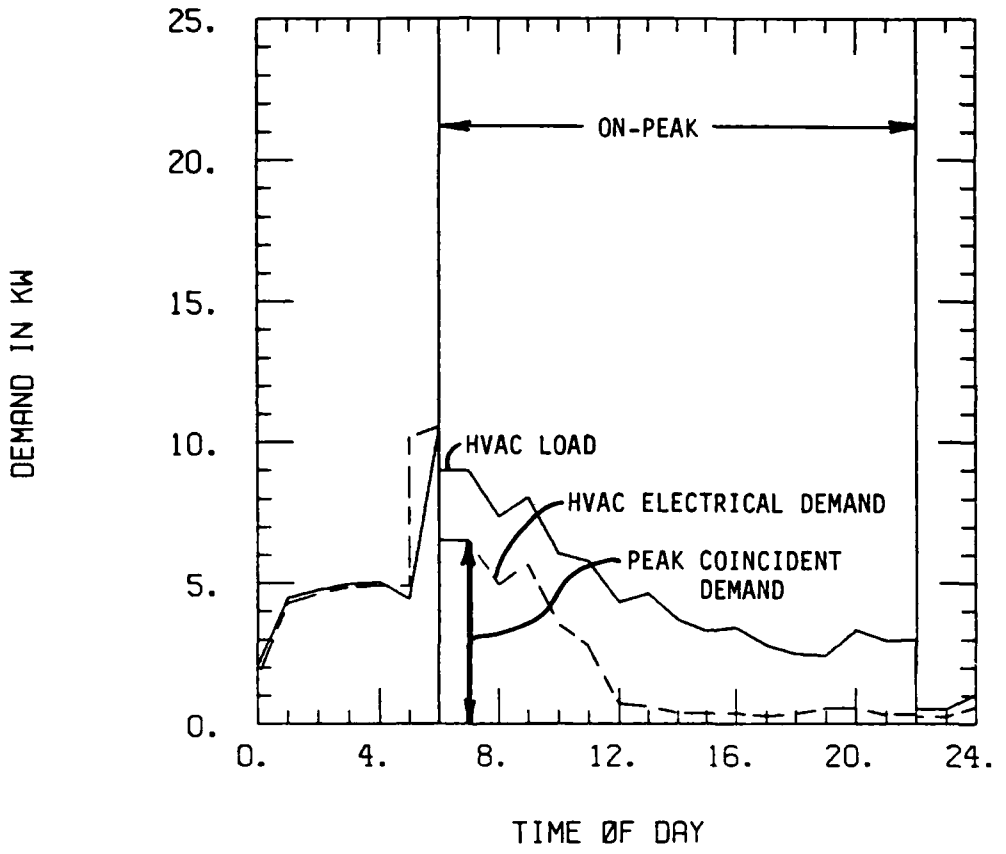

Figure 27. Proportional Strategy for Solar Plus Off-Peak Storage on March 14.

percent as large as the storage for the off-peak system. The storage in the combined system was sized using the standard design ratio of two gallons of storage per square foot of collector; the storage in the off-peak system was sized to meet the load on all but the "worst" days.

Because of the performance of the system at different times of the year, the recommended strategy for the discharge of combined solar plus off-peak storage is a combination of the proportional and conventional strategies. The proportional strategy is used for December, January, and February to reduce the annual peak coincident demand, and the conventional strategy is used for the remainder of the heating season to take advantage of its ability to satisfy a high morning load. For comparison with the results in Table 7, this combination strategy resulted in a coincident demand cost of supply of $1612 and a fuel cost supply of $666. This total of $2278 represents a 42 percent reduction in heating costs relative to the baseline system.

The changes in the load curves on the peak heating load day if 45 percent of the new homes use solar plus off-peak heating systems are presented in Figures 28 and 29. The widespread use of these systems with conventional discharge of storage reduces the morning utility peak but does nothing for the evening peak. The use of proportional discharge reduces the evening peak as well and generally smoothes the entire curve. A saturation of 45 percent results in the most uniform load curve.

IMPLEMENTATION

Implementation of the proportional or weighted proportional discharge strategy can be accomplished by using a microprocessor-based controller. The only input to the controller is the storage temperature. The storage temperature is measured at specified time intervals throughout the on-peak

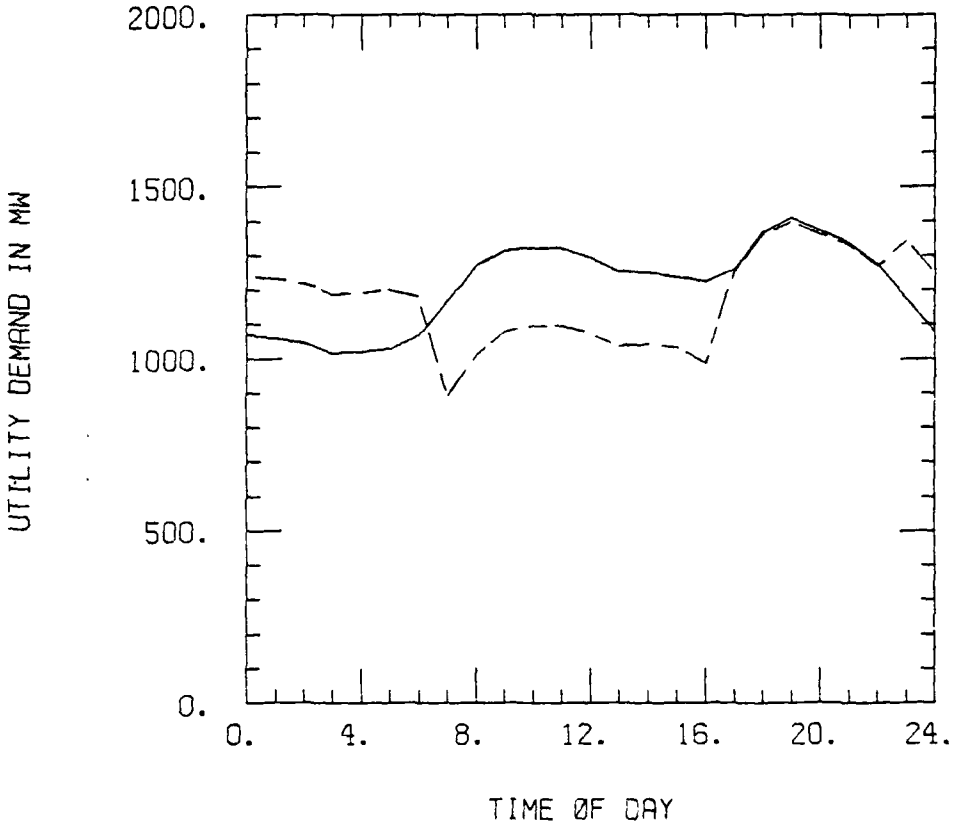

Figure 28. January Peak Day Utility Impact Due to 45% Saturation of Solar Plus Off-Peak Systems With Conventional Discharge.

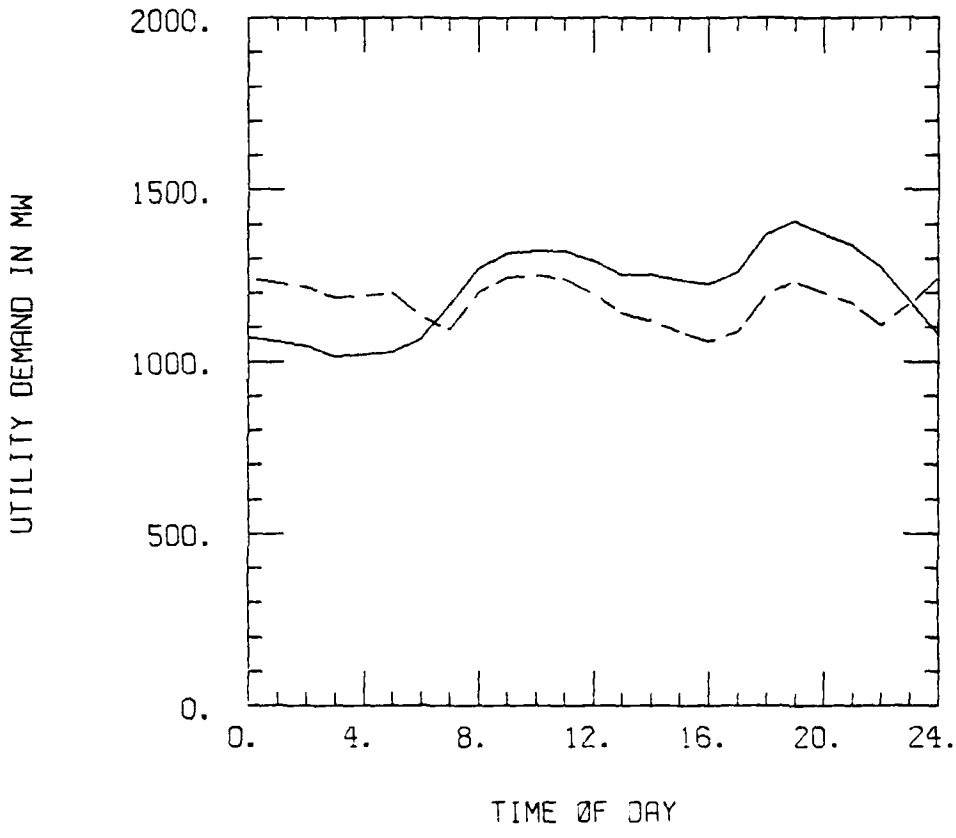

Figure 29. January Peak Day Utility Impact Due to 45% Saturation of Solar Plus Off-Peak Systems With Proportional Discharge.

period. The interval is chosen to coincide with the time period used by the utility in determining the demand charges. For hot storage, the minimum allowable storage temperature is subtracted the current storage temperature to determine the available energy in storage. The available energy in storage is divided by the time remaining until the end of the on-peak period to determine the maximum rate of energy discharge from storage from which the minimum temperature at the end of the time interval is established. The circulating pump is allowed to remove hot water from storage to satisfy the HVAC load until the minimum storage temperature is reached. If the minimum temperature is reached before the end of the time interval, the pump is disabled until the start of the next time interval when the next calculation is made. The process is repeated until the end of the on-peak period. An analogous process is used for discharge from cool storage.

There are some variations to the above implementation procedure which may be necessary for a particular installation. If the storage is stratified, an average temperature or some other means of determining the amount of available energy in storage is required. In addition, a stratified storage or a very large storage may make it difficult to control energy delivery using minimum temperatures as described above. If such is the case, the maximum pump on-time for each time interval can be determined using the difference between the storage outlet and the room air temperatures. Regardless which method is used, the strategy will ensure that storage is not depleted before the end of the on-peak period.

CHAPTER IV

ACTIVE SOLAR ENERGY COLLECTION

The problem of optimally collecting solar energy is presented in this chapter. The control is the mass flow rate through the collector. Provided the storage is sized properly, the storage dynamics have little effect on the optimal control.

INTRODUCTION

The rate at which energy is collected by a solar heating system can be increased by increasing the flow rate through the collectors. Increasing this flow rate, however, increases the power required to drive the fluid mover. This is illustrated in Figure 30. The energy collection rate as a function of mass flow rate is concave downward whereas the parasitic power as a function of mass flow rate is concave upward. These two curves are shown intersecting at a flow rate of $\dot{M}$, which represents an upper bound for $\dot{m}$. Most systems will operate at a maximum flow rate, $\dot{m}_{max}$, which is less than $\dot{M}$ on a sunny day. On a day with relatively low solar radiation, $\dot{m}_{max}$ could be greater than $\dot{M}$. The flow rate in a bang-bang controller will be either zero or $\dot{m}_{max}$. In either event, this would not normally maximize the difference between $\dot{Q}_u$ and P. Ideally, one would choose the flow rate, $\dot{m}^*$, that maximizes the difference between the two curves shown in Figure 30.

The difficulty in determining $\dot{m}^*$ stems from the fact that $\dot{Q}_u$ is a function of solar and weather conditions and is a dynamically changing variable. Therefore, $\dot{m}^*$ also changes with respect to time. The methods of optimal

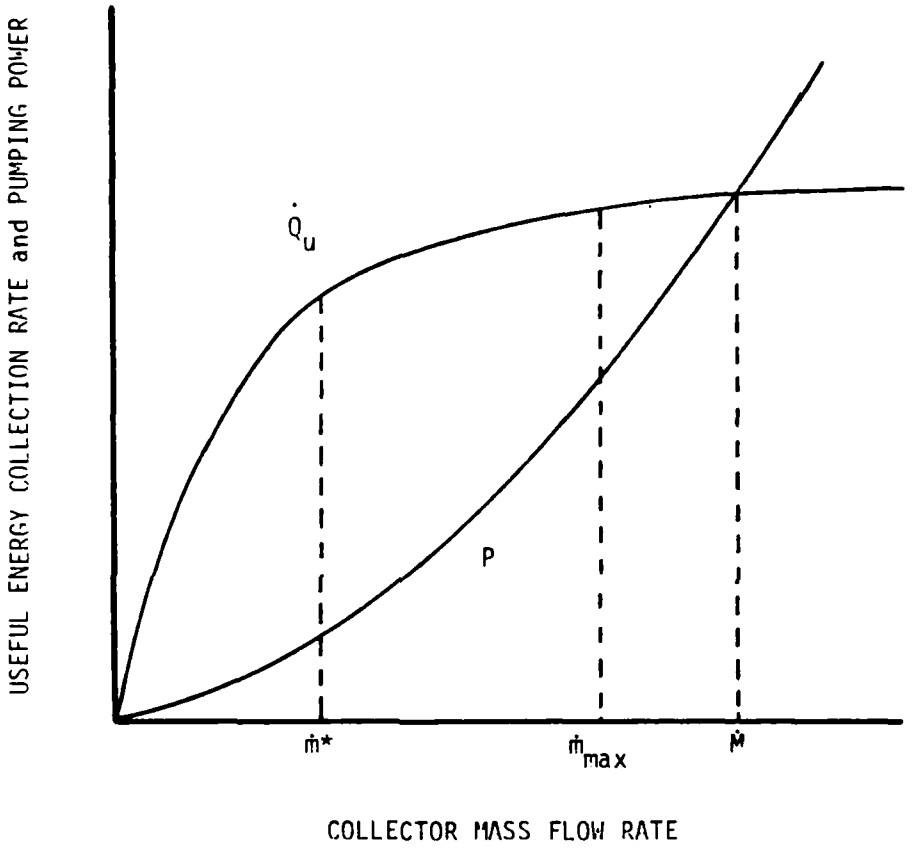

Figure 30. Qualitative Representation of Useful Energy Rate and Pumping Power.

control of dynamic systems should be applied to determine the value for $\dot{m}^*$ at each point in time.

The problem of maximizing the difference between solar power and fluid moving power was first approached by Kovarik and Lesse [6]. Their approach resulted in a two point boundary value problem which was solved numerically. Their solution, however, could not be implemented in a practical controller because it was not a function of measurable states of the system. Winn and Hull presented an approximate analytical solution to the problem which is possible to implement [7]. They showed close agreement between their simulation results and those of Kovarik and Lesse. An optimal controller based on their results has been developed and installed in Solar House II at Colorado State University. The controller's algorithm uses an empirical relationship between collector flow rate and fan power. This chapter describes the optimal control strategy, the development of the empirical fan power relationship, and the implementation of the strategy in a practical controller in Solar House II.

OPTIMAL CONTROL STRATEGY

The optimal mass flow rate in a solar energy collection system depends on the statement of what is to be optimized (the objective function) and the model used to describe the performance of the system (the constraints). Each combination of objective function and constraints results in an optimal, time dependent, flow rate.

If the problem at hand is to maximize the difference between solar energy collected and pumping energy, the objective function can be stated as

$$J = \int_{t_o}^{t_f} [C_3 \dot{Q}_u(t) - P(t)]dt. \tag{16}$$

The energy cost weighting function, C_3, takes into account the difference between the cost of energy to run the fluid mover and that to provide auxiliary heating. For example, if electric resistance heat provides auxiliary heating, C_3 equals 1; if a heat pump is used, C_3 equals 1 divided by the COP of the heat pump. The useful energy collection rate, $\dot{Q}_u$, is given by the Hottel-Whillier-Bliss equation [8].

$$\dot{Q}_u = F_r A_c [H_t \tau\alpha - U_l(T_s - T_a)], \tag{17}$$

where

F_r is the heat removal factor

A_c is the collector area

H_t is the solar radiation incident on the collector

$\tau\alpha$ is the collector transmittance-absorptance product

U_l is the collector loss coeffficient

T_s is the collector inlet temperature = storage outlet temperature

T_a is the ambient air temperature.

The parasitic pumping power, P(t), is expressed empirically as a function of collector mass flow rate, $\dot{m}(t)$, as

$$P(t) = C_4 \dot{m}(t)^a, \tag{18}$$

The appropriate values for C_4 and the exponent, a, depend on the particular installation and will be discussed in detail later in this chapter. The heat removal factor, F_r, is an exponential function of mass flow rate. This function can be expressed by a truncated Taylor's series as

$$F_r = F' - F'^2 U_l A_c / 2\dot{m} c_p, \tag{19}$$

where F' is the collector efficiency factor. Assuming that the collector efficiency factor is constant, the optimal mass flow rate is

$$\dot{m}^* = [C_1 F'^2 U_l A_c / 2aC_4 c_p]^{1/(a+1)}, \tag{20}$$

The available energy, f, was defined in terms of collector outlet temperature, T_c, by Winn and Hull [7]. The available energy is zero if (T_c-T_s) is negative. If (T_c-T_s) is positive, the available energy is determined from either

$$f = \dot{m}c_p(T_c-T_s)/F_r \tag{21}$$

if the collector fluid mover is on, or

$$f = U_l A_c(T_c-T_s) \tag{22}$$

if the fluid mover is off.

The optimal flow rate above can be found using a static optimization procedure which implies that the dynamics of the problem are unimportant in the determination of the optimal control. A derivation of this optimal mass flow rate is presented in Appendix D. In addition, Appendix D contains the derivations of optimal mass flow rates for several different objective functions and system models. Also included is the derivation of the optimal flow rate for a system with a collector efficiency factor which varies with flow rate.

PARASITIC PUMPING POWER

In a well designed solar heating system, the pumping costs are small in relation to the energy collected, and it could be argued that it is not important to determine $\dot{m}^*$. Not all systems, however, are well designed. Some, in fact, have actually increased consumer's utility bills [9]. A controller which selects $\dot{m}^*$ reduces the possibility of this occurring because it controls collector flow rate so as to maximize the difference between the solar power and the associated pumping power.

An accurate determination of $\dot{m}^*$ requires an accurate relationship between flow rate and power required. Some authors suggest a linear

relationship between flow rate and power required [10]. The fan laws suggest a cubic relationship between air flow rate and fan power [11]. A theoretical analysis of each system will yield the proper relationship for each system.

The power required to move a fluid is proportional to the product of the mass flow rate and the pressure increase across the pump or fan. The pressure increase can be determined by analyzing the rest of the system. For an open system, such as with a trickle collector, the head against which the pump moves the liquid is predominantly the result of the increase in elevation from the storage tank below the collector array to the end of the pipe at the top of the array. This head loss (pressure drop) is independent of flow rate. For a closed system, the elevation change throughout the system does not affect the head required of the fan or pump. Except during start up when the fluid is being accelerated, the pressure drop in a closed system is primarily due to viscous effects. If the flow is laminar in a particular section of the system, the pressure drop is linear with flow rate. If the flow is turbulent, the pressure drop is proportional to flow rate raised to some power. For flows just barely turbulent, the exponent is slightly greater than one; for flows with Reynolds numbers above 10^6, the exponent is two [12]. In a system with flow in some sections at high Reynolds numbers and some at low Reynolds numbers, the pressure drop for the entire system is proportional to the flow rate raised to some power between one and two. With power delivered to the flow proportional to the product of flow rate and pressure change, the power is proportional to the flow rate raised to some power between two and three. This analysis of flow in a closed system applies to any fluid, either liquid or gas.

In the system in Solar House II, the Reynolds number varies widely from place to place. The Reynolds number, based on data taken in March 1980, is

about 80,000 in the ducts to and from the collectors, about 3000 in the collectors, and about 200 in the rock box. The head developed by the fan at the different rates is presented in Table 8. A least squares fit of these data shows the increase in pressure to be proportional to the flow rate raised to 1.4; therefore, the power delivered to the air is proportional to the flow rate raised to 2.4.

The fan in Solar House II is a four-speed fan, but the design flow rates ranged from about 0.45 kg/s to 0.51 kg/s. The fan speeds were altered by using transformers to obtain the flow rates shown in Table 8. Because the fan was forced to operate so far from its design conditions, the fan efficiency was very low. If a fan were designed to operate at the flow rates in Table 8, it would be reasonable to expect good efficiency at each flow rate with the best efficiency at an intermediate flow rate. As an approximation to this condition, the fan power used in the simulations to be discussed later is the power delivered to the air divided by a constant efficiency of 29 percent. This is the combined efficiency of the fan and motor in Solar House II when operating at high speed. The equation used to describe fan power in Watts is

$$P = 3175\dot{m}^{2.4}, \tag{23}$$

IMPLEMENTATION

Practical implementation of the solution to this optimal control problem requires some compromises. The equation for the optimal flow rate given earlier requires a fan with an infinitely variable flow rate. This is not practical; however, a multi-speed fan is reasonable. A four-speed, 3/4 horsepower fan has been installed in Solar House II. The optimal controller picks the fan speed with flow rate closest to the optimal flow rate. The solution of the problem also requires continuous measurement of collector

Table 8. Solar House II Flow Rate-Fan Head Relationship.

Flow Rate (kg/s)	Fan ΔP (mm H_2O)
0.156	5
0.263	11
0.378	19
0.510	33

Table 9. Solar Energy Collection System Parameters.

$C_3 = 1.0$

$F' = 0.9$

$U_L = 3.86 \ W/m^2 \ ^oC$

$A_c = 29.0 \ m^2$

$a = 2.4$

$C_4 = 3175 \ W \ s^{2.4}/kg^{2.4}$

$c_p = 1.004 \ kJ/kg \ ^oC$

$\dot{m}_1 = 0.156 \ kg/s$

$\dot{m}_2 = 0.263 \ kg/s$

$\dot{m}_3 = 0.378 \ kg/s$

$\dot{m}_4 = 0.510 \ kg/s$

temperatures and continuous updating of the optimal flow rate. This would result in cycling which would be, at least, bothersome. To avoid this problem, a time interval between updates is established. Slightly more than two minutes was used in Solar House II. A microprocessor-based controller is used to determine the flow rate and maintain the time interval between updates.

Calculating the optimal flow rate from the equation described earlier requires a significant amount of program storage space, which is expensive. To reduce the required storage size, the calculations are replaced by a table search. The new optimal flow rate depends on the flow rate for the previous time interval and the temperature difference across the collector. For a four speed fan, there are only five possible flow rates, zero or one of the four stages. For each of these flow rates, temperature differences are determined which will result in each of five possible flow rates for the next time interval. Thus a table is generated which, with the search program, requires less the 1K bytes of storage. For the parameters in Table 9, the search table in Table 10 results. The reduction in microprocessor size resulting from the use of the table look-up reduced the cost of the controller by about half. In fact, the microprocessor is not even necessary because the table look-up can be accomplished using a Read-Only-Memory (ROM) based state machine similar to those used in the automotive industry, appliance industry, etc. The optimal controller installed in Solar House II cost about 150 dollars in retail parts. If the controller were produced in quantity using a ROM-based state machine instead of a microprocessor, it would cost considerably less.

The optimization takes place when the controller's internal clock signals that it is time for an update. The temperatures at the bottom of storage and at the collector outlet are measured as analog signals. These analog signals are

Table 10. Search Table.

$T_c - T_s$, (°C)		Fan Speed During Last Time Interval				
		0	1	2	3	4
Fan Speed for Next Time Interval	0	<0	<0	<0	<0	<0
	1	0 - 8	0 - 4	0 - 2.	0 - 2	0 - 1
	2	8 - 33	4 - 14	2 - 10	2 - 8	1 - 6
	3	33 - 100	14 - 44	10 - 31	8 - 23	6 - 18
	4	>100	>44	>31	>23	>18

converted to digital signals and subtracted. The resulting digital signal and the digital signal corresponding to the most recent flow rate are used to enter the table. A digital signal corresponding to the new optimal fan speed results and is used to send a signal to the appropriate fan speed relay.

SYSTEM PERFORMANCE

Solar House II operated under optimal control in the energy storage mode from March 21 to April 9, 1980. On a sunny day, the controller starts the fan on its lowest speed and gradually steps it up through the different fan speeds. After about 90 minutes, the fan is operating at its highest speed and remains there until about an hour before sunset. Then, the fan speed is stepped down until the sun sets. On less than full sunny days, the controller picks the optimal fan speed based on the table described earlier. Figures 31 and 32 depict the time history of solar radiation and mass flow rate for March 21-24. Note that the flow rate generally follows the level of solar radiation. The high fan speeds at the beginning and end of the second and third day and at the beginning of the fourth day are caused by an override of the optimization when the house called for heat.

Simulations were used to compare the performance of the system under optimal control with an identical system using bang-bang control. The simulation used the Hottel-Whiller-Bliss equation with U_l, $\tau\alpha$, and F' all held constant [8]. The values used were U_l=3.92W/m^{2o}C, $\tau\alpha$=0.774, and F'=0.8. These values were selected because they produced the best agreement with the measured data. The measure of agreement was the absolute difference between measured and simulated daily energy collected plus the weighted absolute difference between measured and simulated peak daily temperature. Measured ambient temperatures and solar radiation were used to drive the

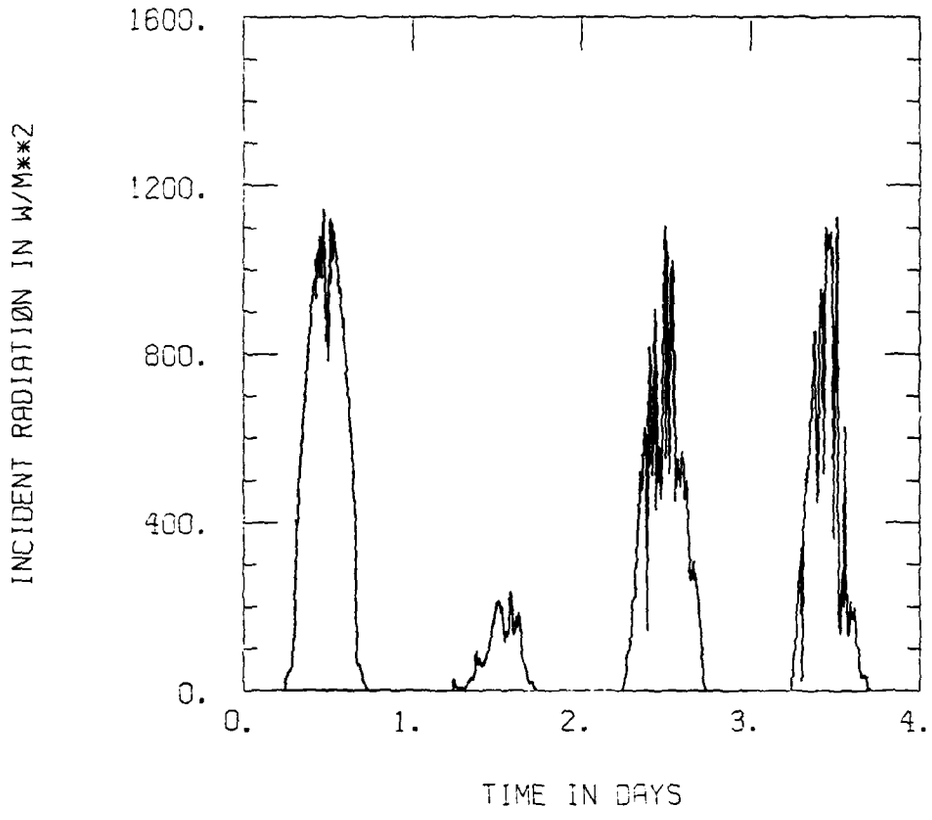

Figure 31. Incident Radiation from March 21 to 24, 1980.

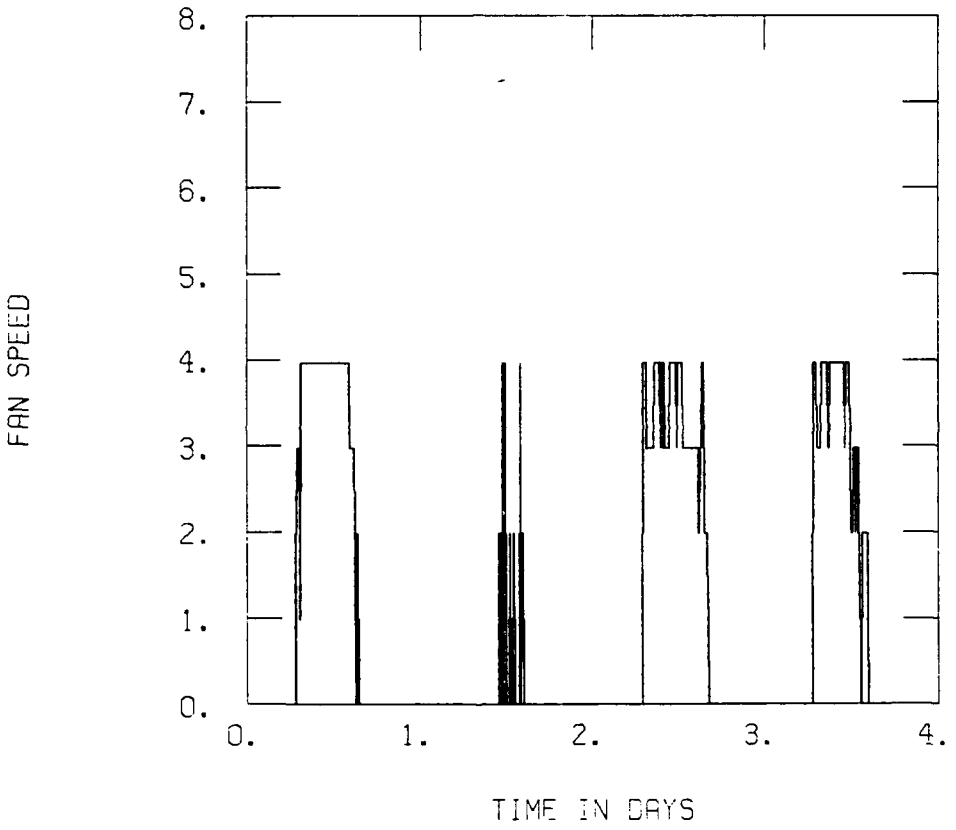

Figure 32. Actual Fan Speed from March 21 to 24, 1980.

simulation. For the period from March 21 to April 9, the simulation agreed with the measured performance quite well except for three days. These were particularly windy days, and, since the model did not allow for the wind, the simulation results were optimistic. Excluding these three days, the average daily difference in energy collected between the simulation and measured performance was 4 percent. Over the entire period, the simulation was within 1 percent of actual energy collected. The average difference between the predicted and actual daily maximum collector temperature was 3.3°C.

This model, which accurately predicted the performance of the system under optimal control, was changed to a bang-bang control strategy with zero dead band. The zero dead band was used to negate the effect of collector capacitance on simulation results. The comparisons of system performance under the two control strategies are shown in Figures 33, 34, and 35. In Figure 33 the increase in the objective function, J, is defined as the objective function with optimal control minus the objective function with bang-bang control. This is actually the net amount of energy savings realized by using optimal control and was 105 MJ over the 20 days. If the performance of the system is extended to cover an entire heating season, about 950 MJ of energy could be saved per house. The optimal controller achieves this savings by decreasing the fan energy required by a substantial amount as shown in Figure 34. Because the flow rate is generally lower with optimal control compared to bang-bang control, there is a corresponding decrease in the energy collected as shown in Figure 35. The decrease in fan energy is much larger than the decrease in energy collected. The performance improvement is the largest on the least sunny days, for example, day two. This implies that optimal control will have its most important application in marginal solar climates.

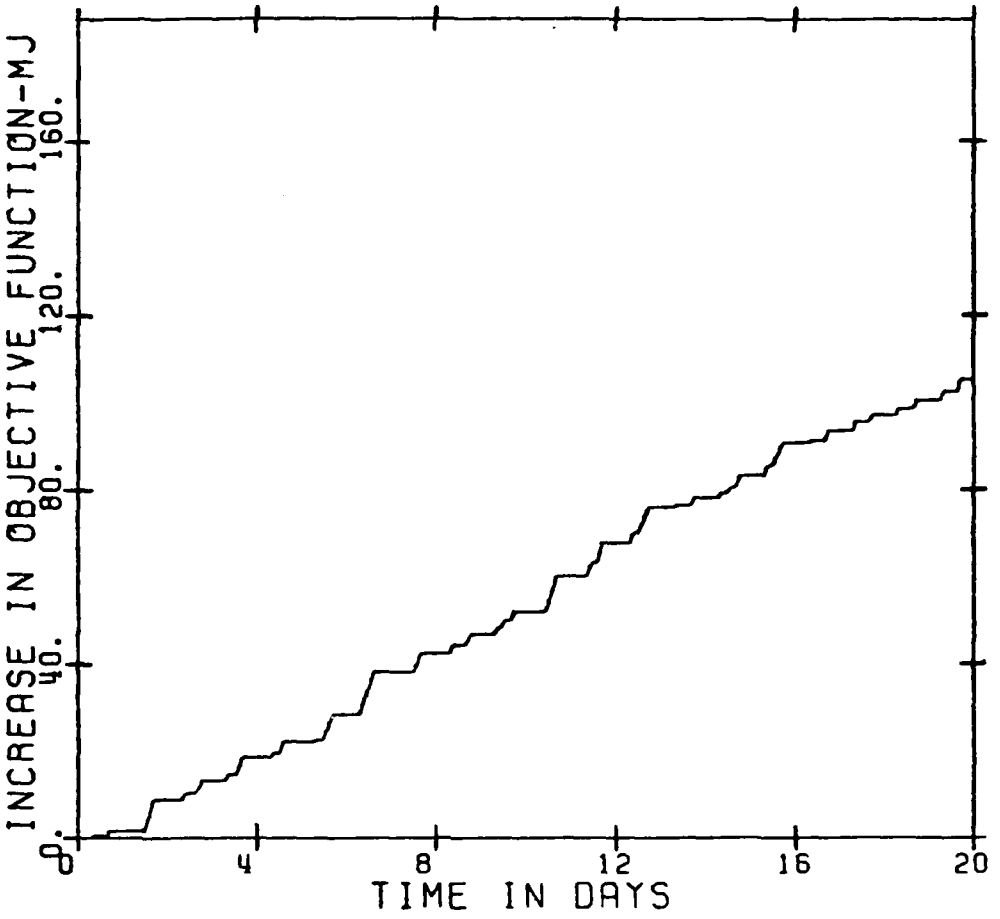

Figure 33. Cumulative Energy Saved from March 21 to April 9,1980.

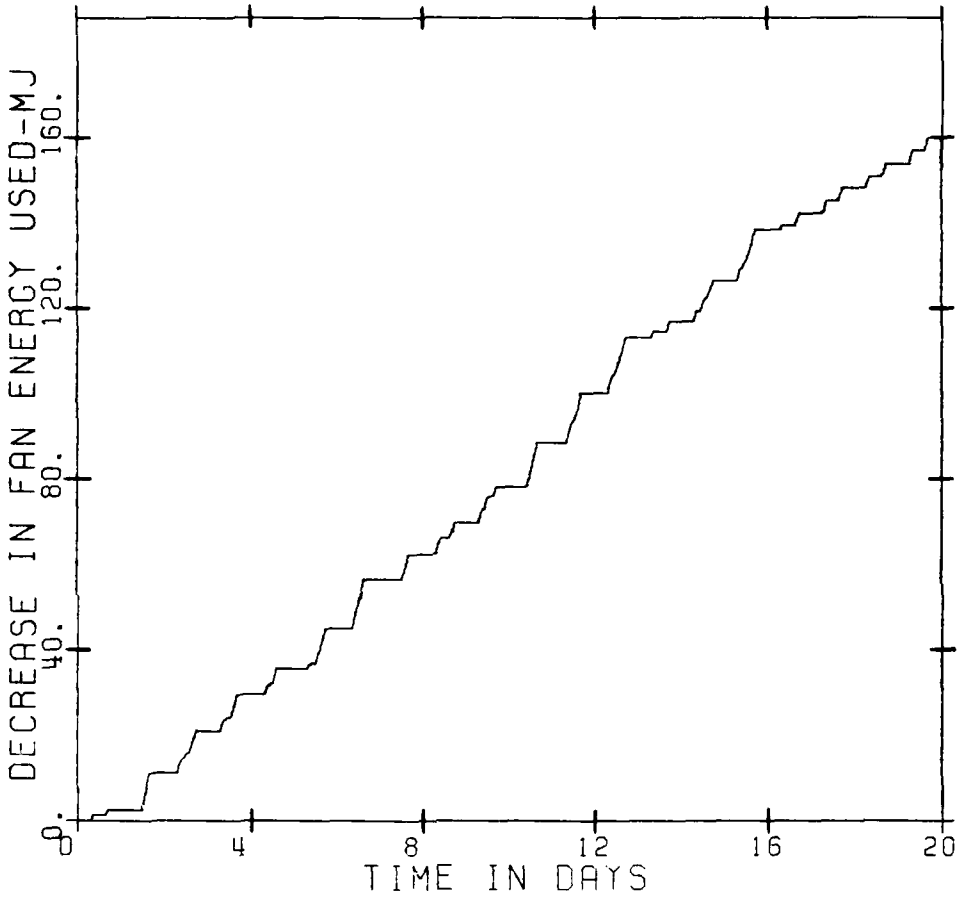

Figure 34. Cumulative Decrease in Fan Energy Required from March 21 to April 9, 1980.

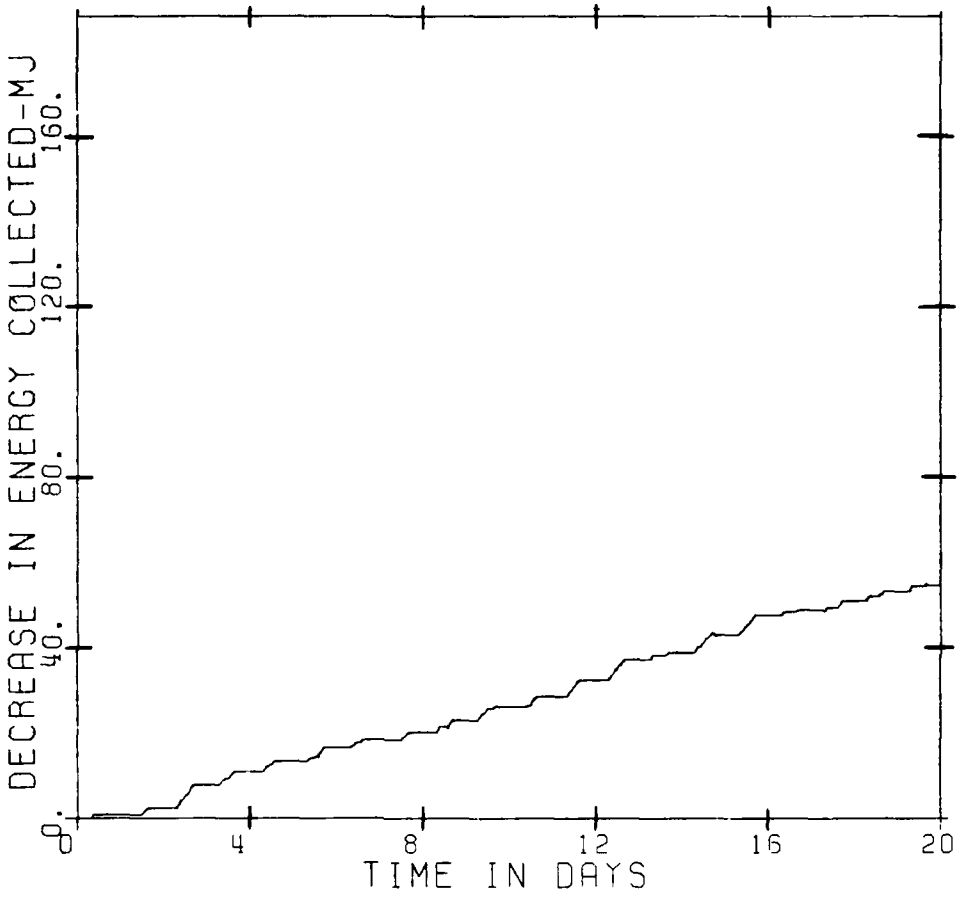

Figure 35. Cumulative Decrease in Solar Energy Collected from March 21 to April 9, 1980.

AD-A119 673 AIR FORCE INST OF TECH WRIGHT-PATTERSON AFB OH F/G 13/1
OPTIMAL CONTROL OF RESIDENTIAL HEATING AND COOLING SYSTEMS.(U)
1982 R C WINN
UNCLASSIFIED AFIT/CI/NR-82-54D NL

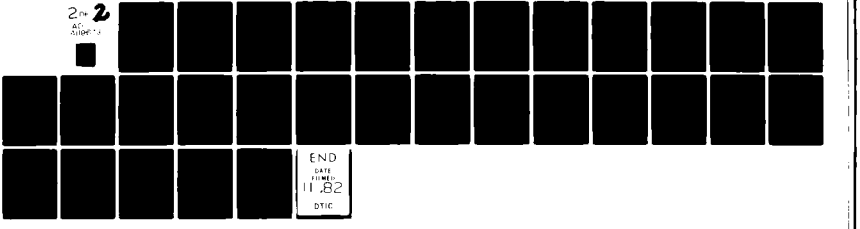

It should be noted that the simulation used the measured storage temperature as collector inlet temperature. This is not accurate when the control strategy is changed to bang-bang, but a bang-bang strategy will collect more energy than an optimal strategy and, thus, will actually have the same or higher storage/collector inlet temperature than the one used in the simulation. Therefore, the simulated performance of the system is optimistic when bang-bang control is used.

The comparison of system performance under the two control strategies only considered one bang-bang flow rate for the installation. The flow rate used was the maximum flow rate for the fan in Solar House II which may or may not have been the best possible. The question of optimal flow control versus several different bang-bang flow controls was addressed by Piessens, et al. [13]. Using TRNSYS simulations, they showed that the optimal controller performed better than any useable bang-bang strategy over the long term. On a low solar radiation day, one would expect a low flow rate bang-bang control to perform nearly optimally, but the same bang-bang control operates far from optimally on high solar radiation days.

CHAPTER V

CONCLUSIONS AND RECOMMENDATIONS

The methods of dynamic optimization have been used to develop optimal control strategies for several different heating and cooling systems. For a passive solar heated residence with an electrically heated thermal energy storage floor, the optimal controls are determined using either numerical methods or a combination of analytical and numerical methods. For each optimal control, some form of weather prediction is required if precise enclosure temperature control is to be maintained. The control varies significantly with the estimate of the future weather; however, because of the large mass of this type building, the temperature inside remains acceptable. Future work on this problem should include the determination of the optimal controls for different passive configurations such as an electrically heated thermal storage wall and a direct gain system with an electrically heated floor. In addition, the control should be implemented in an actual passive solar home.

An optimal control strategy for the discharge of energy stored in an isolated storage has also been developed. Because this optimal strategy is difficult to implement in a practical controller, approximations to the optimal control were studied. The use of the approximations to the optimal control resulted in reductions in annual operating costs of 25 percent for an off-peak storage system, 7 percent for a solar heating system, and 12 percent for a combined solar plus off-peak storage system relative to the costs of operation

when the conventional strategies are used. Future work should include a detailed study of the charging process, particularly for cool storage. The deterioration of the COP of the refrigeration equipment can play an important part in the optimal operation of the system. Again, these control strategies should be implemented to determine the actual savings which can be achieved.

Optimal collection of solar energy has been shown, both analytically and experimentally, to be of practical value. Future work on this problem depends on the development of an efficient, multi-speed fan for use in residential solar heating systems.

The three major problems analyzed in this study differed primarily in the importance and complexity of the energy storage. Systems with complex interactions between the storage and the conditioned space (Chapter II) have optimal control strategies which are difficult to obtain and require accurate weather prediction. Systems with isolated storage (Chapter III) have simpler optimal control strategies which produce excellent results with very simple load models. Solar energy collection performance (Chapter IV) does not depend heavily on the changes in the state of storage, and the optimal control is a series of static optimizations which require no weather prediction.

REPERENCES

1. Murrary, H.S., Melsa, J.L, and Balcomb, J.D., "Control System Analysis for Off-Peak Auxiliary Heating of Passive Solar Systems," Proceeding of the System Simulation and Economic Analysis Conference, San Diego, California, 1980.

2. Bryson, A.E., and Ho, Y.C., Applied Optimal Control, Ginn and Company, Waltham, Mass., 1969.

3. Zaininger Engineering Company, May 11, 1981, Personal Correspondence.

4. Winn, C.B., and Robinson, K., "Use of the ATOP System in the Control of an Off-Peak Storage Device," Proceedings of the 18th IEEE Conference on Decision and Control, Fort Lauderdale, Florida, 1979.

5. Arthur D. Little, Inc., "EPRI Methodology for Preferred Solar Systems (EMPSS) Computer Program Documentation," Arthur D. Little, Inc., Cambridge, Mass., 1978.

6. Kovarik, M., and Lesse, P.F., "Optimal Control of Flow in Low Temperature Solar Heat Collectors," Solar Energy, Vol. 18, 1976.

7. Winn, C.B., and Hull, D., "Optimal Controllers of the Second Kind," Solar Energy, Vol. 23, 1979.

8. Duffie, J.A. and Beckman, W.A., Solar Energy Thermal Processes, John Wiley and Sons, New York, 1974.

9. Ward, J.C., "Electricity and Gas Consumption of 24 Solar Homes Compared With 26 Conventional Homes Having Identical Heating Loads," Proceedings of Solar Heating and Cooling Operationsl Results Conference, Colorado Springs, 1978.

10. Schiller, S.R., Warren, M.L. and Auslander, D.M., "Comparison of Proportional and On/Off Solar Collector Loop Control Strategies Using a Dynamic Collector Model," Proceedings of the System Simulation and Economic Analysis Conference, SERI/DOE, San Diego, California, 1980.

11. ASHRAE Guide and Data Book, Equipment, American Society of Heating, Refrigerating and Air Conditioning Engineers, New York, 1974.

12. Olson, R.M., Essentials of Engineering Fluid Mechanics, International Textbook, Scranton, 1961.

13. Piessens, L.P., Beckman, W.A., and Mitchell, J.W., "A TRNSYS Microprocessor Controller," Proceedings of the Third Annual Operational Results Conference, ASME Solar Division, Reno, Nevada, 1981.

14. Roberts, S.M. and Shipman, J.S., Two Point Boundary Value Problems: Shooting Methods, American Elsevier, New York, NY, 1972.

15. TRNSYS, A Transient Simulation Program, Report 38-10, Engineering Experinment Station, University of Wisoncsin-Madison, 1979.

16. Applications Engineering Manual, Solaron Corporation, Denver, 1978.

APPENDIX A.

SOLUTION TO THE OPTIMAL CONTROL PROBLEMS FOR THE PASSIVE RESIDENCE

Two optimal control problems are posed for the operation of the off-peak heating system in the passive residence depicted in Figure 1. The first problem is to minimize

$$J_1 = \int_{t_o}^{t_f} [f\dot{Q}_{aux}{}^2 + C(T_e - T_{set})]dt$$

which is referred to as the quadratic objective function. The second problem is to minimize

$$J_2 = \int_{t_o}^{t_f} f\dot{Q}_{aux}dt$$

which is called the minimum cost objective function because the integral is, in fact, the total cost of energy for the time of integration. In either case, the optimization is subject to the dynamic equations of the system,

$$g_1 = dT_e/dt = -(a_1+a_2+a_3)T_e + a_1T_w + a_2T_f + a_3T_a$$

$$g_2 = dT_w/dt = a_5T_e - (a_5+a_6)T_w + a_6T_a + a_4H_t$$

$$g_3 = dT_f/dt = a_7T_e - (a_7+a_8)T_f + a_8T_g + Q_{aux}/C_f.$$

The methods of solution for these two optimal control problems differ considerably, and each will be discussed separately.

QUADRATIC OBJECTIVE FUNCTION

$$H = \lambda_1g_1 + \lambda_2g_2 + \lambda_3g_3 - f\dot{Q}_{aux}{}^2 - C(T_e - T_{set})^2.$$

A necessary condition for the Hamiltonian to be minimized with respect to the control is

$$\partial H/\partial\dot{Q}_{aux} = 0 = -2f\dot{Q}_{aux} + \lambda_3/C_f$$

or

$$\dot{Q}_{aux}{}^{*} = \lambda_3/2fC_f.$$

The adjoint variables are defined using the following:

$$d\lambda_1/dt = -\partial H/\partial T_e = (a_1+a_2+a_3)\lambda_1 - a_5\lambda_2 - a_7\lambda_3 + 2C(T_e - T_{set})$$

$$d\lambda_2/dt = -\partial H/\partial T_w = -a_1\lambda_1 + (a_5+a_6)\lambda_2$$

$$d\lambda_3/dt = -\partial H/\partial T_f = -a_2\lambda_1 + (a_7+a_8)\lambda_3$$

The above three equations and the dynamic equations of the system form a set of six differential equations. These equations have initial conditions on each of the temperatures. The final condition on the enclosure temperature is specified as $T_e(t_f)=T_{set}$ but the final conditions are free for T_w and T_f. To determine the two remaining final conditions, the transversality condition is applied resulting in

$$\lambda_2(t_f) = 0$$

$$\lambda_3(t_f) = 0$$

The set of equations with the stated initial and final conditions describes a two point boundary value problem which is solved numerically using the method of adjoints.

The method of adjoints is a shooting technique for determining missing initial conditions in a linear two point boundary value problem. The fundamental identity for the method of adjoints for a linear system of the form

$$\dot{y}_i = A(t)y_i + f_i$$

is

$$\sum_{i=r+1}^{n} x_i^{(m)}(t_o) = y_{i,m}(t_f) - \sum_{i=1}^{r} x_i^{(m)}(t_o)y_i(t_o) - \int_{t_o}^{t_f} \sum_{i=1}^{n} x_i^{(m)}(t)f_i(t)dt$$

where

n is the number of differential equations

r is the number of initial conditions

m is a counter identifying each missing initial condition

t_o is the initial time

t_f is the final time

$x_i^{(m)}$ is the adjoint variable vectors.

The adjoint variable vectors are the solutions to the set of equations

$$\dot{x}_i = -A^T(t)x_i$$

where

$A^T(t)$ is the nxn transpose of A(t).

To use the fundamental identity of the method of adjoints, integrate the adjoint equations backward (n-r) times, that is, one time for each missing initial condition. Each integration has the terminal boundary conditions

$$x_i^{(m)}(t_f) = \begin{cases} 1, & i=i,m \\ 0, & i\neq i,m \end{cases}$$

where i,m refers to the subscripts on the specified terminal conditions. Each integration results in a $x_i^{(m)}(t)$ and the corresponding initial condition $x_i^{(m)}(t_o)$. Substitution into the fundamental identity (n-r) times yields a set of (n-r) linear algebraic equations in the (n-r) unknowns, the missing initial conditions for y_i. The process is theoretically non-iterative, since the solution of the algebraic equations gives the missing initial conditions directly. Once the missing initial conditions are found, the original differential equations are integrated to produce the $y_i(t)$ profiles which satisfy the given final conditions. A complete discussion of the method of adjoints is presented in Reference [14].

Even though the process of determining the missing initial conditions is, in principle, noniterative, in practice, this may not be the case. If the eigenvalues of A(t) are widely separated in value, the set of (n-r) linear algebraic equations is nearly singular. As a result, it may not be possible to determine the missing initial conditions without iteration. This is the case with the set of differential equations resulting from the quadratic objective function. An orthonormalization procedure to cope with these problems is suggested in Reference [14], but this process is complex and requires a significant increase in the number of computations. A gradient improvement technique to improve the estimates of the missing initial conditions is also possible, but this method requires the numerical evaluation of many partial derivatives. For the system of equations in question, six integrations are required for each iteration. An approximation to this technique requires one integration for each iteration. In this modified gradient technique, it is assumed that the value of each variable at the end of the integration is primarily determined by its initial value. Improved values of the missing initial conditions are determined using results from the last two integrations as

$$y_{new}(t_o) = y_k(t_o) - R[y_k(t_f) - y_d][y_{k-1}(t_o) - y_k(t_o)]/[y_{k-1}(t_f) - y_k(t_f)]$$

where

k is the index for the most recent integratin

k-1 is the index for the second most recent integration

R is the relaxation constant (0.7 for this problem)

y_d is the desired final value.

This method does not guarantee convergence; however, sufficient accuracy was achieved in every case with significantly less computer time than would be required for either of the other suggested techniques.

The two point boundary value problem that resulted from the quadratic objective function was solved using the method of adjoints and the modified gradient improvement technique. From this solution, $\lambda_3(t)$ was saved and used in the equation for the optimal control,

$$\dot{Q}_{aux}^{*} = \lambda_3/2fC_f$$

recalling that f, the fuel cost, may be time varying. Typical results of this procedure were presented in Chapter 2 and depicted in Figures 3 and 4.

MINIMUM COST OBJECTIVE FUNCTION

To determine the minimum cost of operation of the system, minimize

$$J_2 = \int_{t_o}^{t_f} f\dot{Q}_{aux}\,dt.$$

The Hamiltonian is

$$H = \lambda_1 g_1 + \lambda_2 g_2 + \lambda_3 g_3 - f\dot{Q}_{aux}.$$

Because the Hamiltonian is linear in the control, $\dot{Q}_{aux}$, the problem becomes one of determining the switching times. Combining the coefficients of $\dot{Q}_{aux}$ in the Hamiltonian results in

$$H = \lambda_1 g_1 + \lambda_2 g_2 + \lambda_3 g_3 - f\dot{Q}_{aux}.$$

The optimal control is, therefore,

$$\dot{Q}_{aux} = \begin{cases} \dot{Q}_{aux,max}, & \lambda_3/C_f - f > 0 \\ 0, & \lambda_3/C_f - f < 0. \end{cases}$$

The solution to this problem depends upon $\lambda_3(t)$ which is defined in the same manner as for the quadratic objective function. The resulting set of differential equations is

$$dT_e/dt = -(a_1+a_2+a_3)T_e+a_1T_w+a_2T_f+a_3T_a$$

$$dT_w/dt = a_5T_e-(a_5+a_6)T_w+a_6T_a+a_4H_T$$

$$dT_f/dt = a_7T_e-(a_7+a_8)T_f+a_8T_g+Q_{aux}/C_f$$

$$d\lambda_1/dt = (a_1+a_2+a_3)\lambda_1-a_5\lambda_2-a_7\lambda_3$$

$$d\lambda_2/dt = -a_1\lambda_1+(a_5+a_6)\lambda_2$$

$$d\lambda_3/dt = -a_2\lambda_1+(a_7+a_8)\lambda_3$$

subject to initial conditions on T_e, T_w, and T_f and the final conditions,

$$T_e(t_f) = t_{set}$$

$$\lambda_2(t_f) = 0$$

$$\lambda_3(t_f) = 0.$$

Notice that the equations for λ_1, λ_2, and λ_3 are uncoupled from the first three equations and can be solved independently. The solution is

$$\lambda_1(t) = K_1\exp(m_1t)+K_2\exp(m_2t)+K_3\exp(m_3t)$$

$$\lambda_2(t) = K_4\exp(m_1t)+K_5\exp(m_2t)+K_6\exp(m_3t)$$

$$\lambda_3(t) = K_7\exp(m_1t)+K_8\exp(m_2t)+K_9\exp(m_3t)$$

where m_1, m_2, and m_3 are the eigenvalues of the system. The K's are constants, six of which are linear combinations of the other three. To determine the values of the remaining three constants, use the boundary conditions; however, there are only two boundary conditions on the adjoint variables,

$$\lambda_2(t_f) = \lambda_3(t_f) = 0.$$

Therefore, the solution to this system of equations is determined except for a constant multiplier. For the paramenters listed in Table 1, the solution for λ_3 is

$$\lambda_3 = K[\exp(.391t)-498\exp(.055t)-6332\exp(.019t)].$$

Several solutions for $\lambda_3(t)$ are presented in Figure 36. As the value for the constant, K, increases, $\lambda_3(t)$ increases. Therefore, according to the

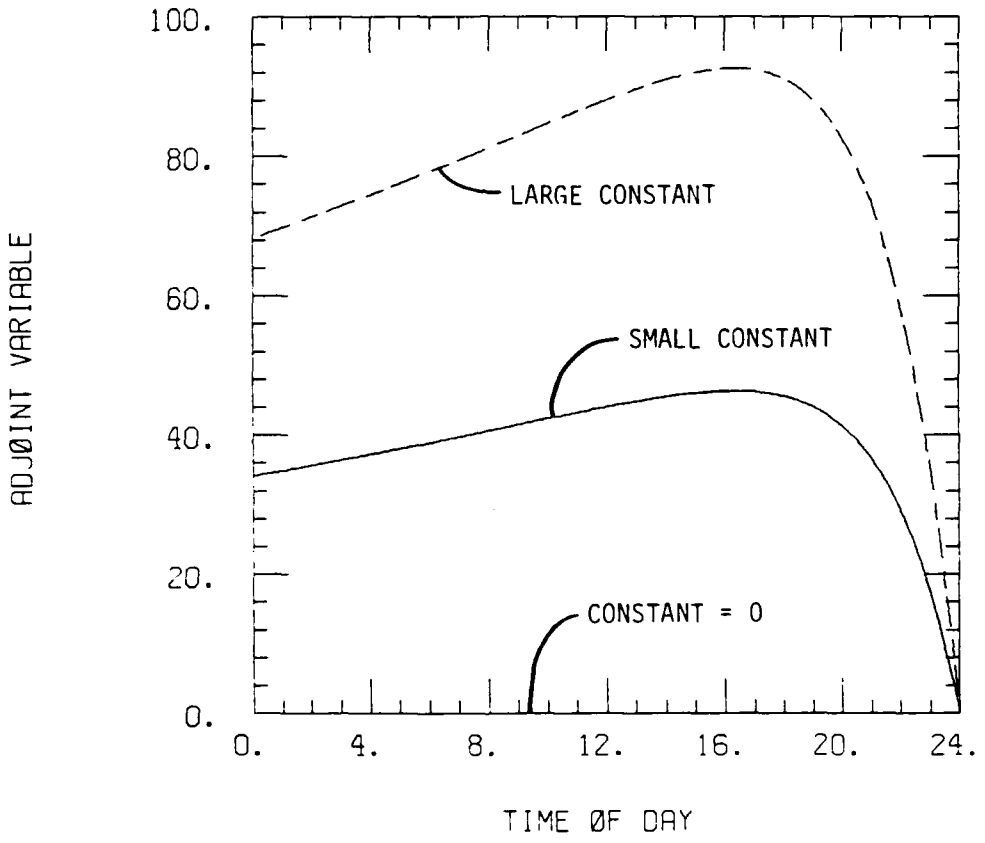

Figure 36. Solution to Adjoint Variable Equation.

equation for the optimal control presented earlier, $\dot{Q}_{aux}^{*}$ is equal to $\dot{Q}_{aux,max}$ more often as K is increased. This is depicted in Figure 37 for the fuel cost function, f, used in Chapter 2. Whenever the decision variable is positive $\dot{Q}_{aux}$ is equal to the maximum value. The correct value for K is determined using the differential equations for the temperatures. Increasing K increases the amount of time $\dot{Q}_{aux}$ is on which increases the final value of T_e. The correct value of K is the one which results in $T_e(t_f)=T_{set}$.

In summary, the solution to the minimum cost problem is determined analytically (to arrive at $\lambda_3(t)$) and numerically (to find the value of K which results in $T_e(t_f)=T_{set}$). Typical minimum cost control strategies are presented in Figures 3 and 4.

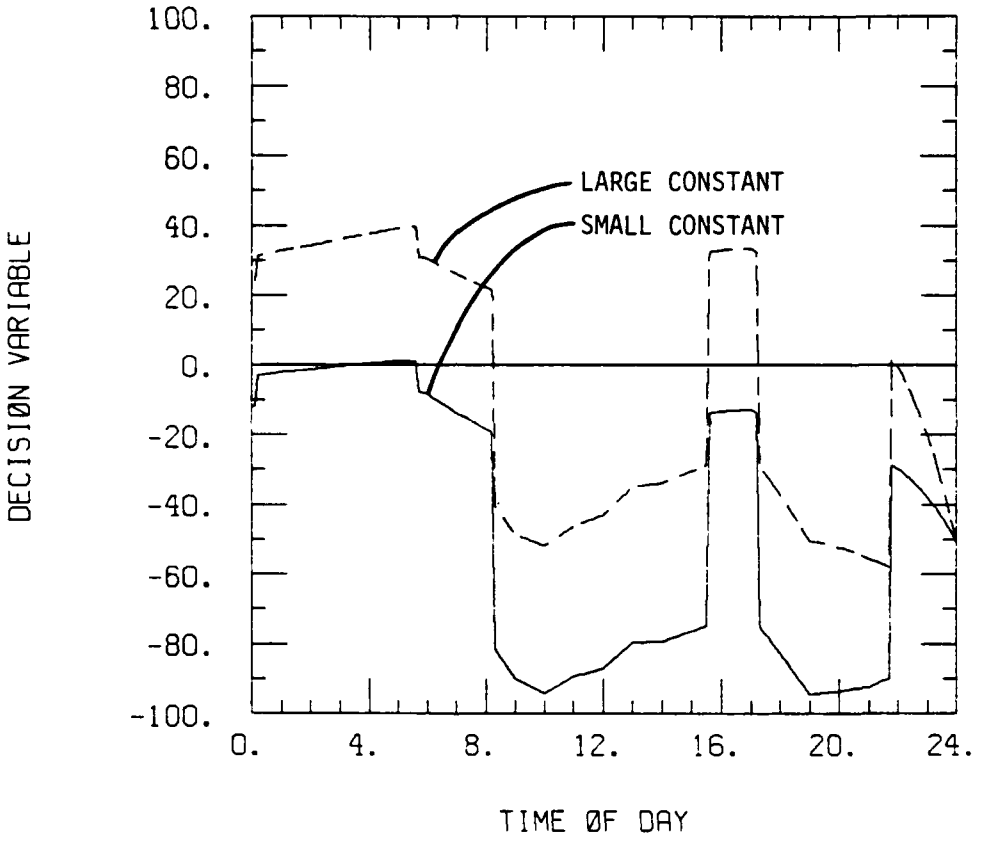

Figure 37. Minimum Cost Control Decision Variable.

APPENDIX B.

OPTIMAL DISCHARGE FROM OFF-PEAK STORAGE

The following is a development of the equations for the optimal discharge rate from the storage of an off-peak storage heating and cooling system. The equations for hot and cool storage are different and are developed separately; however, both are designed to minimize

$$J = \int_{t_o}^{t_f} [\dot{Q}_{on-peak}]^2 dt.$$

HOT STORAGE

The off-peak storage heating system is depicted in Figure 38. Energy balances on the enclosure and the storage yield

$$C_s dT_e/dt = \dot{Q}_{on-peak} + \dot{Q}_{st} - \dot{Q}_{load}$$

$$C_s dT_s/dt = \dot{Q}_{sol} - \dot{Q}_{st} - \dot{Q}_{loss}$$

where all variables are defined in Chapter 3 except

$$\dot{Q}_{loss} = UA_s(T_s - T_o)$$

where

UA_s is the overall storage heat transfer coefficient-area product

T_o is the temperature of the environment of the storage.

As in Chapter 3, it is assumed that the enclosure temperature is effectively constant; therefore,

$$dT_e/dt = 0.$$

The problem now is to minimize

$$J = \int_{t_o}^{t_f} [\dot{Q}_{on-peak}]^2 dt$$

subject to

$$dT_s/dt = [\dot{Q}_{on-peak} - \dot{Q}_{load} + \dot{Q}_{sol} - UA_s(T_s - T_o)]/C_s.$$

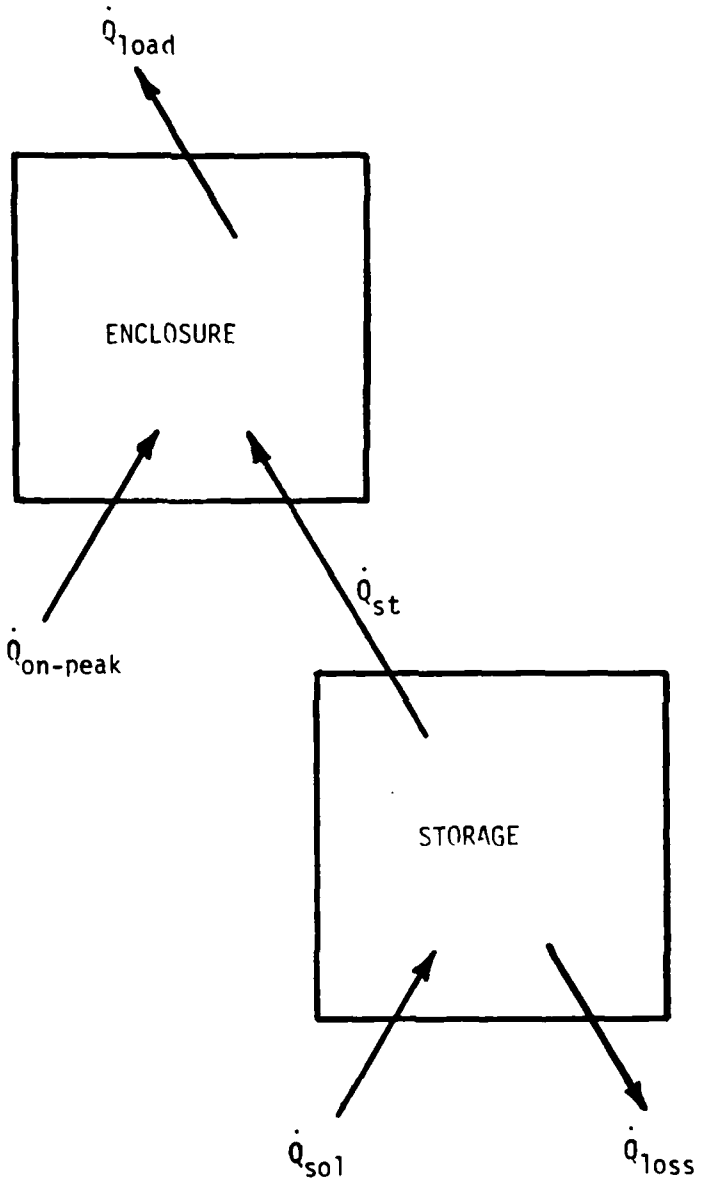

Figure 38. Off-Peak and/or Solar Heating System Schematic.

The Hamiltonian is

$$H = \lambda[\dot{Q}_{on-peak} - \dot{Q}_{load} + \dot{Q}_{sol} - UA_s(T_s - T_o)]/C_s - (\dot{Q}_{on-peak})^2,$$

The optimal control satisfies

$$\partial H/\partial \dot{Q}_{on-peak} = 0 = \lambda/C_s - 2\dot{Q}_{on-peak}$$

or

$$\dot{Q}_{on-peak}^{*} = \lambda/2C_s,$$

The adjoint variable is defined using

$$d\lambda/dt = -\partial H/\partial T_s = UA_s/C_s,$$

Solving this equation yields

$$\lambda(t) = K\exp[(UA_s/C_s)t],$$

Therefore, the optimal control is

$$\dot{Q}_{on-peak}^{*} = K\exp[(UA_s/C_s)t]/2C_s,$$

The problem now becomes one of finding the appropriate value for K. Note that $\dot{Q}_{on-peak}^{*}$ is a constant except for the exponential term. The values for UA_s and C_s which were used in the simulations are about 7.2 Btu/hr-^{o}F and 8250 Btu/^{o}F, respectively. Therefore, the optimal control is

$$\dot{Q}_{on-peak}^{*} = K\exp(.00087t)/2C_s,$$

If the on-peak period is 16 hours, $\dot{Q}_{on-peak}^{*}$ is 1.4 percent higher at the end of the on-peak period than it is at the beginning of the on-peak period. If the storage losses are neglected, that is, if UA_s is equal to zero, at most, a 1.4 percent error in $\dot{Q}_{on-peak}$ is incurred. The storage losses are therefore neglected leaving

$$\dot{Q}_{on-peak}^{*} = \text{constant} = K/2C_s.$$

To evaluate K, integrate the dynamic equation for the storage temperature after substituting for $\dot{Q}_{on-peak}$,

$$C_s\int_{T_o(t_o)}^{T_s(t_f)} dT_s = \int_{t_o}^{t_f} (K/2C_s - \dot{Q}_{load} + \dot{Q}_{sol})dt$$

or

$$C_s[T_s(t_f) - T_s(t_o)] = (t_f - t_o)K/2C_s + \int_{t_o}^{t_f} (\dot{Q}_{sol} - \dot{Q}_{load})dt.$$

Using the initial and final conditions on storage temperature and solving for $K/2C_s$ yields

$$\dot{Q}_{on-peak}^{*} = K/2C_s = \overline{\dot{Q}}_{load} - \overline{\dot{Q}}_{sol} - C_s(T_{s,min} - T_s)/(t_f - t_o)$$

where the overbar indicates an average over the remainder of the on-peak period. Using an energy balance on the enclosure, the optimal discharge from hot storage is

$$\dot{Q}_{st}^{*} = \dot{Q}_{load} - \overline{\dot{Q}}_{load} + \overline{\dot{Q}}_{sol} + C_s(T_{s,min} - T_s/(t_f - t_o).$$

COOL STORAGE

The off-peak storage cooling system is shown in Figure 39. Using the assumptions that the storage losses are negligible and the enclosure temperature is constant, the problem is to minimize

$$J = \int_{t_o}^{t_f} [\dot{Q}_{on-peak}]^2 dt$$

subject to

$$dT_s/dt = (\dot{Q}_{load} - \dot{Q}_{on-peak})/C_s.$$

This problem is identical to the hot storage problem with the exceptions that there is no solar input and the sign of the temperature derivative is reversed. The Hamiltonian is

$$H = \lambda(\dot{Q}_{load} - \dot{Q}_{on-peak})/C_s - (\dot{Q}_{on-peak})^2.$$

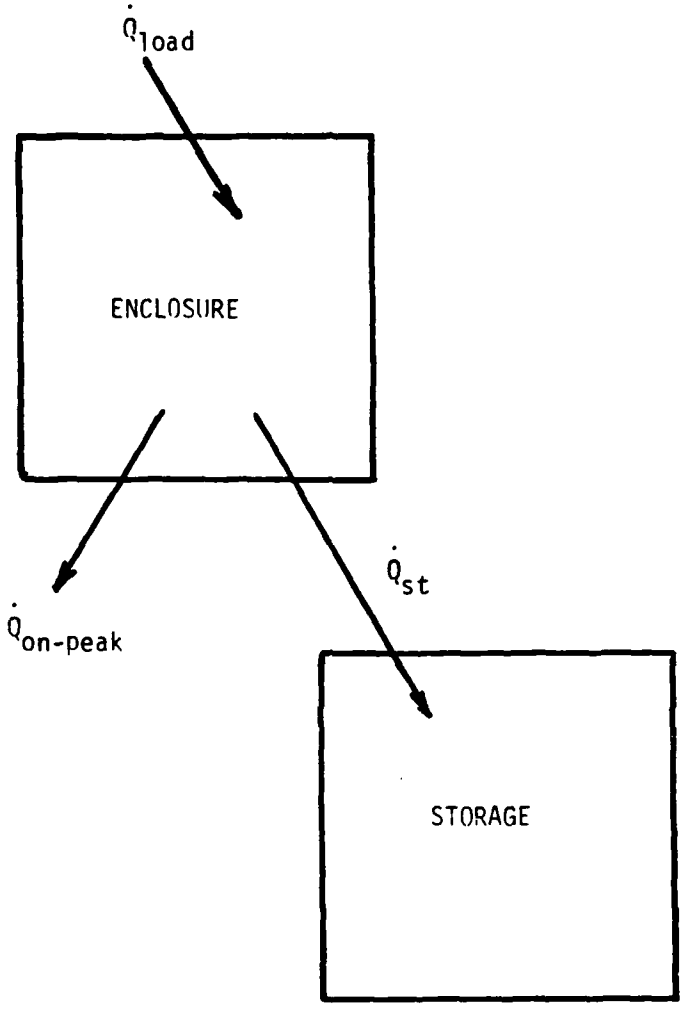

Figure 39. Off-Peak Cooling System Schematic.

The optimal control satisfies

$$\partial H/\partial Q_{on-peak} = 0 = -\lambda/C_s - 2\dot{Q}_{on-peak}$$

or

$$\dot{Q}_{on-peak}^{*} = -\lambda/2C_s.$$

The adjoint variable is defined using

$$d\lambda/dt = 0$$

or

$$\lambda = \text{constant} = K.$$

The value of the constant is determined by integrating the constraint equation

$$C_s \int_{T_s(t_o)}^{T_s(t_f)} dT_s = \int_{t_o}^{t_f} (\dot{Q}_{load} + K/2C_s)dt.$$

Therefore, using the initial and final conditions from Chapter 3, the optimal control is

$$\dot{Q}_{on-peak}^{*} = \bar{\dot{Q}}_{load} - C_s(T_{s,max} - T_s)/(t_f - t_o)$$

and the optimal discharge rate from cool storage is

$$\dot{Q}_{st}^{*} = \dot{Q}_{load} - \bar{\dot{Q}}_{load} + C_s(T_{s,max} - T_s)/(t_f - t_o).$$

It should be noted that the optimal discharge from cool storage was developed using an air conditioner COP which was constant throughout the on-peak period. Further work should include the development of the optimal control with a variable COP.

APPENDIX C.

WEIGHTED PROPORTIONAL DISCHARGE STRATEGY

The weighted proportional discharge strategy uses approximations for $\dot{Q}_{load}$ and $\dot{Q}_{sol}$ which are used in the equation for the optimal storage discharge rate. The following is an example illustrating the development of a weighted proportional discharge strategy. The weighted proportional strategy for discharge from cool storage is used as the example.

The optimal discharge rate from cool storage is

$$\dot{Q}_{st}^{*} = \dot{Q}_{load} - \bar{\dot{Q}}_{load} + C_s(T_{s,max} - T_s)/(t_f - t_o),$$

To establish the weighted proportional strategy, an estimate of $\dot{Q}_{load}$ for the entire on-peak period is needed. For the best effect, this estimate must be for the load on the peak load day. The peak cooling load day is typically characterized by a low cooling load in the morning with the load increasing steadily throughout the day, reaching a peak at about 1800 hours. The cooling load then decreases steadily through the end of the on-peak period. A cooling load such as this can be a combination of linear functions or a sinusoidal function. In this example, the load is modeled as

$$\dot{Q}_{load} = \bar{\dot{Q}}_{load} + A\cos[2\pi(t-18)/24]$$

where A is location dependent and equals the amount that the maximum cooling load on the peak cooling load day exceeds $\dot{Q}_{load}$, the average cooling load during the on-peak period of the peak cooling load day. Substituting this into the equation for the optimal control yields

$$\dot{Q}_{st} = A\cos[2\pi(t-18)/24] + C_s(T_{s,max} - T_s)/(t_f - t_o),$$

This equation represents one possible weighted proportional discharge strategy. Different models for $\dot{Q}_{load}$ will yield different weighted

proportional discharge strategies. The performance of a particular strategy depends on how well the modeled $\dot{Q}_{load}$ approximates the actual load on the peak cooling day.

The procedure described above also applies to the development of a weighted proportional discharge from hot storage. Recall, however, that in most cases, the heating load on the "worst" days in the winter is relatively constant. If the heating load is modeled as constant, the resulting weighted proportional strategy is identical to the proportional straegy described in Chapter 3.

A weighted proportional strategy is also applicable to a solar or combined solar and off-peak storage heating system. For these systems, in addition to the heating load, the total amount of solar energy to be collected must be estimated. Estimation of future solar radiation can be a very risky process; however, the only radiation of interest is the radiation which will occur on the day which has the largest overall heating load during the on-peak period. This "worst" day is quite likely a cloudy one which leads to the estimate of $\dot{Q}_{sol}$ as zero. This is also a safe estimate because, if some radiation is expected and it does not arrive, storage will be depleted before the end of the on-peak period, and a high coincident demand will occur. If radiation is underestimated, energy is simply left in storage for use during the next day. The recommendation, therefore, is that solar energy collection is estimated to be zero unless very reliable prediction is available.

APPENDIX D

OPTIMAL COLLECTOR FLOW RATE

The optimal mass flow rate in a solar energy collection system depends on the statement of what is to be optimized (the objective function) and the model used to describe the performance of the system (the constraints). Each combination of objective function and constraints has an optimal, time dependent, flow rate. To demonstrate this, consider the following examples of analyses using Pontryagin's Maximum Principle.

MAXIMIZE ENERGY COLLECTED WHILE IGNORING COLLECTOR AND STORAGE DYNAMICS

Maximize

$$J = \int_{t_o}^{t_f} \dot{Q}_u(\dot{m},t)dt$$

where $\dot{m}$, the mass flow rate through the collector, is the control. The Hamiltonian is

$$H = \dot{Q}_u$$

where $\dot{Q}_u$ is given by the Hottel-Whillier-Bliss equation

$$\dot{Q}_u = F_r A_c[H_t(\tau\alpha)-U_l(T_s-T_a)]$$

and F_r, the heat removal factor, is

$$F_r = \dot{m}c_p[1-\exp(-F'U_lA_c/\dot{m}c_p)]/U_lA_c.$$

The Hottel-Whillier-Bliss equation is an accepted model for accurately depicting collector performance. With these substitutions, the Hamiltonian is

$$H = \dot{m}c_p[H_t(\tau\alpha)-U_l(T_s-T_a)][1-\exp(-F'U_lA_c/\dot{m}c_p)]/U_l$$

which is a monotonically increasing function of $\dot{m}$. Clearly, to maximize H, the flow rate must be

$$\dot{m}^* = \begin{cases} \dot{m}_{max}, \text{ if } [H_t\tau\alpha - U_l(T_s - T_a)] > 0 \\ 0, \text{ if } [H_t\tau\alpha - U_l(T_s - T_a)] < 0 \end{cases}$$

In other words, to maximize the energy collected with no constraints, the optimal control is bang-bang and the switching condition is based on available net energy.

MAXIMIZE ENERGY COLLECTED SUBJECT TO STORAGE DYNAMICS WHILE IGNORING COLLECTOR DYNAMICS AND PUMPING POWER

Maximize

$$J = \int_{t_o}^{t_f} \dot{Q}_u dt$$

subject to

$$dT_s/dt = \dot{Q}_u/C_s,$$

The Hamiltonian is

$$H = \lambda\dot{Q}_u/C_s + \dot{Q}_u = (\lambda/C_s + 1)\dot{Q}_u$$

where the adjoint variable is defined using

$$d\lambda/dt = -\partial H/\partial T_s = (\lambda/C_s + 1)F_r U_l A_c$$

and, by the transversality condition,

$$\lambda(t_f) = 0,$$

For the final condition on λ to be satisfied it is necessary that

$$0 < \lambda/C_s + 1 \leq 1,$$

Therefore, the multiplier of $\dot{Q}_U$ in the Hamiltonian is positive, and, with the substitutions for $\dot{Q}_U$ and F_r as before, to maximize H, the flow rate must again be

$$\dot{m}^* = \begin{cases} \dot{m}_{max}, \text{ if } [H_t\bar{\tau}\alpha - U_l(T_s - T_a)] > 0 \\ 0, \text{ if } [H_t\bar{\tau}\alpha - U_l(T_s - T_a)] < 0. \end{cases}$$

The addition of storage dynamics to the model does not affect the form of the optimal control. The optimal control remains bang-bang and the condition for switching between the two control levels (0 or $\dot{m}_{max}$) is the same as in the previous case.

MAXIMIZE ENERGY COLLECTED SUBJECT TO STORAGE AND COLLECTOR DYNAMICS WHILE IGNORING PUMPING POWER

Maximize

$$J = \int_{t_o}^{t_f} \dot{Q}_U dt$$

subject to

$$dT_s/dt = \dot{Q}_U/C_s$$

$$dT_e/dt = [\dot{Q}_U - \dot{m}c_p(T_c - T_s)]/C_c$$

where C_c is the thermal capacitance of the collector. The Hamiltonian is

$$H = \lambda_1\dot{Q}_U/C_s + \lambda_2[\dot{Q}_U - \dot{m}c_p(T_c - T_s)]/C_c + \dot{Q}_U$$

where

$$d\lambda_1/dt = (\lambda_1/C_s + \lambda_2 C_c + 1)F_r U_l A_c - \lambda_2 \dot{m}c_p/C_c$$

$$d\lambda_2/dt = \lambda_2 \dot{m}c_p/C_c$$

and

$$\lambda_1(t_f) = \lambda_2(t_f) = 0.$$

The differential equation for λ_2 is solved, giving

$$\lambda_2(t) = K\exp\int(\dot{m}c_p/C_c)dt \ .$$

Since the exponential function is nonzero and $\lambda_2(t_f)=0$, necessarily $\lambda_2(t)=0$. Therefore, the problem reduces to one which is identical to the preceeding one, and the optimal flow rate is

$$\dot{m}^* = \begin{cases} \dot{m}_{max}, \text{ if } [H_t\tau\alpha - U_l(T_s-T_a)]>0 \\ 0, \text{ if } [H_t\tau\alpha - U_l(T_s-T_a)]<0. \end{cases}$$

The addition of collector dynamics does not affect the form of the optimal control.

MAXIMIZE THE DIFFERENCE BETWEEN SOLAR POWER COLLECTED AND PARASITIC LOSSES WHILE IGNORING STORAGE AND COLLECTOR DYNAMICS

Maximize

$$J = \int_{t_o}^{t_f} (C_3\dot{Q}_u - P)dt$$

where C_3 is a weighting factor which takes into account the difference between the cost of energy to run the fluid mover and that to provide auxiliary heating. Here P is expressed as

$$P = C_4\dot{m}^a.$$

The appropriate value for C_4 and "a" depends on the particular installation as discussed in Chapter 4. The Hamiltonian is

$$H = C_3\dot{Q}_u - C_4\dot{m}^a$$

or

$$H = C_3F_rA_c[H_t\tau\alpha - U_l(T_s-T_a)] - C_4\dot{m}^a.$$

Because H does not continuously increase with $\dot{m}$, the optimal control is found by setting

$$\partial H/\partial\dot{m} = 0$$

and solving for $\dot{m}$. To allow an explicit solution for $\dot{m}$, the exponential function in F_r is expressed as a Taylor's series and truncated after second order terms so that

$$F_r = F' - F'^2 U_l A_c / 2\dot{m} c_p,$$

For the system in Solar House II, this approximation for F_r is accurate to within 0.6 percent at the highest flow rate and to within 6.5 percent at the lowest flow rate. The resulting equation for the optimal mass flow rate is

$$\dot{m}^* = (C_3 f F'^2 U_l A_c / 2a C_4 c_p)^{1/(a+1)}$$

where f, the available energy is zero if $(T_c - T_s)$ is negative or, if $(T_c - T_s)$ is positive, determined from either

$$f = \dot{m} c_p (T_c - T_s)/F_r$$

if the collector fluid mover is on, or

$$f = U_l A_c (T_c - T_s)$$

if the fluid mover is off [7]. Note that the optimal control is not bang-bang.

The 6.5 percent error in F_r resulting from the use of the Taylor's series expression causes some error in the selection of $\dot{m}^*$; however, this error is small. Because the exponent in the equation for the optimal control is small, the choice of $\dot{m}^*$ is within 2 percent of the desired value. This results in an insignificant reduction in the objective function, J.

MAXIMIZE POWER COLLECTED MINUS PUMPING POWER SUBJECT TO STORAGE DYNAMICS WHILE IGNORING COLLECTOR DYNAMICS

Maximize

$$J = \int_{t_o}^{t_f} (C_3 \dot{Q}_U - P) dt$$

subject to

$$dT_s/dt = \dot{Q}_u/C_s,$$

The Hamiltonian is

$$H = (\lambda/C_s+C_3)\dot{Q}_u-C_4\dot{m}^a$$

where

$$d\lambda/dt = (\lambda/C_s+C_3)F_rU_1A_c$$

and

$$\lambda(t_f) = 0.$$

Following the same procedure described previously, the optimal flow rate is

$$\dot{m}^* = [(\lambda/C_s+C_3)fF'^2U_1A_c/2\ C_4c_p]^{1/(a+1)}$$

if the term in the brackets is positive, or zero otherwise. The

$$\lambda(t) = C_sC_3\exp[-\int(F_rU_1A_c/C_s)dt]-C_sC_3,$$

A numerical solution of this equation shows that, for a typical system, λ/C_s will begin the day at about -0.2 and gradually increase toward zero. Assuming $\lambda=0$ for all time causes the choice for $\dot{m}^*$ at the beginning of the day to be about 7 percent higher than the true optimal flow rate. As the day progresses, this difference reduces to zero. This difference from the true optimal flow rate results in a very small reduction in the objective function. Therefore, the optimal flow rate is

$$\dot{m}^* = (C_3fF'^2U_1A_c/2aC_4c_p)^{1/(a+1)},$$

This solution is identical to the one obtained while ignoring storage dynamics, that is, assuming that the storage temperature is constant. In other words, this equation approximates the optimal flow rate whether the storage exit temperature is constant, as in an air system, or the storage is well mixed, as in a liquid system or an air system after breakthrough has occurred.

MAXIMIZE POWER COLLECTED MINUS PUMPING POWER SUBJECT TO STORAGE AND COLLECTOR DYNAMICS

Maximize

$$J = \int_{t_o}^{t_f} (C_3\dot{Q}_u - P)dt$$

subject to

$$dT_s/dt = \dot{Q}_u/C_s$$

$$dT_c/dt = [\dot{Q}_u - \dot{m}c_p(T_c - T_s)]/C_c,$$

The Hamiltonian is

$$H = \lambda_1\dot{Q}_u/C_s + \lambda_2[\dot{Q}_u - \dot{m}c_p(T_c - T_s)]/C_c + C_3\dot{Q}_u - C_4\dot{m}^a$$

where

$$d\lambda_1/dt = (\lambda_1/C_s + \lambda_2/C_c + C_3)F_rU_1A_c - \lambda_2\dot{m}c_p$$

$$d\lambda_2/dt = \lambda_2\dot{m}c_p/C_c$$

and

$$\lambda_1(t_f) = \lambda_2(t_f) = 0.$$

As before, solving for $\lambda_2(t)$ and using the final condition on λ_2 yields

$$\lambda_2(t) = 0.$$

Therefore, the problem is exactly the same as the one without considering collector capacitance and the optimal flow rate is approximated by

$$\dot{m}^* = (C_3FF'^2U_1A_c/2aC_4c_p)^{1/(a+1)}.$$

This is the expression for optimal flow rate which was used throughout Chapter 4.

MAXIMIZE POWER COLLECTED MINUS PUMPING POWER WHILE INCLUDING A VARIABLE COLLECTOR EFFICIENCY FACTOR

In each of the above problems, the collector efficiency factor was assumed to be constant for all flow rates. This assumption is consistant with most

simulation programs, for example, TRNSYS [15]. For an air collector, however, the collector efficiency factor may not be constant. Manufacturer's data for the collectors on Solar House II suggest a decrease in collector efficiency factor with flow rate [16]. The decrease in performance at low flow rates is the result of the dependence of air collector efficiency factor on convective heat transfer coefficients [8]. This variation in F' with flow rate can be included in the optimization by assuming a relationship between flow rate and efficiency factor. The derivation of the optimal flow rate for a system with a variable collector efficiency factor follows.

$$J = \int_{t_o}^{t_f} (C_3\dot{Q}_u - P)dt.$$

It was shown earlier that the storage and collector dynamics are not important; therefore, they are not included in this problem. Let the energy collected again be denoted by

$$\dot{Q}_u = F_r A_c [H_t \tau \alpha - U_l (T_s - T_a)]$$

and the heat removal factor by

$$F_r = F' - F'^2 U_l A_c / 2\dot{m}c_p.$$

Now assume that F' is related to flow rate linearly as

$$F' = F'' + b\dot{m}$$

so that

$$F_r = F'' + b\dot{m} - (F'' + b\dot{m})^2 U_l A_c / 2\dot{m}c_p.$$

The Hamiltonian is

$$H = C_3 A_c [F'' + b\dot{m} - (F'' + b\dot{m})^2 U_l A_c / 2\dot{m}c_p][H_t \tau \alpha - U_l (T_s - T_a)] - C_4 \dot{m}^a.$$

The optimal control is found by setting

$$\partial H / \partial \dot{m} = 0$$

which yields

$$(C_4 a/C_3 f)(\dot{m}^*)^{a+1} - [b - U_1 A_C F''^2/2c_p](\dot{m}^*)^2 - U_1 A_C F''^2/2c_p = 0.$$

This equation cannot be solved explicitly for $\dot{m}^*$, but a lookup table similar to the one in Chapter 4 can be developed. The new optimal flow rate again depends on system parameters, the temperature difference across the collector, and the old flow rate.

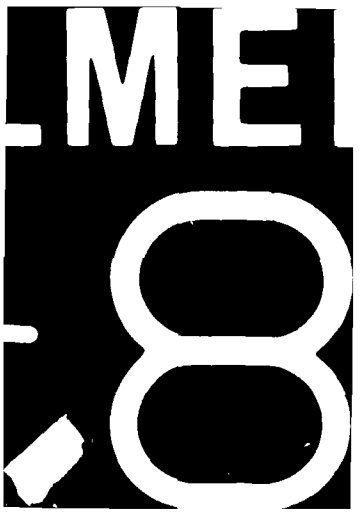
ME
8